공학석사 학위논문

미얀마 Ayeyarwaddy 강 상류유역 유량에 미치는 기후변화 영향평가

Assessment of Impact of Climate Changes on Streamflow in the Upper Ayeyarwaddy River Basin, Myanmar

2021 년 2 월

서울대학교 대학원

건설환경공학부

Paing Myint Mo

Assessment of Impact of Climate Changes on Streamflow

in the Upper Ayeyarwaddy River Basin, Myanmar

지도교수 Van Thinh Nguyen

이 논문을 공학석사 학위논문으로 제출함

2021년 1월

서울대학교 대학원

건설환경공학부

Paing Myint Mo

Paing Myint Mo의 석사학위논문을 인준함

2021년 1월

위 원 장 김 영 오 (인)

부 위 원 장 Van Thinh Nguyen (인)

위 원 서 일 원 (인)

Abstract

The Ayeyarwady is the largest river in Myanmar stretching about 2,170 km long and covering a basin of 413,710 km². The Ayeyarwady River Basin is Myanmar's most economically important area with the population about 39.5 million people. The changes of climate have vital impacts on water resources in the Upper Ayeyarwady River Basin. Therefore, it is necessary to estimate such impacts and their consequences on hydrological processes in this region. In this study, the Soil and Water Assessment Tool (SWAT) has been used as a simulation tool. Before SWAT can be applied to assess the effects of climate changes on hydrological processes in the study region, it has been carefully calibrated and validated against observation data for the period of 1989-2018. During simulation, a three-year warming-up period was given and the total simulation period was set to run from 1993 to 2018 (*i.e.* 26 years). SWAT model was calibrated for 1993 to 2005 and validated for 2006 to 2018 by adjusting the parameters. Model results showed R^2 value of 0.65 (calibration), 0.68 (validation) and Nash-Sutcliffe Efficiency (NSE) value of 0.43 (calibration), 0.55 (validation) at Myitkyina Station, R^2 value of 0.71 (calibration), 0.64 (validation) and NSE value of 0.71 (calibration), 0.64 (validation) at Bamo Station, R^2 value of 0.62 (calibration), 0.65 (validation) and NSE value of 0.5 (calibration), 0.51 (validation) at Katha Station and R^2 value of 0.65 (calibration), 0.7 (validation) and NSE value of 0.69 (calibration), 0.67 (validation) at Sagaing Station, respectively. The model performance indicators (R^2 and NSE) indicated good performance of the model except one station. Climate change data in the Upper Ayeyarwady River Basin was obtained from CMIP5 data set. The climate change scenarios were downscaled from four different GCMs (General Circulation Models), such as EC-EARTH, HadGEM2-ES, MICROC5 and MPI-ESM-MR, under two different Representative Concentration Pathways for medium stabilization scenarios (RCP4.5) and high emissions scenario (RCP8.5). There are various statistical downscaling techniques, such as SDSM, ASD, delta change methods, etc.; among them, LARS-WG developed by Semenov and Stratonovitch was selected for this study, because it can provide a better performance on reproducing monthly meteorological variables than other statistical downscaling techniques, such as SDSM, ASD, and delta change methods. Basically, LARS-WG

has been validated against observed meteorological data (daily rainfall, temperature) for the period of 1989-2015 from a specified site to estimate a set of parameters for fitting probability distributions, which is then used to generate synthetic weather time series of a tributary length by randomly selecting values from appropriate distributions. Projections of four GCMs indicate an increase in both annual Tmax and Tmin for all three future periods under RCP 4.5 and 8.5 scenarios relative to the baseline. Rainy season is projected to receive the greatest precipitation boost in the future than any other seasons in all two periods.

The assessment of impact of climate changes on streamflow in this region was carried out for near futured period 2050s (2021-2050) and the far future period 2080s (2051-2080). Percentage changes in annual average stream flow using four GCMs showed the maximum increase in stream flow (approximately 70%) in the 2050s and (approximately 80 %) in the 2080s under the RCP4.5 and 8.5 using four GCMs at the Katha and Sagaing station. The highest decrease in both annual and seasonal flow (approximately 80%) is observed in all periods by four GCMs under both scenarios at Myitkyina station. The maximum increase in annual flow during the 2050 (9%) and 2080s (15%), is predicted by using EC-EARTH, HadGEM2-ES and MICRO5 and 2080s (15%) decrease by using MPI-ESM-MR under RCP4.5 and 8.5 at Bamo station. For the Changes in average seasonal stream flows at all stations, summer seasonal stream flow for three periods in the century are expected to decrease (approximately 80%) for both scenarios. In the rainy and winter seasonal flow, average flow inclines consistently approaching 84% in 2050 and 107% in 2080 at the Katha and Sagaing stations while approximately 30% in 2050 and 40 % in 2080 at Bamo station under both scenarios by four GCMs.

The range of uncertainty for annual and seasonal stream flow changes are projected roughly 30% to 45% under both scenarios for the future period of all stations. This study proves that projections of stream flow changes under a future climate are uncertain and the greatest source of this uncertainty is also the difference in the climate projections from the four GCMs considered for the whole study area.

The result obtained from this study can provide useful reference to analyze, evaluate and utilize for water resource management under the effects of climate changes in the study region.

Keywords: Climate Change, hydrological process, streamflow, SWAT, CMIP5, GCM, LARS-WG

Student number: 2018-25580

Table of Contents

FIGURES

TABLES

CHAPTER 1. INTRODUCTION

1.1 Background

Over the years, issues relate to water resources are under severe pressure and widely disseminated throughout the world due to the consequences of changes in air temperature and precipitation. Climate change alters the temperature, precipitation and the rate of evapotranspiration which effects hydrological regimes by the volume, peak rate and timing of river flow. The primary climate change impacts driven by global warming are extensive, complicated, and uncertain. Global mean temperature has risen by approximately 0.7 ºC during the twentieth century, with the warming trend accelerating during the last 50 years (IPCC, 2007). Climate change impacts, such as precipitation and temperature changes, are leading to more flood and drought events each year. Climate variability and change have an intensive effect on the communities across the globe. Various aspects regarding the assessment of impact of climate change have to be considered as decisive factors as assessing such effects on the water resources become a problematic.

It has long been possible of generalized precipitation and temperature projection for several years in advance by examining the differences of sea surface temperature and air pressure at key locations all over the countries. It has been widely used in General Circulation Models (GCMs) to predict the future changes in meteorological parameters such as temperature and precipitation. However, their outputs are temporally and spatially very coarse (IPCC, 2001). Although these outputs are useful at continental and global levels, finer resolution outputs are

needed at regional and local levels for investigating the effects of climate change on the environmental flows and water cycle. To use the local and regional scales of 0-50 km and 50 × 50 km, many methods for downscaling have been developed (Bates et al., 2008). As climate models are not perfect, the predicted climatology can differ from baseline climatology. The model state will drift towards a model climate as the forecast progresses and this shift will be confounded by the climate advancement that is being predicted. Moreover, streamflow is an important factor in environmental, agricultural and economical applications. Therefore, investigating changes about streamflow under future climate conditions is important to the discussion of climate change effects. Predicting the impacts of climate change on streamflow is mainly based on hydrological modeling outputs from general circulation models (GCMs). Various researchers have successfully used bias correction technique in impact studies (Berg et al., 2012). Most studies related to forecasting climate change scenarios using Representative Concentration Pathways (RCPs) have been conducted in European countries. Some studies have used bias correction in Asia (Piani et al., 2010). Seasonal climate forecasts are very useful for various communities and decision makers. These forecasting methods also aid in improving water management and the farmers and land owners can get more benefits principally in areas in which precipitation is naturally variable and unreliable. Several past studies have used seasonal climate forecasts (Mahmood et al., 2013; Agarwal et al., 2014; Su et al., 2014). However, many studies have used the SDSM model ASD, and delta change methods to forecast seasonal temperature and rainfall patterns. Beven, (1993) mentioned that the choice of GCMs and different future emission scenarios mainly influence the uncertainty and it is also

calculated by various methods of downscaling and hydrological modelling. Ghosh et al., (2009) mentioned that significant uncertainty exists in the systems of water resources and hydrology analysis by the impacts of climate change. Zhange et al., (2011) pointed out that uncertainties in possible future climate is a good practice for a range of climate projection impact studies. Therefore, investigating the climate change affects is the greatest important task.

1.2 Statement of the Problem

Study area, Ayeyarwaddy River is known as the country's largest main river of Myanmar and it is divided into the upper river basin which has a warm humid subtropical climate and the lower river basin which has a humid tropical climate (Encyclopaedia Britannica 2019).The effects of natural disasters have been visible in this basin with the dawn of the twenty-first century . The changing river flow and precipitation in the Ayeyarwaddy River Basin increase floods and droughts in this watershed because of climate change impacts, and consequently, frequently floods have caused degradation of natural and water resources. There are also serious floods in the Ayeyarwaddy River Basin when cyclones pass through the coastal area. The frequency and severity of floods during rainy season has increased according to the records of Department of Meteorology and Hydrology. It was observed that the Ayeyarwaddy River generally experiences floods above the danger level (9.1 m) once every three years.

Moreover, the drainage systems of the Ayeyarwaddy River Basin are in poor condition and the major cause of flooding. The outflow from this basin is insufficient for the downstream area. During the rainy season, when there is a large amount of watercourse in the river, it has a rapid flow. The average discharge of

the river buries between 2,300 cubic meter per second for low and 32,600 cubic meter per second for high. The large water quantity in the river at the flood measure of 11.3 m causes it to regain its flowing rate as the flood level becomes higher reaching a point of 9 m, there is an increase in the flow rate, for instance, 2000 people were homeless, 20 people were killed, over 2000 people injuries, cultivated area was damaged, and land was inundated with water in 2010. In 2016, the water level reached to 9.6 m at the highest level, causing 4000 people to become homeless and 20 people were killed and paddy fields have been inundated during the past 47 year due to the tow times flooding (DMH 2016).

Increase in surface runoff, land cover change, forest degradation, and soil erosion are the major impacts instigated by climate change in the Ayeyarwaddy River Basin. Climate change has rendered the poor people more vulnerable to water scarcity, food security, and hunger (Hlaing et al., 2008). The local people rely on water resources from this watershed for their livelihoods of fishing and seasonal farming. Farmers account for 40% of the local population, farming over (890 km2) annually. The farmers face a water shortage when planting during summer, with floods in the rainy season during harvest time. This water crisis becomes a constraint impinging on the economic growth in the Ayeyarwaddy River Basin. The loss of agricultural farms is rapidly increasing in this area (Ministry of Agriculture and Irrigation, 2012). Most local people have a poor living standard because of their low GDP (almost US$2). The local people are more vulnerable to water scarcity due to the recent degradation of the forest environment (Ministry of Environmental Conservation and Forestry, 2014). With increasing population

growth, urbanisation and industrialisation are continually expanding in the municipal area of this watershed.

To the best of our knowledge, there is insufficient funding, equipment, and trained staff in government offices to provide resilience and restoration for this watershed. Accordingly, because of these problems caused by climate change and land cover change, it is necessary to study the climate and how they impact on the hydrology and water resources of the Ayeyarwaddy River Basin. Hydrological models are substantial instrument for water resource managements, development and future planning. Therefore, many models have been applied to hydrological modeling and water resource management. Among those models, the Soil and Water Assessment Tool Model (SWAT) model, developed by the United States Department of Agriculture-Agricultural Research Service (USDA-ARS), is applied in this study. However, climate change involves uncertainty due to use of different GCMs and emission scenarios. The uncertainty in projecting future climates seriously impairs water resource planning in the Ayeyarwaddy River Basin. The lack of analysis for extreme events also increases future risks to water-related programmes and projects.

1.3 Research Objectives

The overall objective of this study is to analyse the impact of climate change on hydrology and uncertainty of GCMs in emission scenarios in the Upper Ayeyarwaddy River Basin. The specific objectives are divided into four parts:

1. To project the future climate with scenarios RCP 4.5 and RCP 8.5 for the Upper Ayeyarwaddy Basin
2. To simulate the streamflow of the Upper Ayeyarwaddy Basin

3. To analyse the impacts of climate change on hydrology under various climate change scenarios and quantify the uncertainty of climate change projection and changes in hydrology of the Upper Ayeyarwaddy River Basin.

4. In aid of considering for decision making processes in the field of adaptation and mitigation strategies for preparation of future climate changes in watershed

CHAPTER 2. LITERATRUE REVIEW

2.1 Introduction to Climate Change

Climate change is normally expected to lead to an intensification of the global water cycle as a result of changes in hydrologic variables such as precipitation and temperature (Huntington, 2006). Around the world, the global climate change and human activities strongly change water resources and hydrological regimes, raised by great concern of general public, scientific groups and government agencies (Sangmanee et al., 2011). Nowadays, man-made activities release greenhouse gases, and of these, carbon dioxide poses the most serious threat to global warming. With an increasing rate of global warming, glaciers and snow packs are melting rapidly, causing sea levels to rise thereby resulting in flooding and salt intrusion and destroying agriculture. Raising strong concerns over the stream flow changes, natural pond abasements and water shortage in the region are caused by escalated man-made activities and global weather change. As a result of meteorological changes, cyclones, drought, cold waves, and heat waves have an effect on livelihoods, property, and agriculture. The population suffers water scarcity and food insecurity, with the hunger rate increasing mostly in developing countries.

In developed countries, governments are able to maintain the watersheds, however in some developing countries, they cannot be maintained due to the poor management and financial issues. Therefore, the watersheds are more vulnerable to climate change. The watershed ecosystem has changed because of climate change (Bryon et al., 2013) and drought and floods have an effect on loss of water input by reducing storage capacity. With extensive ranging results of the ecosystem and society, climate change has strong probable affecting on water resources to be

more susceptible in the world (Dowa et al., 2007). Hydrological cycle is changed by weather changes indicating increased amount of water vapor, the patterns of precipitation changes, causing extremes and intensity, snow cover reduction, and extensive ice melting and soil moisture and discharge changes (Chinvanno, 2004). Global warming causes glaciers and snow packs to start melting earlier in the year, with the timing of stream flow being unstable. In mountainous areas, the local people rely on stream flow. From a health point of view, people and animals need more drinking water because of drought. In Africa, women and children die from water scarcity. Wealthier people can buy drinking water but the poor cannot afford it.

Hydropower production depends on stream flow. If there is only a small amount of water available, energy production is reduced. With decreasing hydroelectricity, countries will be turning to the alternative energy sources of petroleum and coal and they also release more greenhouse gases, which are very hazardous to climate change. Irrigated water is essential for farmers as if they cannot get sufficient water, there will be decreased in yield production (Field et al., 2007). Hunger is based on harvest production and floods erode the soil and damage crops. Water temperature affects certain fish species: for example, salmon cannot exist in warm temperatures, and there are many other ways in which climate change can be affected by water resources.

2.2 Climate Change Projections

2.2.1 General Circulation Models

Generally, there are two types of climate models; GCM and RCM. The difference between the GCM and RCM is that the RCM is a high-resolution climate model

and can be used in a limited area. It can focus on an area of 5000 km × 5000 km and its typical horizontal resolution uses a 50 km mathematical equation with a three-dimensional grid. As with the GCM, certain boundaries influence the RCM such as wind, temperature, water vapour, and surface pressure. To evaluate assessment for regional areas, small scales are needed. The output from GCMs is too large and too low in resolution to give a clear picture of specific regions. GCMs are good at characterizing large scale atmospheric circulation of the whole planet. In addition, GCMs do not incorporate landscape features, water bodies, or other characteristics. According to climate models and their evaluation (EPRI, 2009), GCMs show increasing atmospheric carbon dioxide. From simulations of GCMs, it can be seen that in the twenty-first century, the increasing concentration of the average precipitation and water vapor under future scenarios. For example, in Southern Asia, from reports of different GCMs, the projected precipitation will be increased by 15%.

Water resources are affected by variation in meteorology across the globe. GCMs can predict temperature and precipitation changes in Southern Asia. The Center for International Climate and Environmental Research, Oslo (CICERO) estimated that temperature will increase by 0.9 and 1.8 in 2025 and 2050 respectively. Precipitation will change by ± 3% and 6% in 2020 and 2050 respectively. The rise in sea levels may increase by 0.2 m and 0.3 m in 2020 and 2050 respectively. By using GCMs, long range precipitation and temperature in a region can be ascertained. For example, in Southern Asia, the CSIRO, Australian global climate model can provide a long range of 5 to 50% for precipitation. Similarly, other GCMs such as CCCMAUKMOH and GFDLLH can give projected precipitation

increases of 20%, 24%, and 59% respectively. However, GCMs outputs cannot be used directly for hydrologic modelling. GCMs were increasingly developed to impact on GHG concentrations. GCMs can predict mean temperature, precipitation, and runoff ranging from 1 to 4.5 ºC and -20 to +30% respectively in the twenty-first century. GCMs focus on very large scales because of their coarse resolution ranges. These ranges are from 200 to 600 km (CICERO).

2.2.2 Selection of GCMs

The correct selection of GCM for a modeler is important to explain the magnitude and variability of local variables (T, P). According to Smith and Hulme in 1998, a modeler will consider the vintage and resolution of a GCM. It will choose GCM with a higher resolution because it can apprehend more local weather information than that of a rough resolution. For instant, a researcher wants to seize complex features: discharges in alpine area, he will use a very fine resolution GCM. It will be important to find sounder and more current climate producing GCM during the period of validation. For a level of region, a different range of climate variables can be simulated by various GCMs. Therefore, where many models are to be chosen, then representation of climate changes range in area will be considered for these models (Sharma et al., 2007). According to Liu and Smedt (2005), many modelers used 24 GCMs in the Fourth Assessment Report of Intergovernmental Panel on Climate Change (IPCC). Although most of these models have a higher resolution, and provide more recent and advanced climate models, some have output data starting from 2000. Since the observed meteorological data is available for the period from 1980 to 2009 and the observed baseline is selected for the

period 1980-2009, these models cannot be used now. Thus, modellers are using GCMs in Climate Model Intercomparison Project Phase 5 (CMIP5).

IPCC Fifth Assessment Report (AR5) released the CMIP5 which is the principal framework for a coordinated climate modelling experimentation in 2013. Approximately 20 modelling divisions from around the world are campaigning the CMIP5 researches and model data is hosted on the Earth System Grid, which consists of international data nodes and gateways. The CMIP5 experimental protocol provides four emission scenarios based on the RCPs, which are identified by amount of net radiative forcing into the Earth's climate system at the end of the twenty-first century. There are many updated GCMs in CMIP5. In a series of global atmosphere models, at the National Center for Atmospheric Research (NCAR), they originally developed the latest version 5.1 of the Community Atmosphere Model (CAM). The modeler will choose GCMs for particular research objectives and study area.

2.2.3 Representative Concentration Pathways

IPCC AR5 adopts the four greenhouse gas concentration trajectories namely Representative Concentration Pathways (RCPs) which are used for modelling and research linked with the climate change. Depending on the concentrations of greenhouse gases emission, the scientists describe these four RCPs to be possibly considered. A broad range of climate outcomes is represented by the RCPs to be chosen dependent upon a review of literatures. The policy recommendations and forecasting are not considered for that case. The basic concept is that of RCPs, which are expressed in terms of watts per square metre of radiative forcing (W/m2). Therefore, when looking at phenomena such as future temperature change or sea

level rise, there is no ‘business as usual’ (BAU) scenario. The names of four RCPs, 2.6, 4.5, 6, and 8.5 are given the radiative forcing values corresponding to the values before industrialisation as +2.6, +4.5, +6.0, and +8.5 W/m2, respectively (Su et al., 2014). Table 2.1 and Figure 2.1 explain these RCPs: one high greenhouse gas emission policy scenario, two stabilisation scenarios, and a very low forcing level (a mitigation scenario).

The future data of institute, technology, economy, policy and demography provide the RCP results. As an instance, it can be assumed that the mitigation scenario is to be moderated (Su et al., 2014). Although B1 scenario among SRES scenarios can reduce greenhouse gas emissions, the secondto-lowest RCP cannot aimed as a target in itself. However, it is also considered as a worldwide enlargement scoping on adjustment for industry service and technological refinements. During 2010-2020 with emissions lessening subsequently, the peak of global annual GHG emissions can be assumed as RCP 2.6. RCP 4.5 which is measured in CO2 equivalents, reaches at the peak in 2050, and then reduces. In RCP 6 climax for 2080 year, then shrinks (Deng et al., 2013). RCP 8.5 emissions continue to rise across the twenty-first century. The last RCP8.5 is perhaps the equivalent of BAU or ‘no climate change’. Multi-model ensemble data is obtained by using an arithmetic mean of 21 GCMs under the latest RCP scenarios from the World Climate Research Programme's (WCRP's) CMIP5 with a spatial resolution of 1.0˚ × 1.0˚. The 21 GCMs are listed in Table 2.2. Seeing this table, only the three countries: China, Japan and South Korea can produce the CMIP5 models. The others are USA and Europe countries. Now many research groups especially Japan are trying to produce new CMIP5 GCMs to investigate the greatest challenges of

climate variables. Now some GCMs have not completed all four emission scenarios but can be produced in next years.

All detailed RCPs data with their bounds and proper uses can be seen at the websites. International Institute for Applied Systems Analysis (IIASA) provides the Integrated Assessment Modeling Consortium database, for Applied Systems Analysis. The numberless groups developed the central data sets supported by IIASA (http://www.iiasa.ac.at/web-apps/tnt/RcpDb). The modelling groups can use a specific CMIP5 nominated database and also an enlightenment for RCP usage can do. With expansion to 2300, the historical atmospheric data and RCPs concentrations data during 2005 to 2100 are comprised in the data set. A vast range of data was supported to the Montreal Protocol with ozone expending materials control and the Kyoto Protocol with gases control. A vast range of data was provided, including gases controlled under the Kyoto Protocol, ozone expending materials controlled under the Montreal Protocol, and a huge range of aerosols and materials. The system of IAMC is operating for the review and release of the emission scenarios to initialize the integrated assessment models and also arranging supplementary modelling and intercomparisons (http://cmip-pcmdi.llnl.gov/cmip5/). Integrated Assessment Models can project RCPs towards 2100. For long term climate response research, the climate modeling sodality requested extra scenario information out to 2300.

Table 2.1. IPCC climate scenarios specified in Representative Concentration Pathways (RCPs) (Source: (IPCC, 2007))

Scenarios	**Radiative forcing**	**CO_2 Equiv (p.p.m)**	**Temperature anomaly (°C)**	**Pathway**	**SRES temperature anomaly equivalent**
RCP 8.5	Rising radiative forcing pathway leading to 8.5 W/m2 in 2100	1,370	4.9	Rising	SRES A1F1
RCP 6	Stabilisation without overshoot pathway to 6 W/m2 at stabilisation after 2100	850	3.0	Stabilization without overshoot	SRES B2
RCP 4.5	Stabilisation without overshoot pathway to 4.5 W/m2 at stabilisation after 2100	650	2.4	Stabilization without overshoot	SRES B1
RCP 2.6	Peak in radioactive forcing at ~ 3 W/m2 before 2100 and decline	490	1.5	Peak and decline	None

Table 2.2 : CMIP5 GCMs, their sources, scenarios available, resolution, parameters, and data sources

SN	Model	Description	Research Center	Grids (Long-lat) (Degree)
1	BCC-CSM 1-1	Beijing Climate Center Climate System Model version 1	BCC, China Meteorological Administration, China	128 x 64
2	BNU-ESM	Beijing Normal University Earth System Model	The College of Global Change and Earth System Science (GCESS), BNU, China	128 x 64
3	CanESM2	Canadian Earth System Model version 2	Canadian Centre for Climate Modelling and Analysis, Canada	128 x 64
4	CCSM4	The Community Climate System Model version 4	National Center for Atmospheric Research, USA	288 x 192
5	CNRM-CM5	Centre National de Recherches Météorologiques Climate Model version 5	CNRM/Centre Européen de Recherche et Formation Avancée en Calcul Scientifique, France	256 x 128
6	CSIROMk3-6-0	Commonwealth Scientific and Industrial Research Organisation Mark Climate Model version 3.6	CSIRO in collaboration with Queensland Climate Change Centre of Excellence, Australia	256 x 128
7	FGOALS-g2	Flexible Global Ocean Atmosphere-Land System Model-grid version 2	State Key Laboratory of Numerical Modelling for Atmospheric Sciences and Geophysical Fluid Dynamics, Institute	128 x 60

			of Atmospheric Physics, Chinese Academy of Sciences, and Tsinghua University, China	
8	FIO-ESM	The First Institution of Oceanography Earth System Model	FIO, State Oceanic Administration (SOA), Qingdao, China	128 x 64
9	GFDL-CM3	Geophysical Fluid Dynamics Laboratory Climate Model version 3	GFDL, National Oceanic and Atmospheric Administration, USA	144 x 90
10	GFDLESM2 M	Geophysical Fluid Dynamics Laboratory Earth System Model version 2 with Modular Ocean Model version 4.1	GFDL, National Oceanic and Atmospheric Administration, USA	144 x 90
11	GISS-E2-H	Goddard Institute for Space Studies Model E version 2 with Hycoml Ocean Model	GISS, National Aeronautics and Space Administration, USA	144 x 90
12	GISS-E2-R	Goddard Institute for Space Studies Model E version 2 with Russell Ocean Model	GISS, National Aeronautics and Space Administration, USA	144 x 90
13	HadGEM2AO	The Met Office Hadley Centre Global Environment Models version 2 with the new Atmosphere–Ocean	Jointly with Met Office Hadley Centre and National Institute of Meteorological Research (NIMR), Korea Meteorological	192 x 1

		Component Model	Administration (KMA), Seoul, South Korea	
14	IPSLCM5A-LR	Institute Pierre Simon Laplace Climate Model 5A-Low Resolution	IPSL, France	96 x 96
15	MIROC5	Model for Interdisciplinary Research on Climate-Earth System, version 5	Atmosphere and Ocean Research Institute (AORI), National Institute for Environmental Studies (NIES), Japan Agency for Marine Earth Science and Technology, Kanagawa (JAMSTEC), Japan	256 x 128
16	MIROCESM	Model for Interdisciplinary Research on Climate-Earth System	JAMSTEC, AORI, and NIES, Japan	128 x 64
17	MIROCESM-CHEM	Atmospheric Chemistry Coupled Version of Model for Interdisciplinary Research on Climate-Earth System	JAMSTEC, AORI, and NIES, Japan	128 x 64
18	MPI-ESMLR	Max-Planck Institute Earth System Model-Low Resolution	MPI for Meteorology, Germany	192 x 96
19	MRICGCM3	Meteorological Research Institute Coupled General Circulation Model version 3	MRI, Japan	320 x 160

20	NorESM1-M	The Norwegian Earth System Model version 1 with Intermediate Resolution	Norwegian Climate Center, Norway	144 x 96

2.2.4 Downscaling Model

In a specific region, the climate change can be defined as permanent and steady. It will be shifting in the long-term by means of climate variables statistics over the entire globe. From different groups of stakeholders and researchers, it is drawing attention of the assessment for climate change impacts on both regional and global scales. In fine-scale impact studies, the spatial resolutions of GCM outputs are too coarse and cannot be directly used although they are typical sources for future climate predictions. Cannon et al., (2001) explained that a great deal of biases can be involved by all model outputs. Moreover, it can lead to significant errors in impact assessment if it is not corrected. Recently, GCM precipitation was developed with the simpler downscaling methods to be directly used as a predictor which involves bias correction of model outputs (Harpham et al., 2005). In different hydroclimatological studies, it can be proved satisfactory for the statistically downscaled climate model and the performance of bias corrected outputs. It is necessary of making correction procedures for biased representations of observed time series provided by climate models (Teutschbein et al., 2004). Between observed and simulated climate variables, the identification of possible biases is the underlying idea forming the basis for correcting both control and scenario GCM/RCM runnings.

According to theory, all moments of distributed function can be adjusted by bias correction for each day. But a good approximation can be noted if a 2-parameter fit to the transform function for most regions in practice. Specific regions use 3 or 4 parameter transfer functions. It may not be adequate for using larger number of parameters because it is needed for correction to be time in dependent on climatological time-scales (>10 years). For temperature, the monthly transfer functions with smooth transitions are used. In many regions of the globe, both the fields of mean and the variance of the precipitation and temperature are effectively improved by bias correction (Mehrotra et al., 2014). To simulate climate variables, many published studies use the comparison of GCM capacities and it can be outstandingly relevant in water resources.

Generally, downscaling is defined as a factor which creates relationship between largescale cycles (predictors) and weather variables at local-scale (predictands). As a matter of fact, downscaling refers to the process of moving from large-scale predictors to predictands at local scale (Mearns et al. 2003). There are various statistical downscaling techniques, such as SDSM, ASD, delta change methods, etc.; LARS-WG (Long Ashton Research Station Weather Generator) is a stochastic weather generator which is used for simulation of weather data at a particular station under current and future conditions affected by the climate change phenomenon. Its data are in the form of daily time series of weather variables such as precipitation (mm), minimum and maximum temperature (°C) and solar radiation (MJm2 day -1) (Semenov, 2008). Basically, LARS-WG was developed by Semenov and Stratonovitch and it has been validated against observed meteorological data (daily rainfall, temperature)

from a specified site to estimate a set of parameters for fitting probability distributions, which is then used to generate synthetic weather time series of a tributary length by randomly selecting values from appropriate distributions. The assessment of impact of climate changes on streamflow in this model was carried out for near future period near future period 2050s (2021-2050) and the middle future period 2080s (2051-2080). The climate change scenarios were downscaled from five different GCMs (General Circulation Models), such as GFDL-CM3, EC-EARTH, HadGEM2-ES, MICROC5 and MPI-ESM-MR, under two different Representative Concentration Pathways for medium stabilization scenarios (RCP4.5) and high emissions scenario (RCP8.5). Many studies have used the SDSM model to forecast seasonal temperature and rainfall patterns for Ayeyawaddy Basin of Myanamar. LARS-WG model was selected for this study, because it can provide a better performance on reproducing monthly meteorological variables and no studies have investigated the analysis of climate change impacts relative to water resources of the Ayeyarwaddy River Basin using LARS-WG model.

2.3 Hydrological Modelling

In the analysis and collection of hydrological data, advances in the understanding of physical, chemical, and biological processes can influence water quality, coupled with improvements. It can provide exploring and modelling the process of watershed-scale with opportunities for significant innovations in the manner. Several methods were developed to assess the hydrological effects of environmental change. The main three methods are statistical methods namely time series analysis, hydrological modelling and approaching paired catchment. At different stages, it may be changing significantly

the same catchment, therefore application of the paired catchment approach is difficult for anything other than small catchments. Time series analysis is a statistical method which simply analyses the hydrological effects of environmental change (Schwank et al., 2014). Setegnet et al., (2011) stated that a framework is provided by hydrological models explaining the relationships between climate, human activities, and water resources to investigate and conceptualise. Jiang et al., (2006) stated that depending on the data available, a hydrological model will be chosen according to the purpose of study. Current watershed models generally adequately represent the surface water component, but simplify the dynamics of groundwater.

On the other hand, groundwater models ignore the dynamics of surface water (Cherkauer et al., 2010). A distinct strategy of parallel-computing is needed and the computational characteristics should be learned for each hydrological model. As an instance, a rainfall–runoff model (HBV) can be used in case of simulating present and future discharges of a river. For example, at Lake Nasser in the River Nile upstream, allocation modelling with RIBASIM was used for the Upper Nile and integrated water distribution for HBV was run. By combining these two models, it is called NHSM known as Nile Hydrological Simulation Model. Chen et al., (2013) explained about HSAMI hydrological model developed by Hydro-Québec for forecasting natural inflows hourly and daily. They used this model in two North American River Basins calculating annual and seasonal mean discharges and extremes with changes. For hydrological modelling, the properties of sediment variability will be importantly considered at the catchment scale (Hölzel et al., 2013).

In the Hebei province of China, there was a research in Qingshuihe watershed using Fully Sequential Dependent Hydrological Model to perform channel flow and overland flow routings (Liu et al., 2014). A distributed model can be simulated for the transport of water and contaminated sediment in a watershed hydrological system, and applied to a partially forested mountain catchment located in an area highly contaminated by radioactive fallout as in the Kuchibuto River catchment (Kinouchi et al., 2015). A MIKE SHE model can perform as well as global hydrological model and an earlier semi-distributed, conceptual model. SLURP catchment model can be compared with Mac-PDM.09 model and also MIKE SHE when they projected the same direction of change in mean discharge of Mekong River. Therefore, Thompson et al., (2013) proved that , MIKE SHE perform very well in river flow projections. SWAT, is developed by USDA-ARS (Arnold et al., 1998). The hydrological practices can constantly simulated by SWAT for an extensive periods (Abbaspour et al., 2007), as well as a physically based, distributed parameter continuous simulation model. The sub-basins are generated from SWAT fixing with surface flows (Dechmi et al., 2012). The hydrological response units (HRUs) are extracted from each sub-basin, based on topography, land cover, and soil properties. In the study area of the Hoeya River Basin, Korea, the researchers used SWAT and predicted over ten years; the impacts of land demands on water resources, sedimentation, and agricultural chemical loadings in large multiplex river basins with changing soil properties and land demands (Kim et al., 2013). To analyse the impact of climate change on hydrology, particularly on a regional scale, SWAT is a good tool for using and very effective for investigating the impact of climate change. In uncertainty sources on future extreme flows, SWAT is also useful.

In the Lanjiang catchment, East China, SWAT model results indicated that the model performed well through calibration and validation (Zhang et al., 2014).

Table 2.3: Summary of previous studies about simulation of streamflow studies

Author	Year	Research Title	Research Objective	Model
Su Wai Ag	2016	Simulation of Stream Flow Using Soil and Water Assessment Tool (SWAT) in Upper Ayeyarwady Basin	to simulate the stream flow in Ayeyarwady Basin.	SWAT (2003-2013)
Han Thi Oo	2019	Assessment of Future Climate in Upper Ayeyarwady River Basin Using MRI-AGCM3.2S Model	to predict the future climate projection	Linear Scaling -MRI-AGCM3.2S
Han Thi Oo	2019	Assessment of Future Climate Change Projections Using Multiple Global Climate Models	to assess the projections of future climate	Linear Scaling -CanESM2 -CCSM4 -MIROC-ESM-CHEM -CFDL-ESM2G -MRICGCM3
Han Thi Oo	2019	Analysis of Streamflow Response to Changing Climate Conditions Using SWAT Model	to project the future climate impact on streamflow	SWAT Linear Scaling (2003-2013)

2.4 Impacts of Climate Change on Hydrology

There is a wide issue for analysing of the climate change impacts on hydrology. The human activities causing climate change substantially influence on the hydrological cycle. The vulnerability of water resources to climate change is therefore of utmost importance because regional water management is needed in order to understand

potential future water resource changes and water-related disasters particularly on a regional scale and water-related disasters zone (Xu et al., 2013). Cherkauer et al., (2010) pointed out that the quality and quantity of water availability are affected by changes in meteorological parameters resulting in livelihoods, domestic and irrigated water, hydro-energy and ecosystem are devastated. Reduced rainfall causes less inflow leading to a water crisis. Some areas rely on the inflow for their livelihoods, with floods and droughts generally affecting the watershed due to climate change. When the floods impact on the watershed, the infrastructure, agricultural farms, and water supply are deteriorated, creating water shortage problems for farmers and the local population. Water scarcity is also associated with drought, resulting in insufficient water supplies for municipal and irrigation users (Arora et al., 2001).

Most Asian countries have experienced storm water and water shortage frequently over the past decades as a consequence of natural disasters and human activity (Chinvanno, 2004). Regional communities in climate-sensitive sectors are seriously vulnerable to climate crisis especially the farmers, women, children and poor people although climate change is a global issue. Overall, the intensifying sea levels and extreme cold and hot waves have been increasing due to global warming, affecting the water resources of coastal areas (Chinvanno, 2011). The report from the Asian Development Bank (2013) indicates that the most affected disasters are prevalence in the Asia-Pacific countries all over the world. Migration is emerging from disaster affected area to safety area. Therefore, humanitarian crises caused by climate change are expanding. During the past five years alone, natural disasters forced approximately 45 million people in this region leave their homes and that progress is promptly increasing now. In the Asia-

Pacific countries, some people are inhabiting in low-lying coastal zones for their livelihoods and have high risks for sea level rising (Abrishamchi et al., 2005). Investigation of floods for different sectors showed that agricultural production, livelihoods, scio-economics, and the ecosystem were affected and devastated with increasing at least 6% per year in Asia-Pacific countries (Lioubimtseva et al., 2009).

Myanmar Department of Meteorology and Hydrology stated in 2013 that floods and droughts have been rapidly seen over the last six decades. Some area have increasing overall precipitation but some experience declining trend with increasing in mean temperature. Aung et al., (2013) surveyed during early termination in the period 1991-2010 of the south-west monsoon, and late onset. He pointed out that precipitation patterns were changed too much representing extreme weather event as a major crisis which placed Myanmar in seven place globally. The disaster preparedness is very low in the current time and cannot immediately response to the potential impacts (Khin et al., 2000). Representation of disaster risks, the rank of Myanmar is within the world top countries which are experienced in floods, droughts and cyclones in the present (Wang et al. 2013). He studied the vulnerabilities of poor people in the underdeveloped Southeast Asia and reported the 10 % of local people in Myanmar are staying nearby coastal area and affected by tidal waves and sea level rising (between 1-5 m). In the Ayeyarwaddy Delt having more populated farmers, floods are frequently evidence. Myanmar's threat levels are raised dramatically (National Adaptation Programme of Action, 2012).

CHAPTER 3. METHODOLOGY

3.1. Research Methodological Framework

This chapter outlines the summary of methodology applied to complement this study. The detailed methodology to achieve each specific objective is explained in each chapter separately. In general, the aim of this dissertation is to analyse the impacts of climate change on stream flow changes of the Upper Ayeyarwaddy River Basin under two RCP scenarios for the future 2021-2080 period by using SWAT modelling. CMIP5 GCMs are used to predict climate change scenarios under RCP4.5 and 8.5 scenarios for an early-century period 2021 to 2050 (2050s) and a late-century period 2051 to 2080 (2080s). Global future climate data obtained from these GCMs are downscaled using LARS-WG for the six meteorological stations. LARS-WG has been validated against observed meteorological data (daily rainfall and temperature) a specified site to estimate a set of parameters for fitting probability distributions, which is then used to generate synthetic weather time series of a tributary length by randomly selecting values from appropriate distributions. This method can be used confidently for this study because statistical analysis for GCMs model performance at all the observed meteorological stations is well done during the baseline period by using statistical indicators R2 and RMSE. LARS-WG was used in downscaling Tmax, Tmin and precipitation for all stations of the Upper Ayeyarwaddy River Basin to be good agreement in the simulated and observed time series.

The impacts of climate change on water resources of the Upper Ayeyarwaddy River Basin are analysed using SWAT model to show the monthly, seasonal and annual stream flow changes for future periods. The 90 m x 90m resolution of land use map derived from MIMU is used in SWAT model for land use classification. The 7 km x 7

km resolution of soil map in SWAT model is extracted from FAO. The 30 m resolution DEM is used in SWAT model for watershed delineation and subbasins. The indicators of R2 and NSE are measured as satisfactory performance in the SWAT model during calibration (1993-2005) and validation (2006-2018) with 3 year warm-up period. In addition, this research is expected to quantify the uncertainties of climate change projection and stream flow changes due to RCP4.5 and 8.5 scenarios and GCM structures. Figure 3.1 shows the whole methodology applied in this study to achieve all objectives.

3.2. Downscaling of GCM Data

The methodology framework for downscaling as applied to this study is mentioned in Table 3.1.

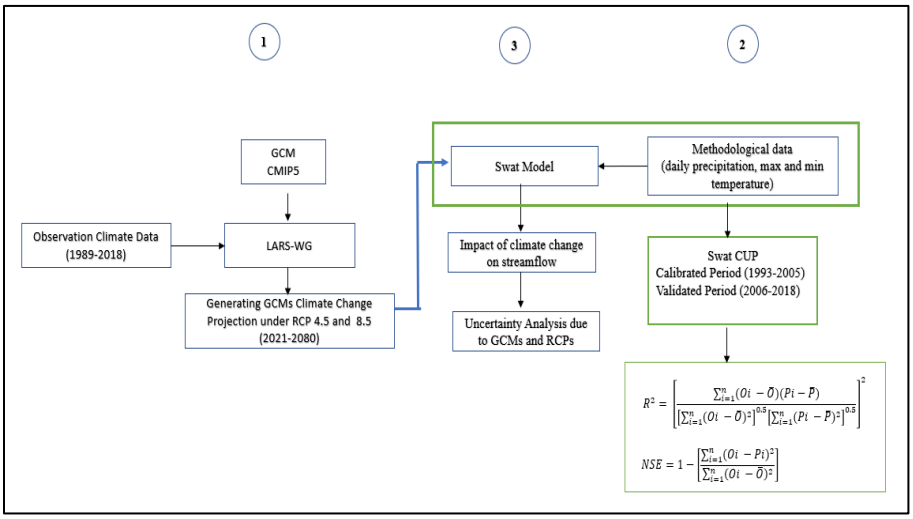

Figure 3.1: Research methodological framework

LARSWG-WG IS used for future climate projections in basin scale of the whole study area. The CMIP5 GCM data are available in ESGF and IS-ENES websites and downscaled with observed meteorological data at six stations. The time series of GCMs

show a bias in duplicating twentieth century meteorological fields and therefore cannot directly be used to input hydrological models in order to appraise the projected climate change impacts on certain constituents of the hydrological cycle. The schematic diagram for LARS-WG is shown in Figure 3.2.

Table 3.1: Methodology for projecting climate change scenarios

Objective	Activities	Tasks Performed	Tool/source
To translate the global scale climate projections to basin level and analyse the uncertainty in future climate projections in the Upper Ayeyarwaddy River Basin	Selection of GCMs	Analysis of GCMs resolution, scenario, and parameters available Data source and data available (daily, monthly)	ESGF IS-ENES
	Selection of Downscaling methods	Performance analysis of GCM downscaling for the study region	LARS-WG
	Basin scale future climate projections	Generated data from 4GCMs for RCP4.5 and 8.5 scenarios for the observation stations	LARS-WG

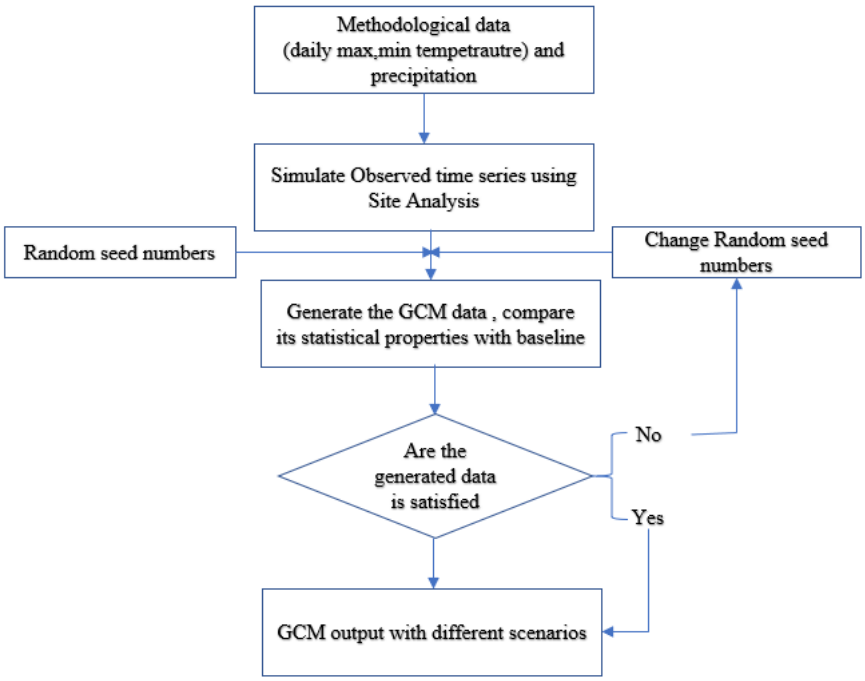

Figure 3.2. The schematic diagram for LARS-WG

3.3 Hydrological Modelling

Advancement of understanding the physical, chemical, and biological processes distressing water quality, coupled with enhancements in the collection and inspection of hydrological data, provide opportunities for significant innovations in the manner and level with which river basin scale processes may be explored and modelled (Fujihara et al., 2008). There are many watershed models which can be grouped into various categories depending on the modelling practices used. Gosain et al., (2010) noted that the main distinctions to perceive watershed-scale modelling approaches include the nature of the employed algorithms such as empirical, conceptual, or physically-based algorithms. On the other side, the modellers use a stochastic or

deterministic approach for model input or parameter specification, and whether the spatial depiction is lumped or distributed. Watershed mathematical modelling is a tool to assess water resources. The present watershed models practically demonstrate the surface water component adequately, but they simplify the groundwater dynamics (Chiew et al., 2010).

3.3.1 Soil and Water Assessment Tool (SWAT)

Srinivasan (1998) and Gosain (2010) proved that SWAT is not required more calibration and thus can be used ungauged in large and varied watersheds. A HRU is defined as the basic spatial unit for the simulation of hydrological components and water allocation for surface, soil, and ground water. Each HRU in a subbasin provides flow generation, sediment yield, and non-point source loading and then the resulting loads are routed through channels, ponds, and reservoirs to the watershed outlet (Jayakrishnan et al., 2005). SWAT can simulate the hydrological procedures of the entire study area including natural ponds and different land use types. Researchers are using SWAT for predicting the land management and demand impacts on water supply, sediment yields, and agricultural pesticide loads in huge, composite watersheds with differing soil properties, land covers, and management practices over long periods of time. Plant water evaporation is simulated as a linear function of potential ET, leaf area index, and rooting depth, and can be limited by soil water content. Tile drainage occurs when the soil water content exceeds the field capacity. According to Zhang et al., 2014, the nine major components: weather, hydrology, crop growth, sediment, nutrients, pesticides, soil temperature, land management, and bacteria in land phase can be simulated by SWAT. Arnold, et al., (2012) stated that Soil Conservation Service (SCS)

in the SWAT model is the modified curve number method which can estimate surface runoff.

3.3.2 Data requirements for SWAT

The Digital Elevation Model (DEM) is an important input parameter for SWAT because topography, landscape, elevation, slope applicable information of the study area, land use, land cover, soil types, hydrological, and meteorological data are to be provided. The physical characteristics of the basin as well as the direction of flow is determined by DEM. DEMs are based on airborne interferometric synthetic built structures and vegetation (Liu et al., 2014). Automatically the digital terrain model can solve the hydrographical network and can be produced via a map. Other important data includes land use and soil because these significantly influence the stream flow. To delineate the basin, DEM is required in an Arc-info grid format. The stream network is generated based on the threshold area. The threshold value for land use, slope, and soil is defined by limitation of the number of HRUs. After HRU processing, weather data is used for input. At this step, different methods of rainfall-runoff routing, channel water routing, potential evaporation define setting of the basic model with default methods and properties. On the basis of its topographical features, the basin is delineated and subdivided into a number of subbasins in SWAT modelling. The schematic diagram for SWAT below shows the steps of systematic model running. Sensitive parameters will be identified for sensitivity analysis for stream flow, sediments etc. The sensitivity parameters are optimised for model calibration. The land use, slope, and soil properties are classified to determine the land use, soil, and slope combination for different subbasins.

3.3.3 Hydrological modelling using SWAT

The schematic diagram for hydrological modelling using SWAT is shown in Figure 3.2. The characteristics of slope, subbasin areas, length of rivers and longest flow paths, etc obtained by using DEM data into SWAT model. Watershed delineation is atomically done on the basis of the topographic characteristics and then subbasins are appeared. The sensitivity analysis is needed to perform the best sensitive parameters for stream flow based on this research. In SWAT model calibration, optimazation of the parameter values are important. In validation, this calibrated model will be run for an independent time interval.

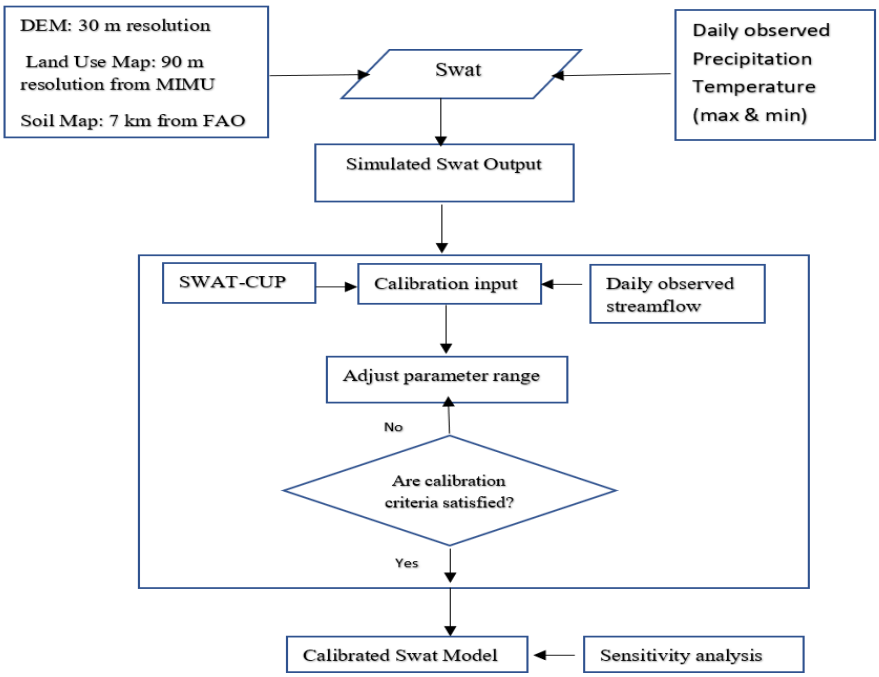

Figure 3.3. Schematic diagram for SWAT modelling

3.3.4 SWAT Model performance evaluation

In statistical analysis, there are many kinds of error parameters such as efficiency index (EI), standard deviation, root mean square error (RMSE), mean absolute error (MAE), Nash Sutcliffe Efficiency (NSE), percent volume error (PVE), percent bias (PBIAS), correlation of determination (R2) etc. for testing and accuracy assessment of the SWAT model. R2 determines the agreement between predicted and observed variables. NS shows the goodness of fit of observed and simulated data with 1:1. PBIAS evaluates whether the simulated data tends to be larger or smaller than the observed values (Strauch et al, 2012). In this study, statistical analysis was checked using NSE and R2 for satisfactory calibration of the parameters. Zhang et al., 2014 stated that NSE and R2 values are greater than 0.6 meaning a perfect match. The following equations show these error parameter formulations. R2 is calculated as

$$R^2 = \left[\frac{\sum_i\left(Q_i^{obs}-Q_i^{mean}\right)-\left(Q_i^{sim}-Q_i^{mean}\right)}{\left[\sum_{i=1}^{n}\left(Q_i^{obs}-Q_i^{mean}\right)^2\right]^{0.5}\left[\sum_{i=1}^{n}\left(Q_i^{sim}-Q_i^{mean}\right)^2\right]^{0.5}}\right]^2 \qquad 4.3$$

NSE is defined by

$$\mathrm{NSE} = 1 - \left[\frac{\sum_{i=1}^{n}\left(Q_i^{obs}-Q_i^{sim}\right)^2}{\sum_{i=1}^{n}\left(Q_i^{obs}-Q_i^{mean}\right)^2}\right] \qquad 4.4$$

Where Qi^{obs} is the measured daily stream flow, Qi^{sim} is the simulated daily stream flow of the given year and Qi^{mean} is the average daily stream flow for the simulation period and n is the number of daily stream flow values.

3.4 Analysis of Climate Change Impacts on Hydrology

After calibration and validation of the SWAT model, analysis of future climate change impacts on hydrology and water resources can be done in the Upper Ayeyarwaddy River Basin. The analysis was completed for the Upper Ayeyarwaddy River Basin as well as for the six meteorology stations: minimum and maximum temperature and precipitation downscaling with LARS-WG for all stations in the Upper Ayeyarwaddy River Basin was used for evaluating the hydrological parameters and stream flow in the subsequent spells. The other needed data such as solar radiation, relative humidity, and wind speed could not collected in this basin due to lack of available skilled technicians and staff in the area.

In this study, to detect the impacts of climate change on hydrological parameters, the following indices simulated by different GCMs and emission scenarios (RCP4.5 and 8.5) were considered. The uncertainty of future seasonal and annual stream flow changes under different scenarios was calculated using the following indicators:

- Average changes in annual stream
- Average monthly changes in stream flow
- Average seasonal stream flow changes

CHAPTER 4. STUDY AREA AND DATA

4.1 Geographical Characteristics

This study was conducted in the Upper Ayeyarwaddy River Basin. The Ayeyarwady is the largest river in Myanmar stretching about 2,170 km long and covering a basin of 413,710 km². The Ayeyarwady River Basin is Myanmar's most economically important area with the population about 39.5 million people. The Ayeyarwady River runs through the country from south eastern Himalayas to the Andaman Sea in the Bay of Bengal. The whole river system is divided into two parts; the upper river basin which consists of central dry zone and the lower river basin which consists of tropical dry forest zone. About 91% of the basin is situated in Myanmar, while the rest is in Chinese (5%) and Indian (4%) territories. The changes of climate have vital impacts on water resources in the Upper Ayeyarwady River Basin. The 169,917 km2 upper basin area lies within latitudes 20˚22'- 28˚50' N and longitudes 94˚56'- 98˚42'E and 13 subbasins will be included in this study area. A location map of the Upper Ayeyarwaddy River Basin is shown in Figure 4.1.

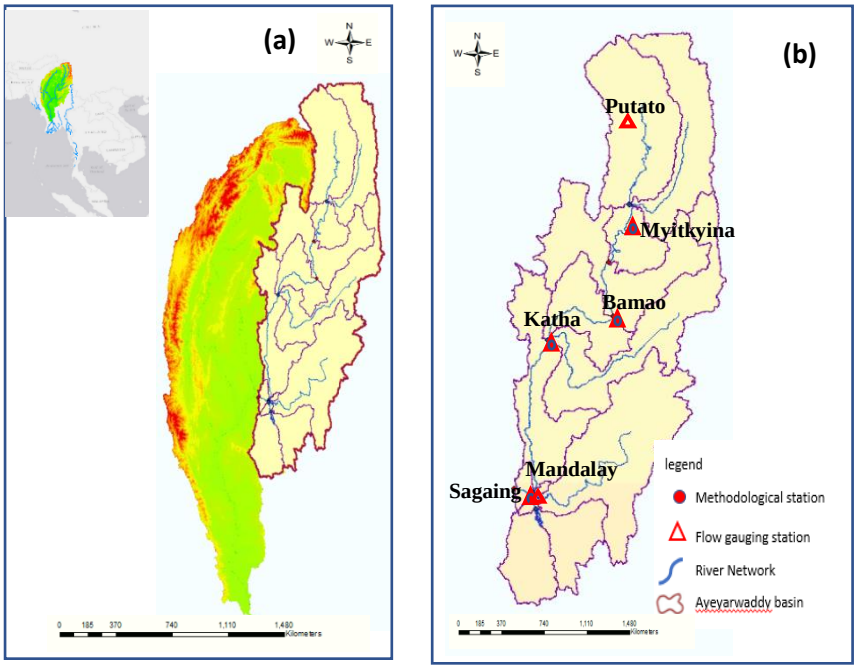

Figure (4.1) : Study area (the Upper Ayeyarwaddy Basin) (a) location of the basin (b) delineated watershed and methodological stations

The Upper Ayeyarwaddy River Basin has (<750 masl) in lower elevation of lower proportion and (>750 masl) in higher proportion of higher elevation. This study area has six meteorological stations (Putato, Myitkyina, Bamo, Katha, Mandalay and Sagaing) and only four hydrological stations (Myitkyina, Bamo, Katha and Sagaing) located beside the main river for stream flow data.

4.2 Demography of the Ayeyarwaddy River Basin

The Ayeyarwaddy River Basin is surrounded by the most vulnerable environments in Myanmar and is a repository of biodiversity, rivers, and many ecosystem services. According to a government survey, the total population of the Ayeyarwaddy River Basin was 36.1 million and population density is 73

people/km^2. The local people rely on the water resources of this watershed for their livelihoods of fishing and seasonal farming. Farmers represent 40% of the local population, farming over 89 thousand hectares of annual farms (Minister of Irrigation, 2012). Fishermen comprise 30% of the population, 20% are traders, while the rest are in government service. Most of the local people have a poor living standard because of their low GDP (almost 2 USD). Water scarcity during the dry season and annual floods are the biggest challenges in the Ayeyarwaddy River Basin (Thiam and Yee, 2004).

4.3 Meteorological Data

The daily precipitation and temperature regimes of all the meteorological stations (Figure 4.1) used in this study for the period of 1989-2018 are as shown in Table 4.1. The daily time series data of precipitation, temperature, and stream flow were acquired from Department of Meteorology and Hydrology (DMH), Myanmar. The data availability period of the four hydrological stations is also shown in Table 4.1. These four stations also generally measure the water levels of the Ayeyarwaddy River. The data availability period of the hydrological stations is also shown in Table 3.1. Whenever the River reaches high flood level of 8.7 m, the DMH station records every 3 hours and reports to the Department of Irrigation. If it exceeds the danger level (9.2 m), the water level is recorded every hour.

Table 4.1: Statistics of meteorological and hydrological parameters at DMH stations in the Upper Ayeyarwaddy Basin

Station	Latitude	Longitude	Elevation (m)	Avg annual Rainfall (mm)	Avg Tmax (°C)	Avg Tmax (°C)	Avg annual streamflow (m^3/s)
Putato	27.3094	97.4173	409	334.194	13.9	9.8	-
Myitkyina	25.3618	97.3959	142	247.603	19.7	12.6	4470
Bamo	24.2619	97.1993	89	174.465	31.9	26.2	5935
Katha	24.1277	96.3160	103	184.705	32.1	19.1	4819
Mandalay	21.9431	96.0578	71	79.3	35.3	27.8	-
Sagaing	21.9218	95.9635	920	68.382	32.9	22.7	6989

According to meteorological records, January and December are the coldest months, whereas April is the hottest month. Table 3.1 illustrates that Bamo, Katha Mandalay and Sagaing stations have slightly greater average maximum temperature. All stations experience one big peak of maximum temperature and minimum temperature in April as shown in Figure 4.2. The basin scale average

annual values for maximum and minimum temperature are 35 ºC and 27ºC respectively.

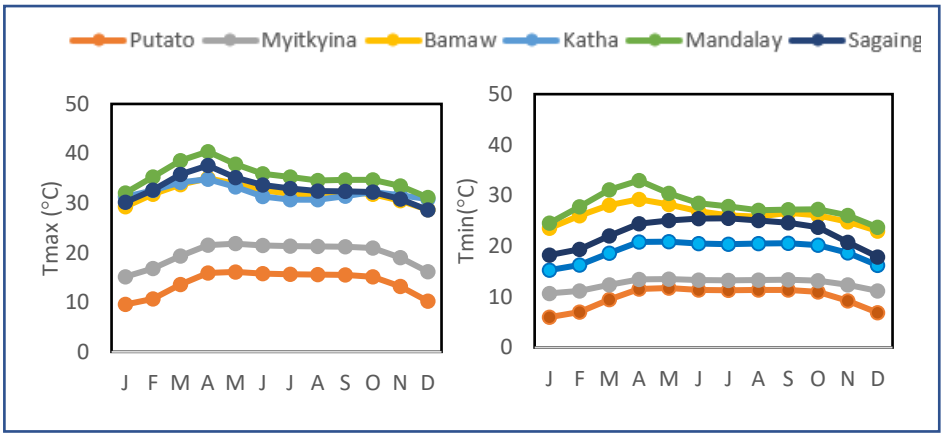

Figure 4.2: Distribution of average monthly Tmax and Tmin at all the meteorological stations in the Upper Ayeyarwaddy River Basin for 1989-2018 (the baseline period)

Figure 4.3 shows the average annual maximum and minimum temperature for all stations during 1989-2018. Analysis of time series data showed that in 1998 the Mandalay station was the hottest for both maximum and minimum temperatures during the baseline period for the whole basin. However, taking spatial variability into account the annual range will be less in the south compared to the north because the upper basin is located further inland than the lower. The basin scale average maximum temperature peaks in April to 40 ºC and plunges down in July to 29.4 ºC. Increases in temperature have a significant influence on water supply in the region.

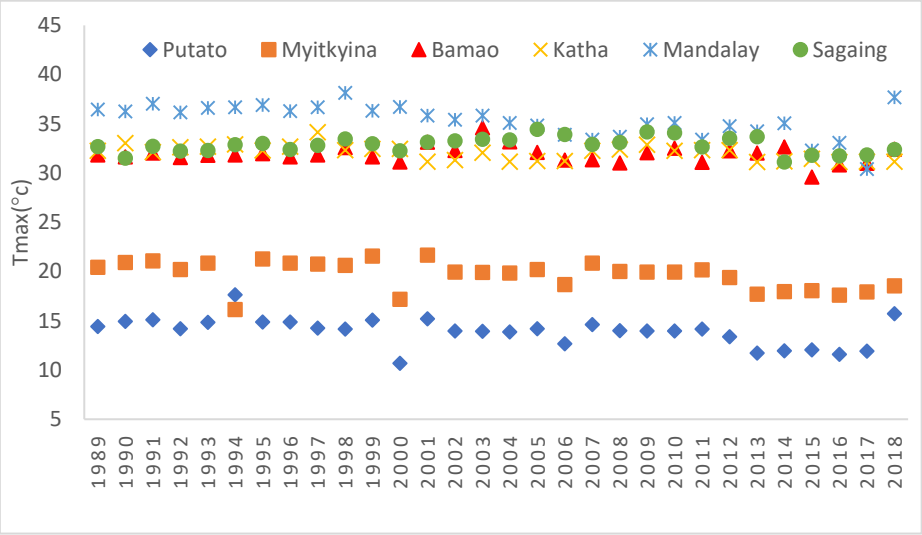

Figure 4.3(a). Distribution of average maximum temperatures at all the meteorological stations in the Upper Ayeyarwaddy River Basin

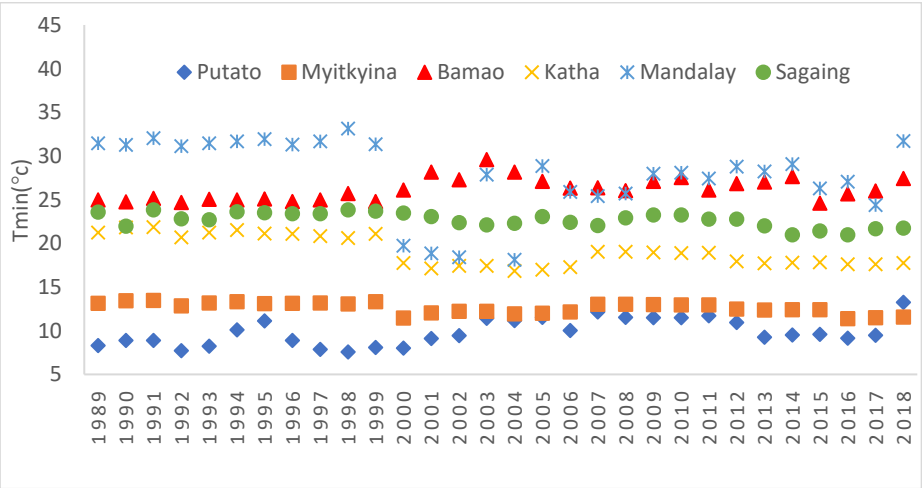

Figure 4.3(b). Distribution of average minimum temperatures at all the meteorological stations in the Upper Ayeyarwaddy River Basin

During the last 30 years from 1989-2018, July has been the wettest month in the whole basin (Figure 4.4). Table 4.1 illustrates that the Putato station, with an average annual precipitation of 334 mm, is the wettest location. Figure 4.4(b) shows average annual precipitation for all stations during 1989-2018 and the Putato station was also the wettest station in 2001. The highest average annual precipitation of 17 mm occurred in 2001 for the whole basin scale. Within the baseline period, the monthly distribution of precipitation is directly related to the southwest monsoon. On the other hand, January to March are the driest months. The prevalence and magnitude of extreme events have gradually increased over the last ten years. Extreme events are more challenging than the gradual changes in this area. Floods and droughts change livelihoods when extreme climate events occur concurrently.

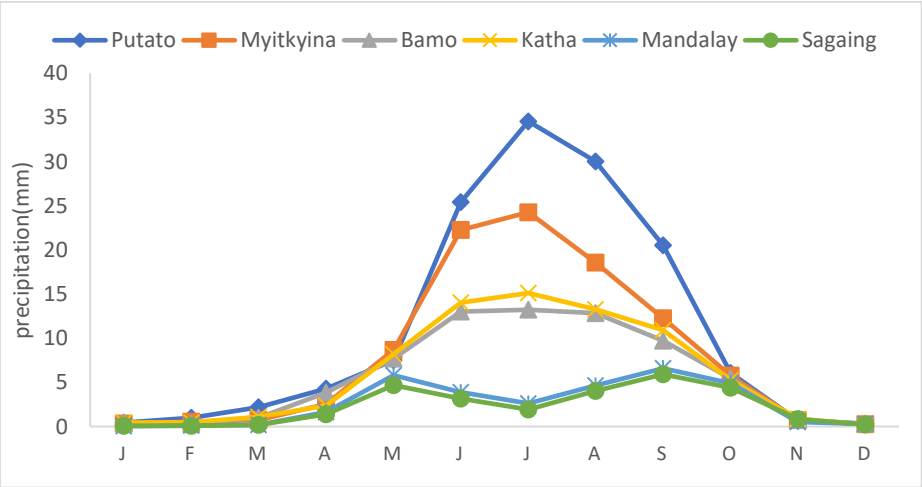

Figure 4.4 (a) : Distribution of average monthly precipitation for all the meteorological stations in the Upper Ayeyarwaddy River Basin

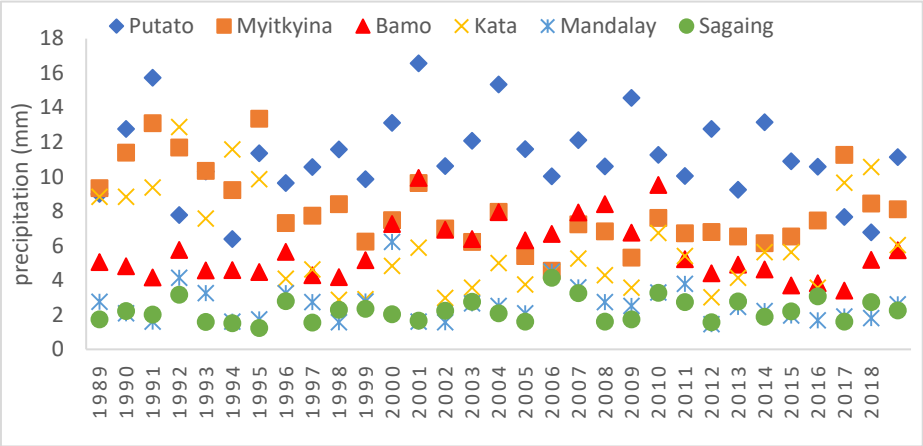

Figure 4.4 (b): Distribution of average annual precipitation at all the meteorological stations in the Upper Ayeyarwaddy River Basin

The floods in the Upper Ayeyarwaddy River generally occur during the monsoon season. In some years, although above-normal annual precipitation was the main cause of floods in the Ayeyarwaddy River, it did not correspond with floods of the whole River Basin.

4.4 Hydrological data

Most of High flows occur in July except Sagaing station. The low flows can be seen in January, February, March, April, and December. The period of stream flow data availability for the four stations is mentioned in Table 4.1. According to Department of Human Settlement and Housing report (2013), the local people in flood prone area of Upper Ayeyarwaddy are always affected by seasonal floods every year.

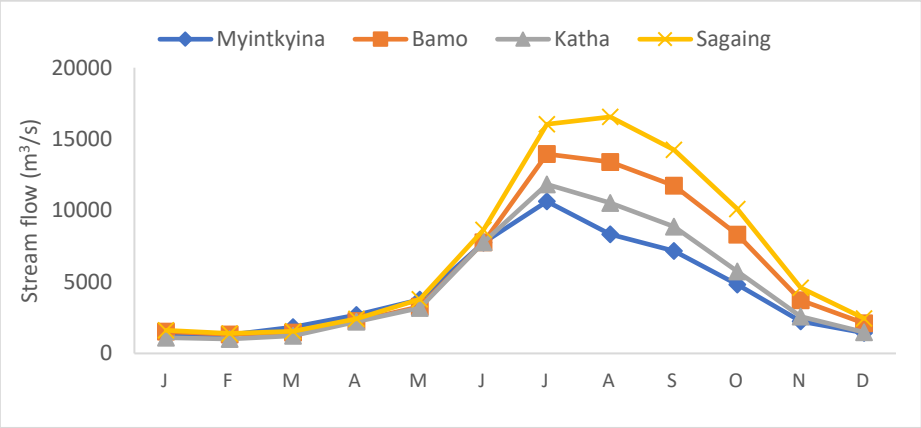

Figure 4.5 (a): Distribution of average monthly stream flow at all the stream flow stations in the Upper Ayeyarwaddy River Basin for 1989-2018 (the baseline period)

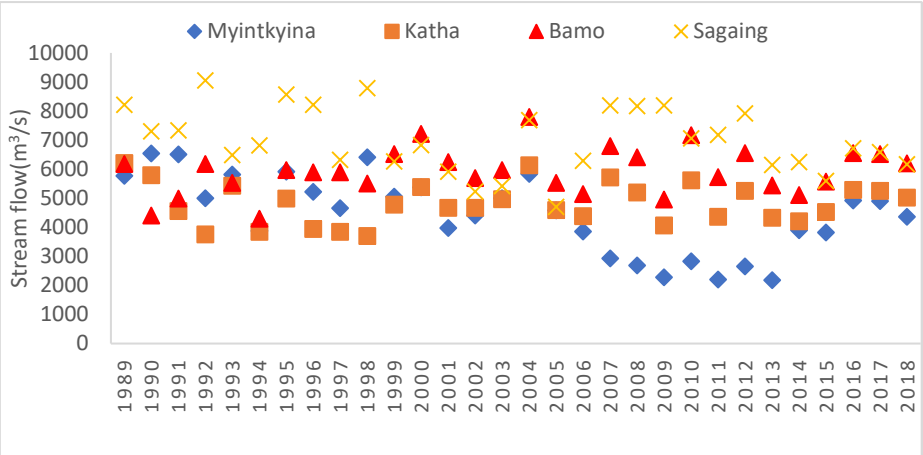

Figure 4.5 (b): Distribution of observed annual average stream flow at all the stream flow stations in the Upper Ayeyarwaddy River Basin for 1989-2018 (the baseline period)

Comparison of the four stations shows that the average monthly stream flow at Sagaing is greater than the other stations. However, at the beginning of year until March, average monthly stream flow is almost the same as shown in Figure 4.5 (a). The distribution of observed annual average stream flow from Sagaing is shown to be higher than other stations until 2013.The stream flow has changed in the Myitkyina station after 2004 until 2013 (Figure 4.5(b)).

4.5 Future Climate Data

The future climate data in this study was downloaded from ESGF (Earth System Grid Federation), IS-ENES, and Climate4impactportal websites. Four GCMs included in the Coupled Model Intercomparison Project Phase 5 (CMIP5) were considered in this study as shown in Table 4.2. These GCMs cover different resolutions, varying from 1.1215 x 1.1215 º to 1.8653 x 1.875 º, and come from different climate centers around the world and have vintage after 2010. The future climate projections derived from these RCP4.5 and 8.5 scenarios represent updated research for climate change. For the IPCC AR5, simulations from the new generation of state-of-the-art global climate models are available for analysis within the CMIP5 (Taylor et al., 2012).

Table 4.2: GCMs with a brief indication of their origin, resolution, and the number of realisations available for each climate change scenario

No	Centre	Country	GCM	Resolution
1	European Centre for Medium Range Weather Forecasts	Europe	EC-EARTH	1.1215 x 1.1215 º
2	UK Met Office	United Kingdom	HadGEM2-ES	1.25 x 1.875 º
3	Meteorological Research Institute	Japan	MIROC5	1.4008 x 1.40625 º
4	Max-Planck Institute for Meteorology	Germany	MPI-ESM-MR	1.8653 x 1.875 º

4.6 Spatial Data from the Study Area

The spatial data needed to develop a physically based hydrological model includes: the Digital Elevation Model (DEM), land use, and soil. There are many available global sources for this data. DEM is important for the SWAT model for good watershed delineation and sub-basins because it can be used effectively as input data particularly for climate change, environmental impacts, hydrological modelling, and geographical studies (Zhang et al., 2014). Generally, spatial resolution of 30 m × 30 m DEM derived from SRTM (earthexplorer.usgs.gov) is used to run the SWAT model. Some researchers also use 90 m resolution DEM downloaded from, gdex.cr.usgs.gov/gdex and gdem.ersdac.jspacesystems.or.jp websites. This study used 30m resolution DEM for the whole basin created from topographical and channel survey maps by using certain steps as shown in figure 4.6 (a). The first step creates elevation data for the whole basin by geo-referencing and digitizing channel survey maps provided by the

Directorate of Water Resources and Improvement of River Systems (DWIR) and topographical maps (published in 1944 by the Burma Survey Bureau) with the aid of ArcGIS. Obtaining more elevation points can support more accurate DEM. In addition, ArcMap10.3 software was used to create 30 m resolution of the DEM form to produce elevation points together with streams, counter lines, water bodies, and boundaries.

Many researchers use the Moderate Resolution Imaging Spectroradiometer (MODIS) land cover map (http://reverb.echo.nasa.gov/reverb) and global land use data from the European Space Agency (ESA). In this study, land use map was developed from 90 m x 90m resolution raster data with a projection of WGS_1984_Zone_47N from Myanmar Information Management Unit (MIMU) using image processing for 2020 latest updated. This study area has been classified into four major land use class namely 38.8% of Evergreen forest, 22.5 % of Deciduous forest, 16.2% of Agriculture and 22.5%of Scrubland as shown in figure 4.6(b).

For a soil map, the Digital Soil Map of the World (DSMW) was produced for the whole basin. The DSMW consists of ten map sheets: Africa, North America, Central America, Europe, Central and Northeast Asia, Far East, Southeast Asia, and Oceania. The maps can be downloaded in three different formats: one vector format (ARC/INFO Export) and two raster formats called ERDAS and IDRISI (or flat raster) formats. This soil map has 1: 5000,000 resolution scales with good quality and soil maps were also acquired from the SOTER website (http://eusoils.jrc.ec.europa.eu/). 7 km x 7 km resolution of Soil map is downloaded from the Food and Agriculture Organization of the United Nation (FAO) for this study. As per DSMW, only six major classes of soil were found in the Upper Ayeyarwaddy River Basin as shown in Figure 3.6. The dominant soil types

are 19.7% of Mountainous brown forest (Ao89-2-3b-4282), 10.7% of Red brown forest (Ao76-2-3c-4276), 4.1% of Red earth and yellow earth (Gh16-2-3a-3766), 49.2% of Meadow and meadow alluvial (Ao90-2-3c-4284), 15.8% of Savanna(Lc12-2-3a-3766) and 0.5% Mangrove forest(Vp40-3a-4426) as shown in Figure 4.6 (c) and Table 4.3. The properties of different soils are defined by depth, appearance, and hydraulic conductivity.

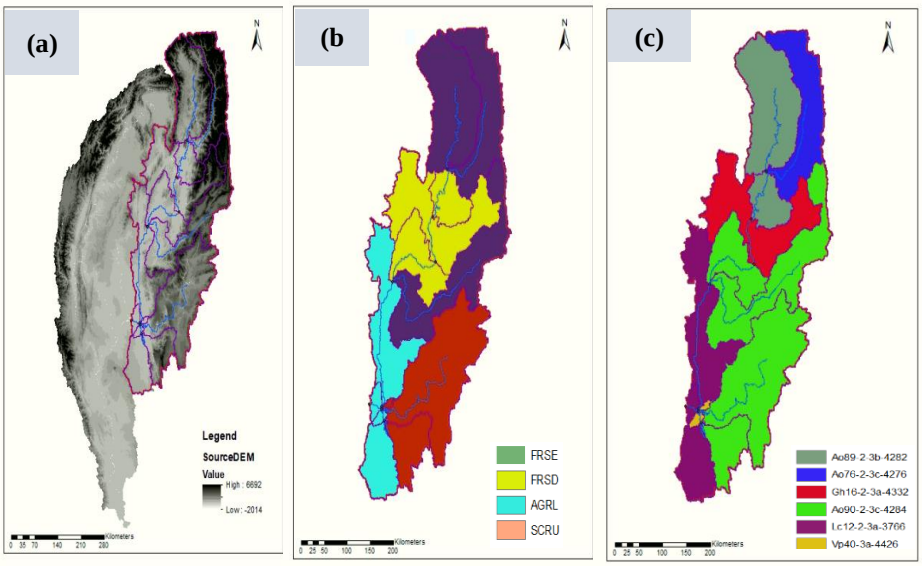

Figure 4.6 : Model input data (a) Digital Elevation Map (DEM) (b) Land Use Map (c) Soil Map of Upper Ayeyarwaddy Basin

CHAPTER 5. RESULTS AND DISCUSSIONS

5.1 Performance of LARS-WG Model

The performance of the LARS-WG model was assessed against the observed data (precipitation, daily Tmin and Tmax) for the baseline period (1989–2005) using mean monthly bias and coefficient of determination (R2) as objective functions. The mean monthly biases for Precipitation, Tmin and Tmax, for all the six stations are used in this study. The figure 5.1 compares observed data and bias correction GCM data by LARS-WG for average monthly precipitation, Tmax and Tmin at six stations in the period from 1989 to 2018. Overall, average monthly precipitation and temperature after bias correction are closer to the observed data and has the best pattern which are match well with observed data. Mean , R2 and RMSE were calculated with monthly average values of observed and simulated data for all six stations as described in Table 5.1. The R2 value is above 0.9, RMSE value is closer to 1 and mean value of simulated precipitation, Tmin and Tmax are close to the observed value for all the station. The mean monthly values and the temporal distribution of Precipitation, Tmin and Tmax simulated by the model for the baseline period are in close agreement with the observed values for all stations. These results indicate that LARS-WG can reliably simulate precipitation, Tmin and Tmax at all the stations and thus is an appropriate tool for downscaling.

(b) Putato

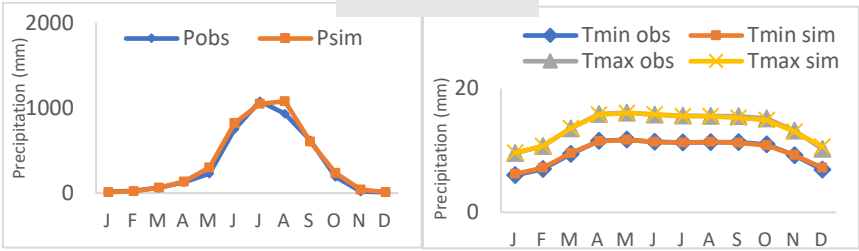

(a) Myitkyina

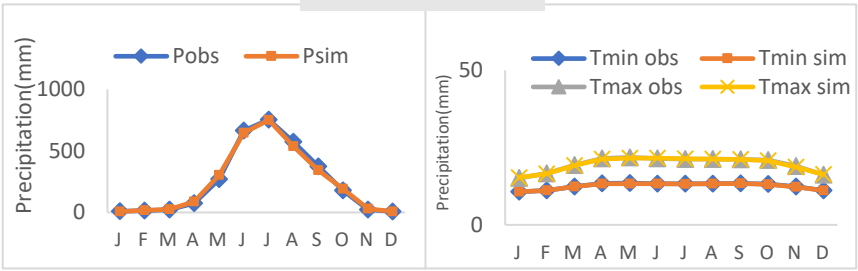

(c) Bamo

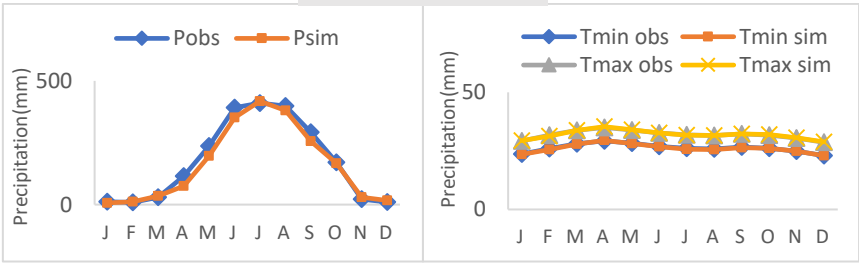

(d) Katha

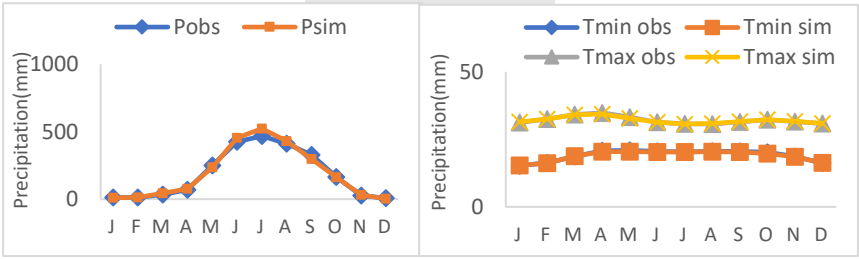

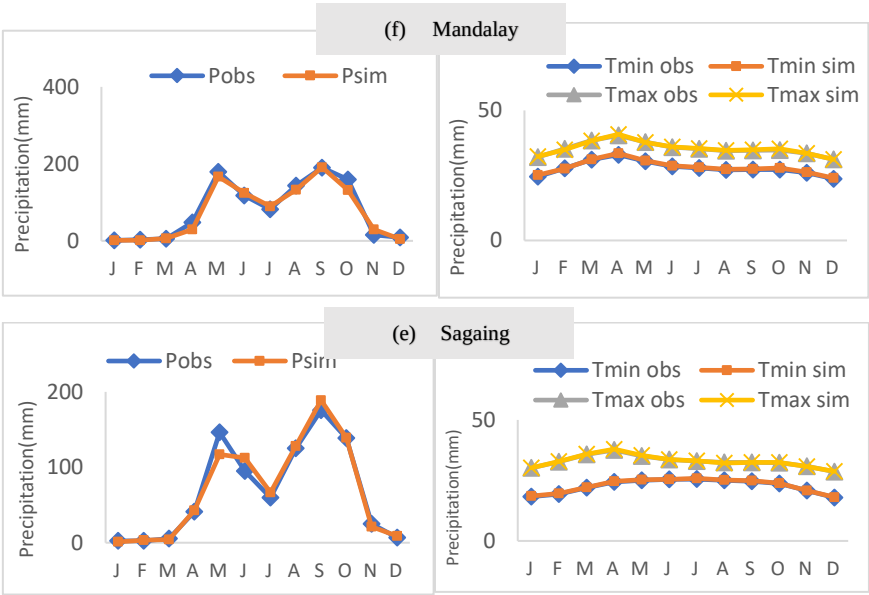

Figure 5.1 : Observed and LARS-WG simulated historical precipitation, Tmin and Tmax for the baseline period (1989-2005) in the Upper Ayeyarwaddy River Basin

Table 5.1: Summary statics of observed and simulated data at six stations in the Upper Ayeyarwaddy River for the baseline period 1989-2005

Stations		Precipitation (mm)		Tmin (°C)		Tmax (°C)	
		Obs	Sim	Obs	Sim	Obs	Sim
Putato	Mean	339.05	364.97	9.845	9.898	13.92	13.88
	R^2	0.993		0.999		0.998	
	RMSE	27.7956		0.1417		0.1627	
Myitkyina	Mean	247.13	245.53	12.59	12.54	19.65	19.59
	R^2	0.998		0.998		0.998	
	RMSE	18.88		0.0779		0.1455	
Bamo	Mean	174.79	161.84	26.20	26.06	31.91	31.94
	R^2	0.993		0.996		0.994	
	RMSE	23.685		0.2094		0.1967	
Katha	Mean	184.266	190.099	19.087	18.927	32.075	32.027
	R^2	0.994		0.996		0.991	

	RMSE	21.7548		0.2521		0.2346	
Mandalay	Mean	79.5366	75.847	27.889	28.178	35.326	35.397
	R^2	0.988		0.995		0.996	
	RMSE	11.9165		0.366		0.2592	
Sagaing	Mean	68.6666	69.509	22.686	22.873	32.874	32.955
	R^2	0.984		0.999		0.998	
	RMSE	10.8011		0.213		0.1591	

5.2 Future Precipitation Projection

In this section, to understand the variations in temperature, the projected changes in both variables were analysed for two periods: 2050s (2021-2050), and 2080s (2051-2080) relative to the 1989-2005 climatology under the RCP4.5 and 8.5 scenarios. The simulation of average monthly precipitation under RCP 4.5 and 8.5 scenarios can be compared with baseline period of the whole basin. These flowing figures shows the result of future precipitation projection by using EC-EARTH, HadGEM2-ES, MICRO5 and MPI-ESM-MR models for the period of 2050s and 2080s with scenarios RCP 4.5 and RCP 8.5 at Putato, Myitkyina, Bamo, and Mandalay stations.

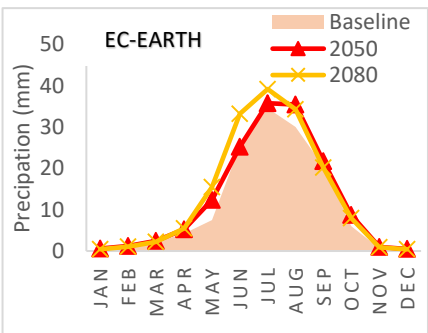

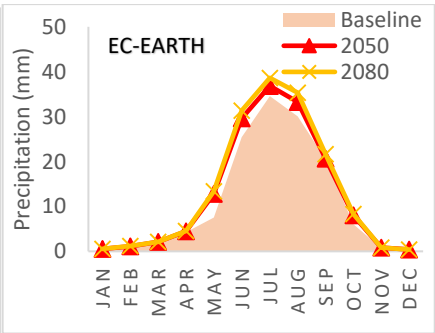

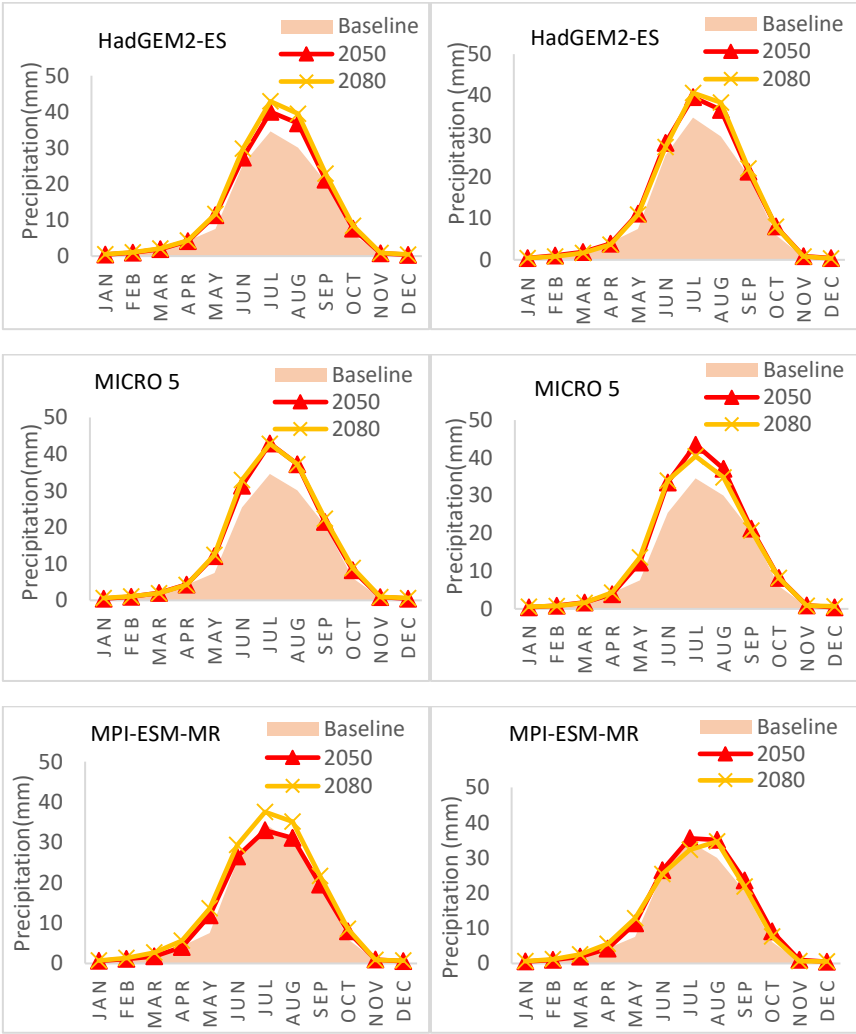

Figure 5.2: Projected future monthly temperature for the periods of 2050s and 2080s with scenarios RCP 4.5 (Left) and RCP 8.5 (right) and baseline period (1989-2018) at Putato Station

The figure 5.2 shows the future average monthly precipitation projected by four GCM Models for the period of 2050s and 2080s with scenarios RCP 4.5 and RCP 8.5 and baseline period (1989-2018) at Putato Station. An overlook is that from January to April, the future average monthly precipitation projected by the both

four GCMs models changes insignificantly compared to the precipitation of the baseline period. For the remaining months, EC-EARTH, HadGEM2-ES and MICRO5 show the upward trends while MPI-ESM-MR changes insignificantly. These trends are clearest in July which is the moth having the highest precipitation in the year.

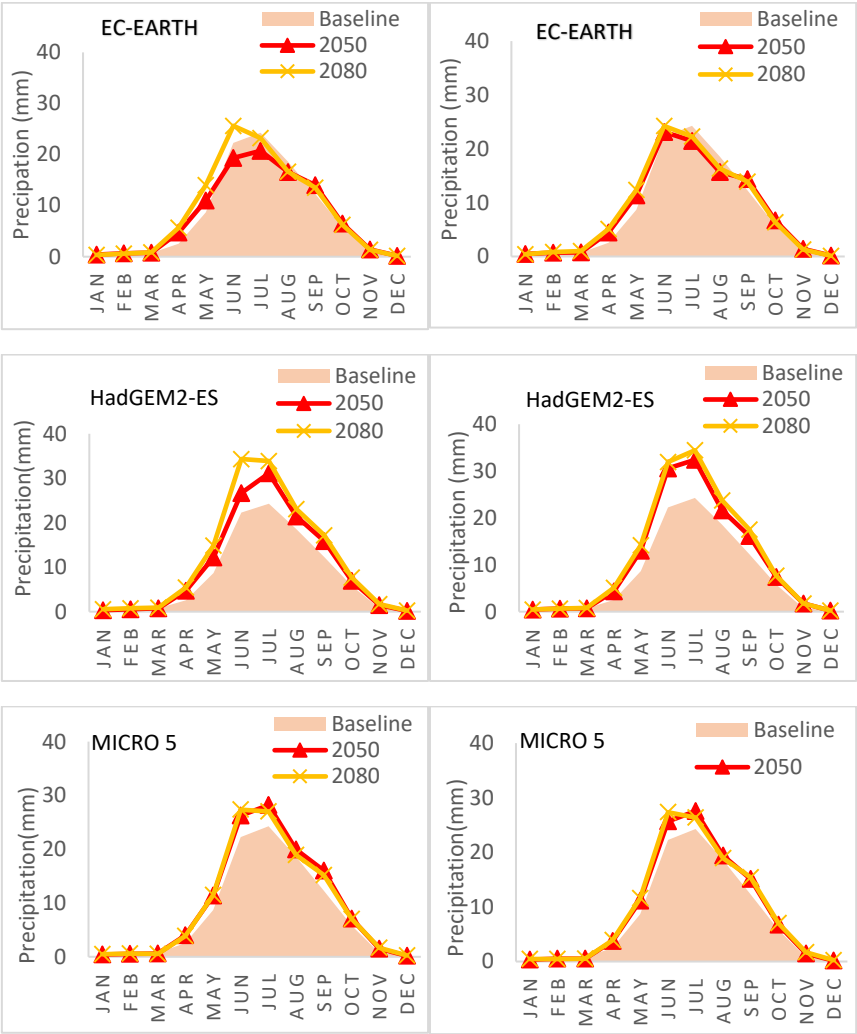

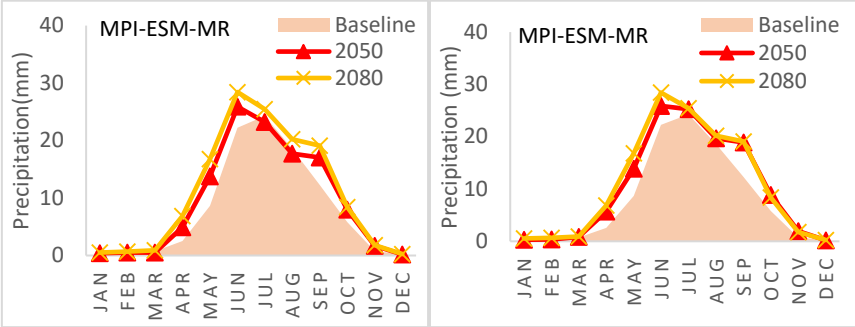

Figure 5.3: Projected future monthly temperature for the periods of 2050s and 2080s with scenarios RCP 4.5 (Left) and RCP 8.5 (right) and baseline period (1989-2018) at Myitkyina Station

The overlook for the figure 5.3 is that from January to March, the future average monthly precipitation projected by the both four GCMs models changes insignificantly compared to the precipitation of the baseline period. These trends are clearest in June which is the moth having the highest precipitation in the year. The trends are slightly increased in EC-EARTH, MICRO5and MPI-ESM-MR while HadGEM2-ES changes significantly for the remaining months.

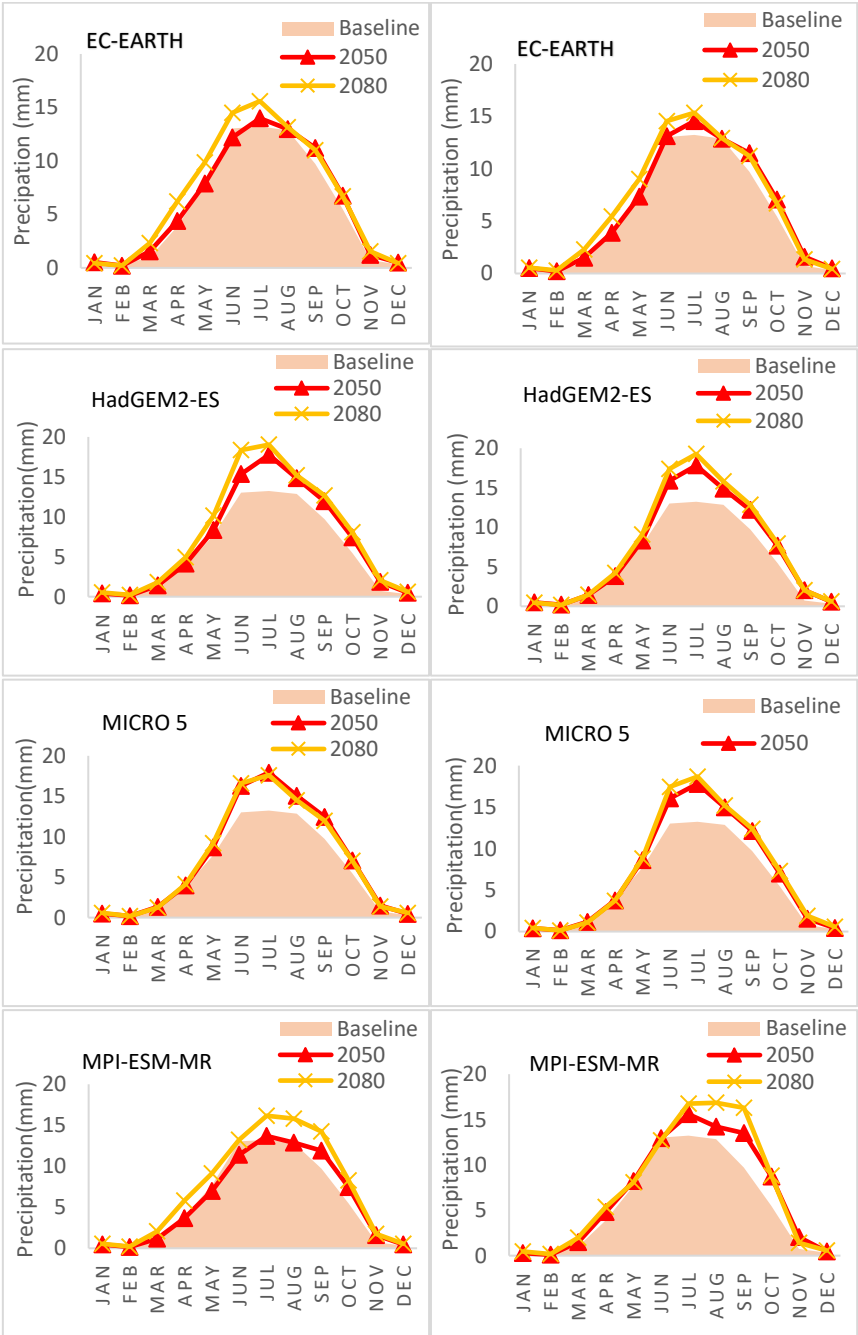

Figure 5.4: Projected future monthly temperature for the periods of 2050s and 2080s with scenarios RCP 4.5 (Left) and RCP 8.5 (right) and baseline period (1989-2018) at Bamo Station

From the above figure (5.4), it can be seen for all the cases, the precipitation changes insignificantly from January to May compared to the baseline period. The trend for EC-EARTH changes insignificantly while the remaining models are significantly increased. The similar result is found for Katha Station.

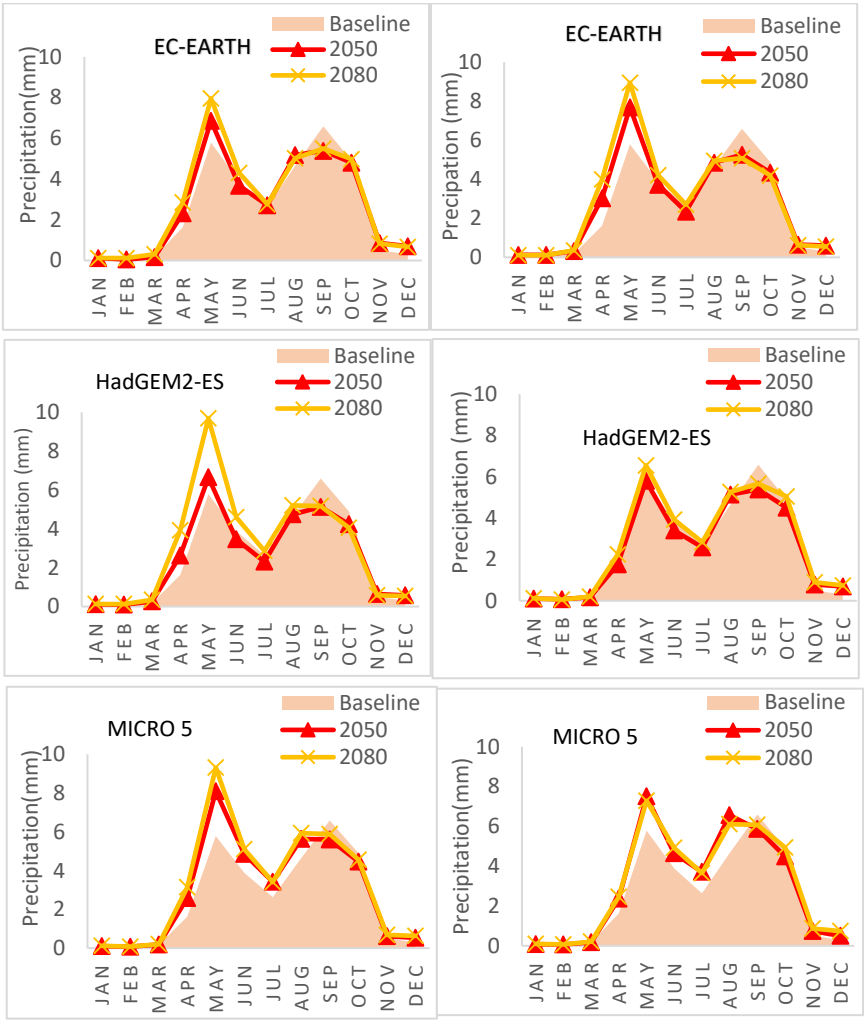

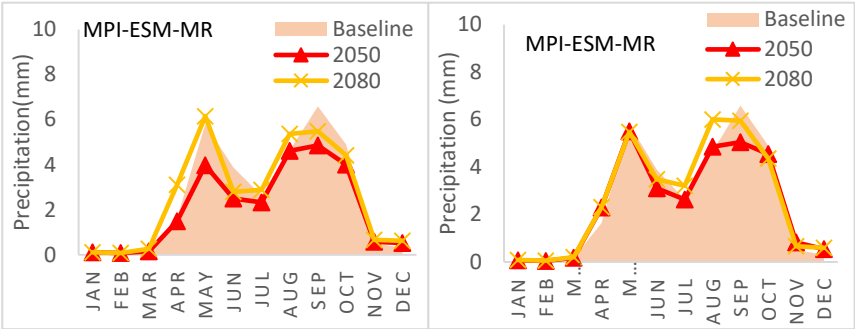

Figure 5.5: Projected future monthly temperature for the periods of 2050s and 2080s with scenarios RCP 4.5 (Left) and RCP 8.5 (right) and baseline period (1989-2018) at Mandalay Station

The figure 5.5 shows the future the average monthly projected for Mandalay station. It is seen that the future average monthly precipitation projected by all GCMs models insignificantly from January to March compared to the precipitation of baseline period. All the GCMs models show the downward trend in September and October. For the remaining months, the trends is significantly increased in EC-EARTH, HadGEM2-ES and MICRO5 models while HadGEM2-ES for RCP 8.5 and MPI-ESM-MR changes insignificantly. The similar result is found for the Sagaing stations.

5.3 Future Temperature Projection

5.3.1 Future Minimum Temperature Projection

The projected changes in temperature can cause considerable shifts in climate regimes over the study area. The changes in temperature will dominate the shift of weather conditions when the strong temperature becomes more pronounced in 2021-2080.

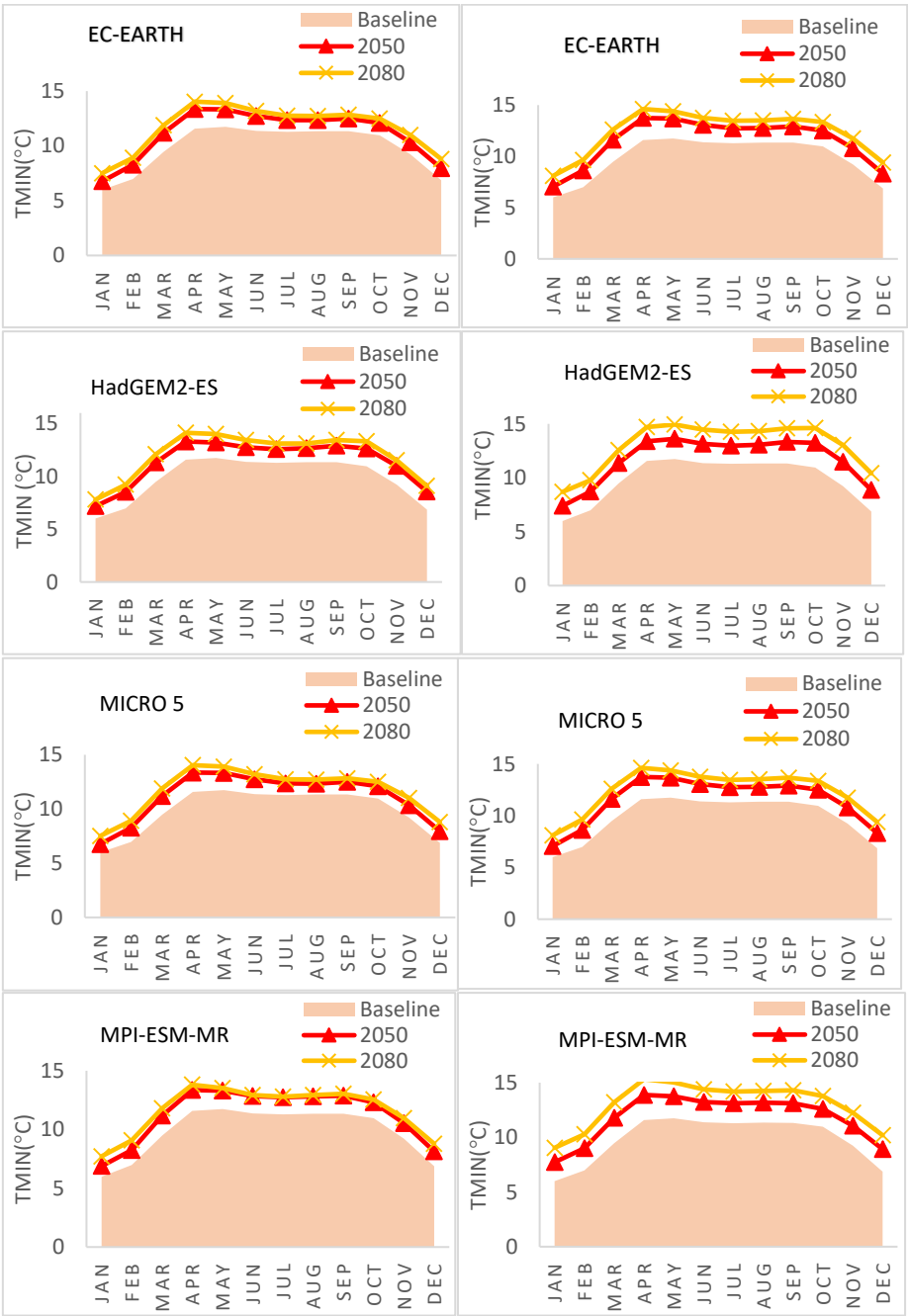

Figure 5.6: Projected future monthly minimum temperature for the periods of 2050s and 2080s with scenarios RCP 4.5 (Left) and RCP 8.5 (right) and baseline period (1989-2018) at Putato Station

In term of visual, the figure 5.6 shows the simulated minimum temperature is projected to be highest in April under both of RCP 4.5 and RCP 8.5 which is slightly increased about 2°C for all the models compared with baseline period. The overall look is that the monthly minimum temperature will be significantly increased in all periods under both RCP 4.5 and 8.5.

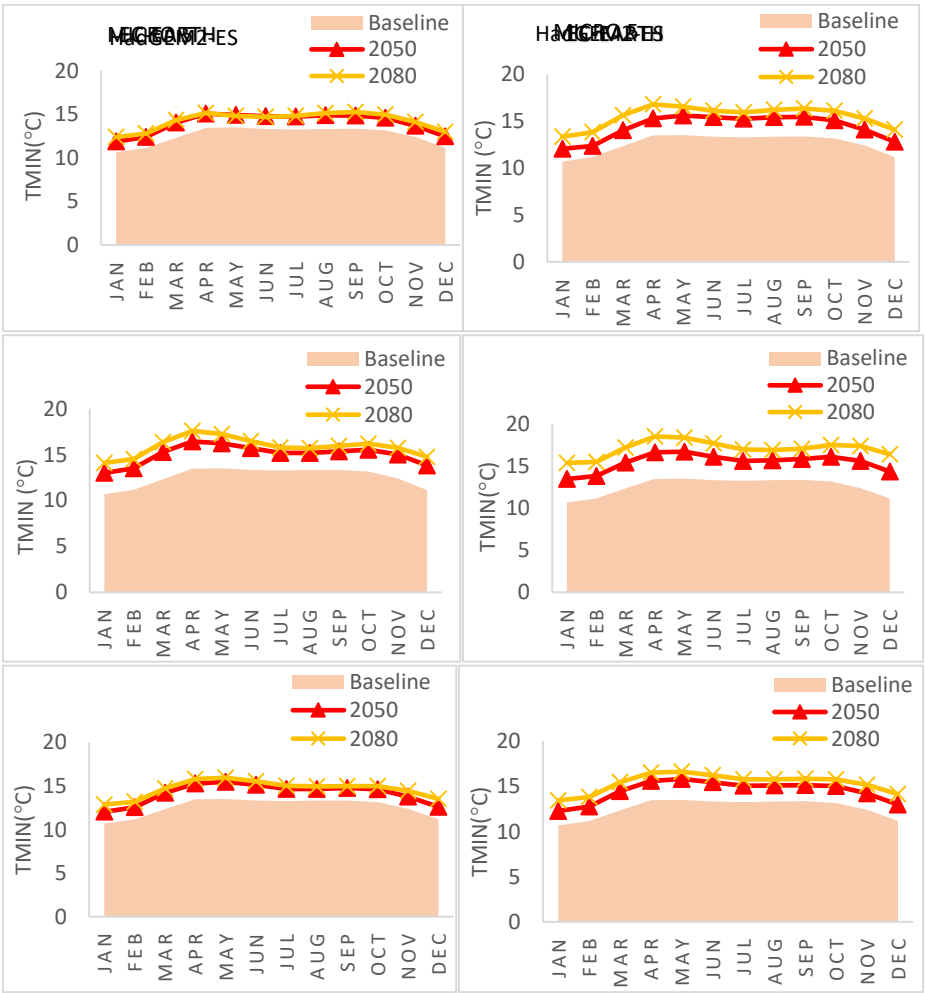

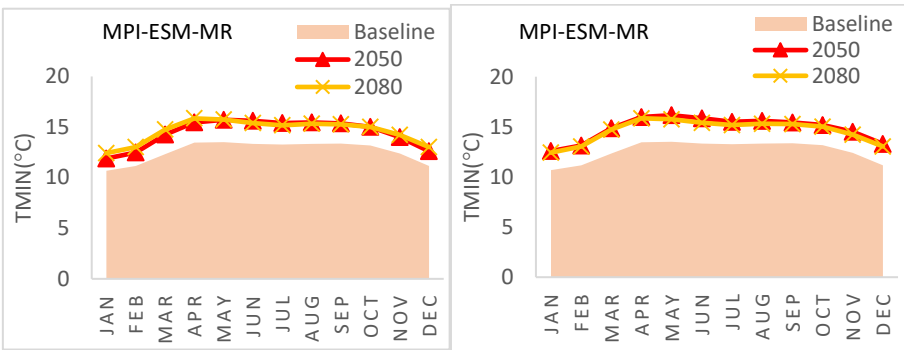

Figure 5.7: Projected future monthly minimum temperature for the periods of 2050s and 2080s with scenarios RCP 4.5 (Left) and RCP 8.5 (right) and baseline period (1989-2018) Myitkyina Station

According to figure 5.7, minimum temperature is projected to be highest in April under both of RCP 4.5 and RCP 8.5 which is slightly increased about 4°C in 2050 s and 2080s for EC-EARTH, MICRO5 and MPI-ESM-MR models while the temperature is increased about 3°C in 3.5°C in 2050 s and 5°C in 2080s HadGEM2-ES compared with baseline period. The overall look is that the monthly minimum temperature will be significantly increased in all periods under both RCP 4.5 and 8.5.

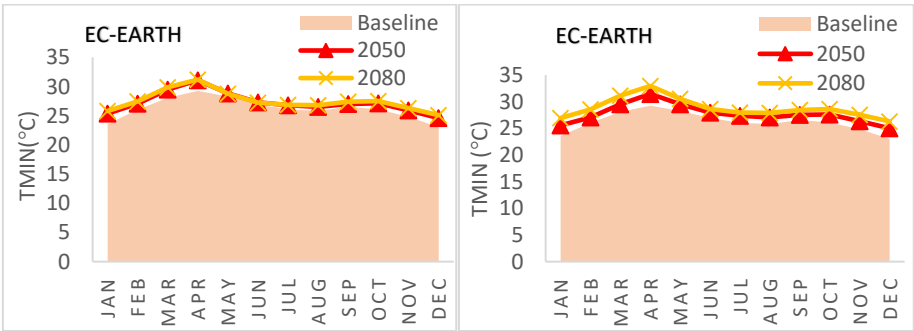

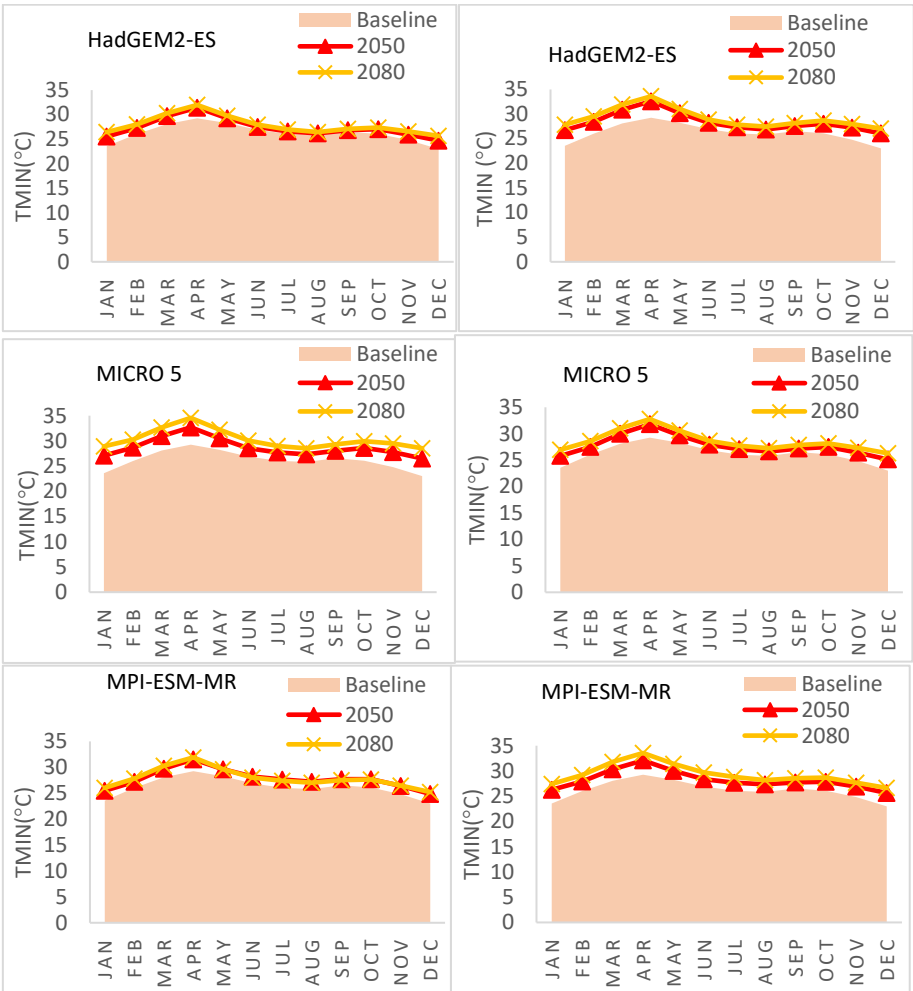

Figure 5.8: Projected future monthly minimum temperature for the periods of 2050s and 2080s with scenarios RCP 4.5 (Left) and RCP 8.5 (right) and baseline period (1989-2018) Bamo Station.

According to the figure 5.8, it can be seen clearly, the minimum temperature is intended to increase until 35°C under both of the scenarios for all models. This station has the similar result with above station which shows highest projected temperature in April and insignificantly increased about 2.5°C in 2050s and 6°C in 2080s compared to

baseline period under both of RCP 4.5 and RCP 8.5. For the remaining months, the temperature is slightly increased than baseline period for all models respectively.

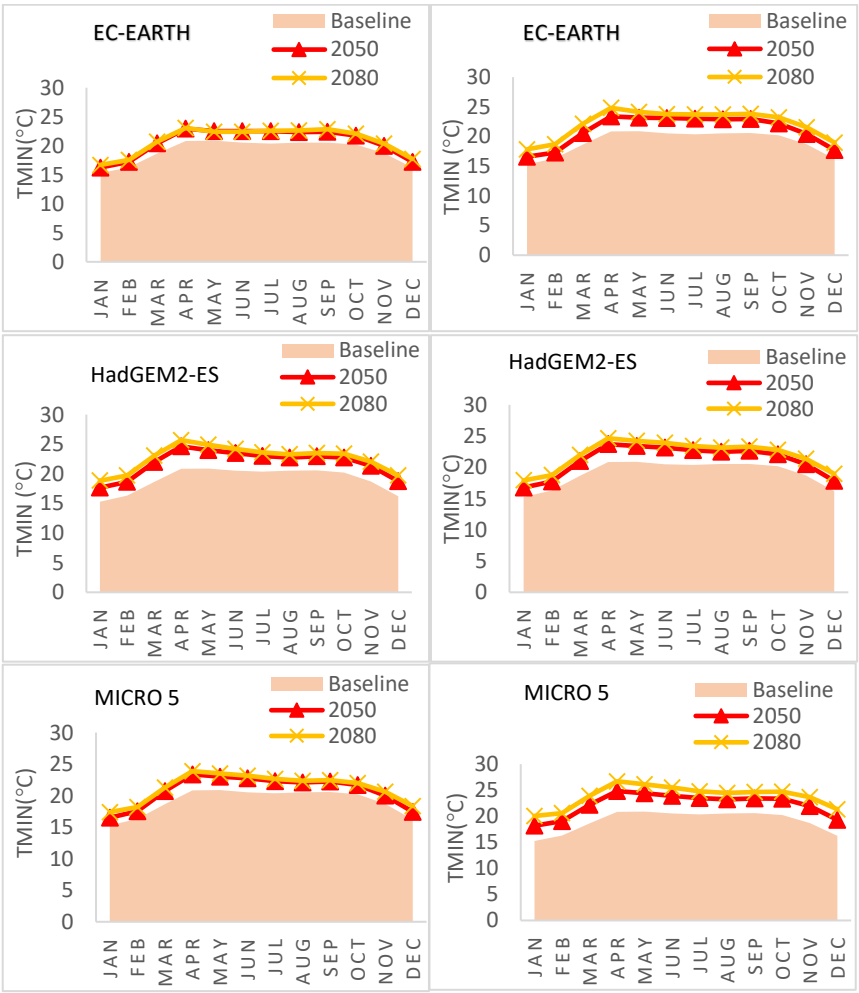

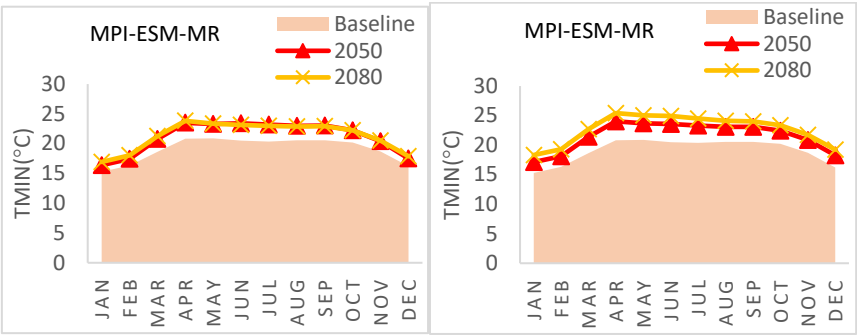

Figure 5.9: Projected future monthly minimum temperature for the periods of 2050s and 2080s with scenarios RCP 4.5 (Left) and RCP 8.5 (right) and baseline period (1989-2018) Katha Station.

An overall look for Kata station is that the highest temperature occurs in April which is increased about 6°C in 2050s and 2080s under RCP4.5 and increased about 2.5°C in 2050s and 6°C in 2080s under RCP 8.5 for all models. For the remaining months, all the models change slightly compared with the baseline period.

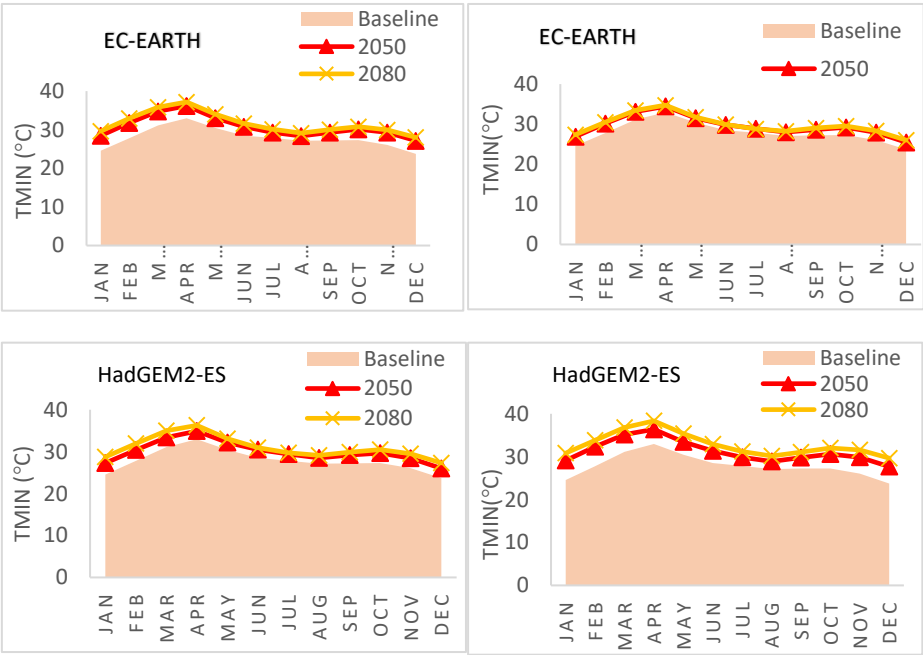

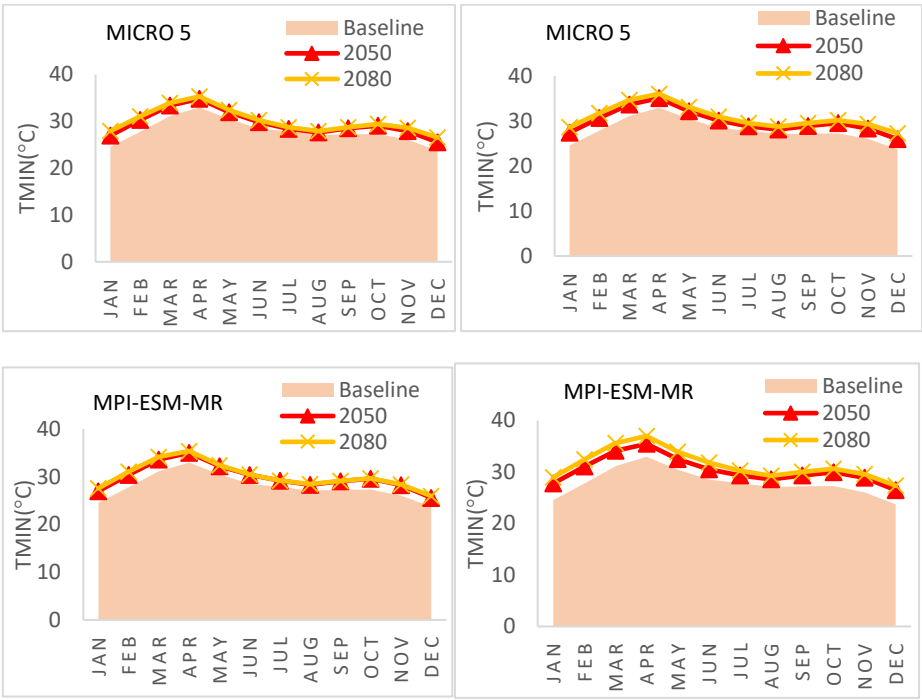

Figure 5.10: Projected future monthly minimum temperature for the periods of 2050s and 2080s with scenarios RCP 4.5 (Left) and RCP 8.5 (right) and baseline period (1989-2018) Mandalay Station.

Both of the maximum and minimum temperature in Mandalay station is projected to be the highest out of five stations. It is observed to be at peak in April under both RCPs for all three periods as shown in figure 5.10. The minimum temperature is projected to be at about 34.5ºC (2050s), and 34.7 ºC (2080s) in April under RCP4.5 and at 34.9ºC (2050s), and 36.3ºC (2080s) under RCP8.5 for four GCMs. Projections of all the GCMs under both scenarios indicate an increase in Tmin in each month for all two future periods under both scenarios.

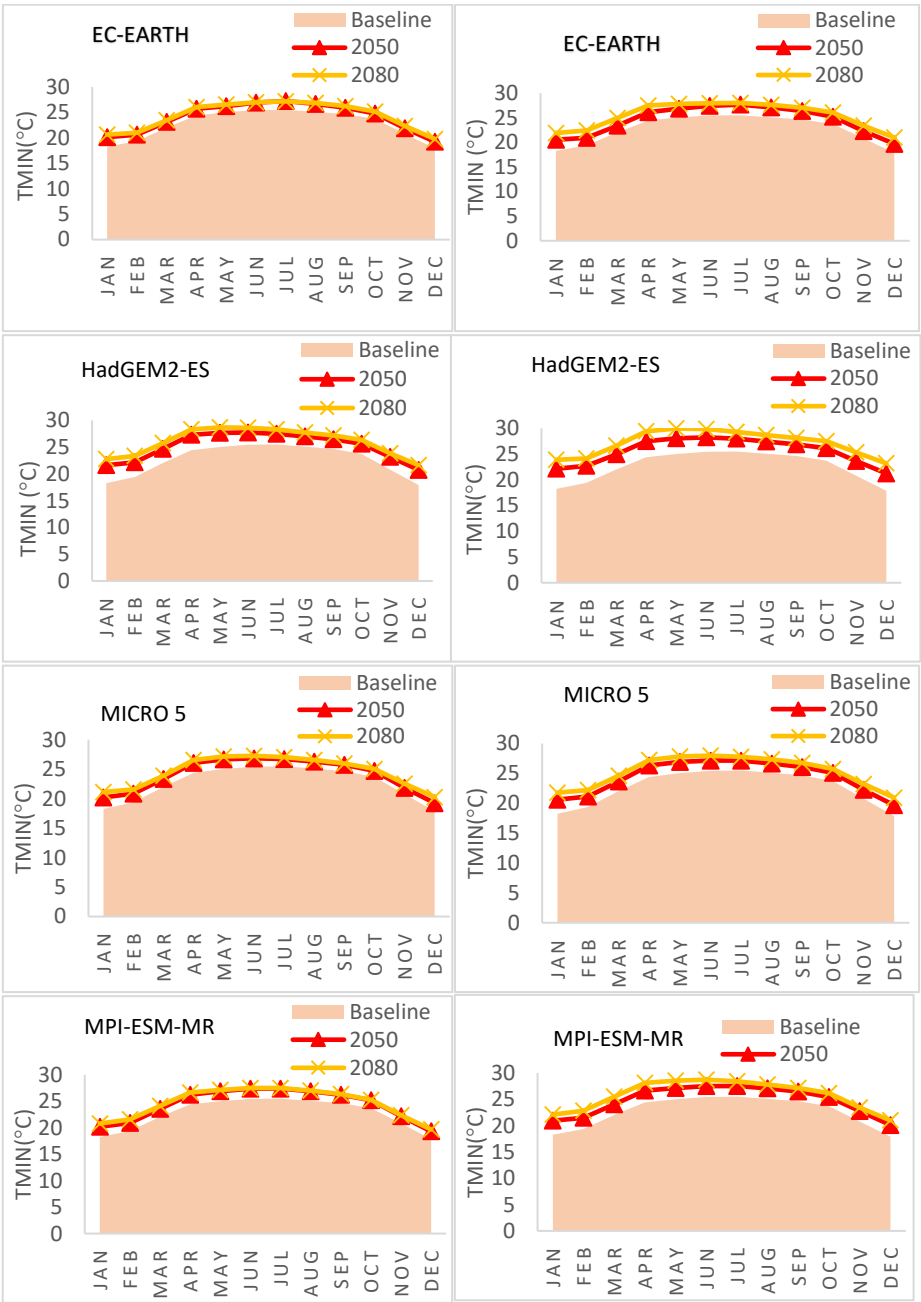

Figure 5.11: Projected future monthly minimum temperature for the periods of 2050s and 2080s with scenarios RCP 4.5 (Left) and RCP 8.5 (right) and baseline period (1989-2018) Sagaing Station.

The average monthly minimum temperature in Sagaing station does not have the peak trend like the other stations as shown in figure 5.11. However, the significant increment of temperature occurs from April to September. The minimum temperature is constantly projected to be at about 2050s and 2080s of April, May, June, July, August and September for four GCMs under RCPs.

5.3.2 Future Maximum Temperature Projection

The projected change in maximum temperature was analyzed monthly. Figure 5.12 to Figure 5.17 show the monthly average maximum temperature in 2050s and 2080s under RCP 4.5 and RCP 8.5 for six stations.

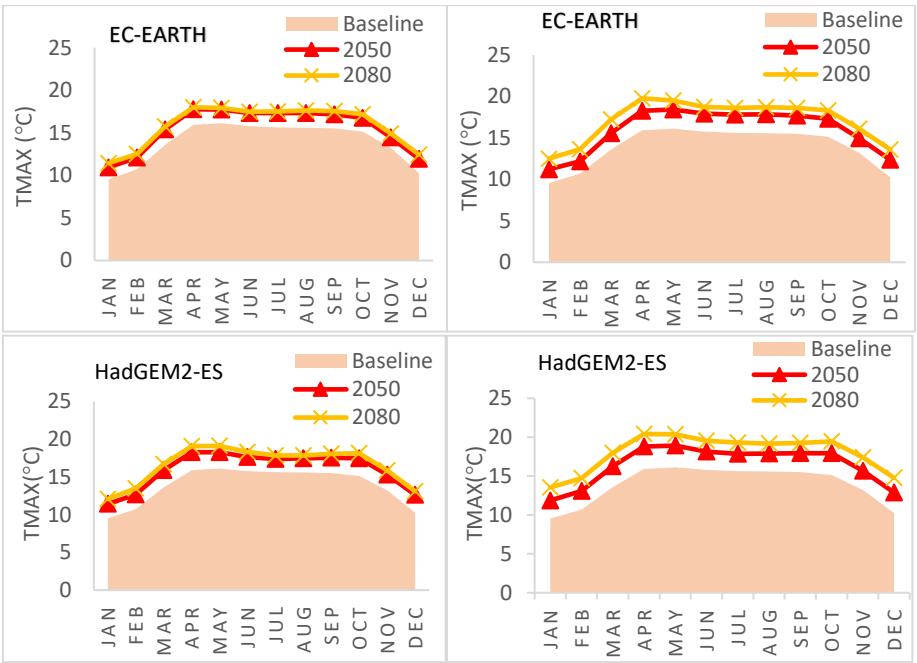

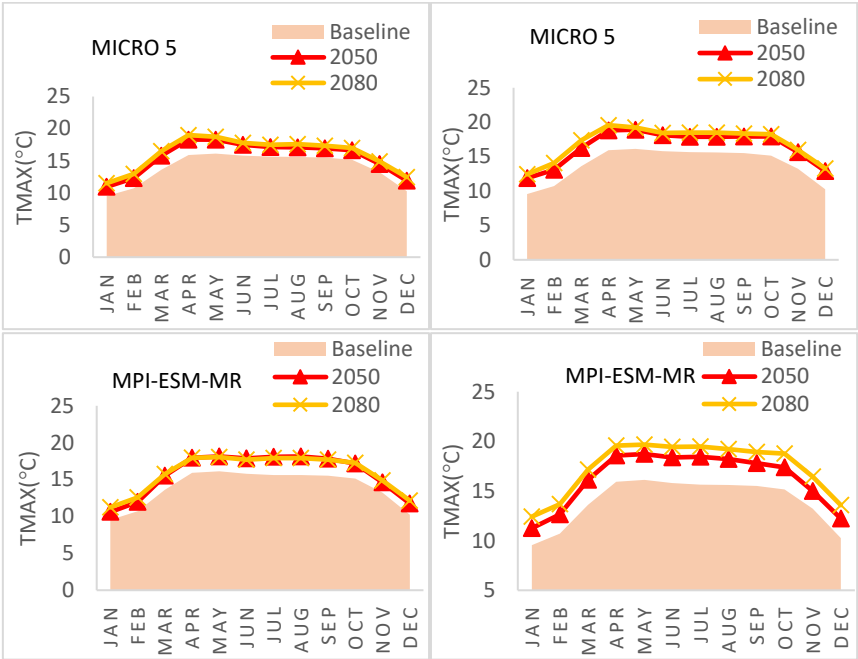

Figure 5.12: Projected future monthly maximum temperature for the periods of 2050s and 2080s with scenarios RCP 4.5 (Left) and RCP 8.5 (right) and baseline period (1989-2018) Putato Station

In term of visual, the figure 5.12 shows the simulated maximum temperature is projected to be peak in April in 2050s and 2080s under both of RCP 4.5 and RCP 8.5 which is slightly increased about 2°C for EC-EARTH, HadGEM2-ES and MICRO5 models while MPI-ESM-MR shows constantly increase trends as the highest temperature from April to October compared with baseline period. The overall look is that the monthly minimum temperature will be significantly increased in all periods under both RCP 4.5 and 8.5.

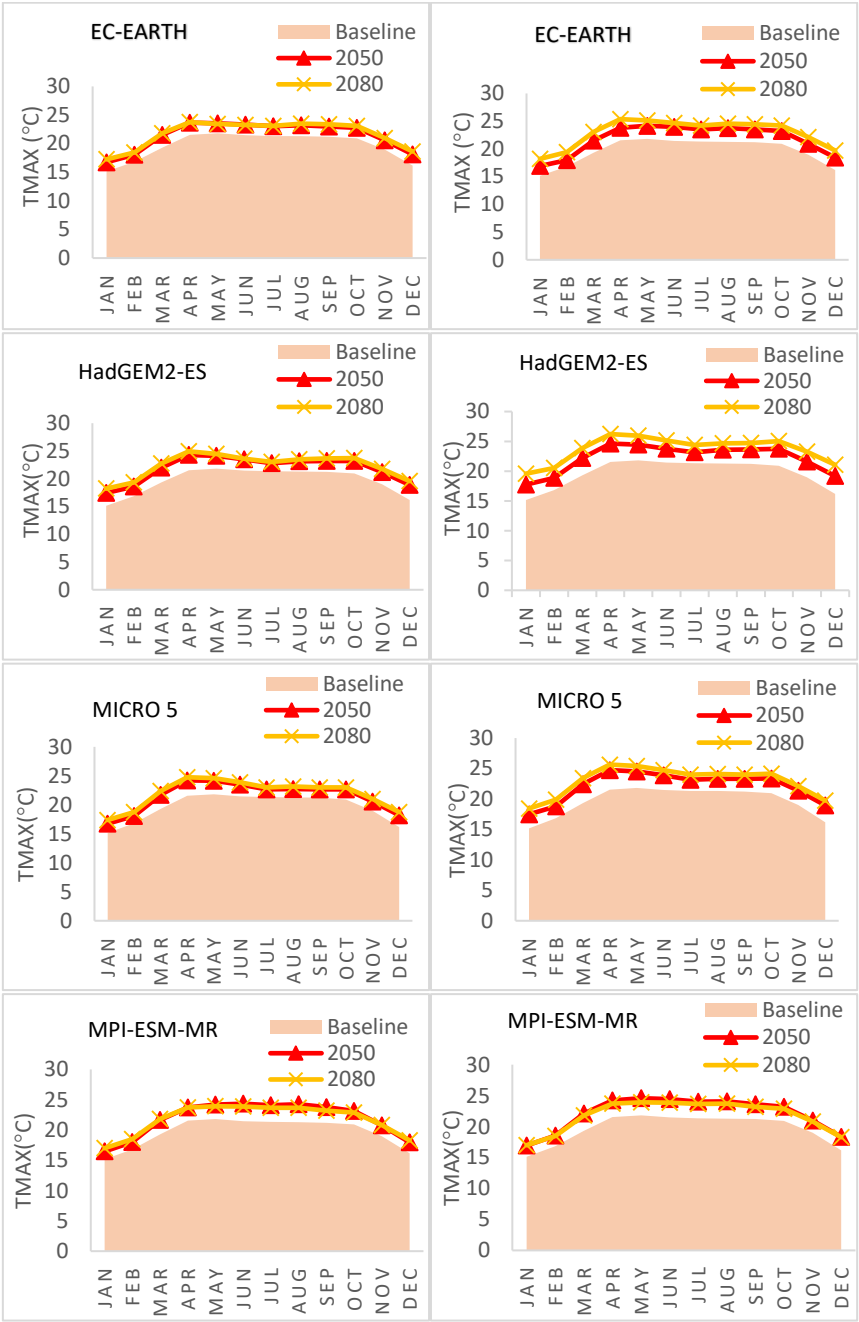

Figure 5.13: Projected future monthly maximum temperature for the periods of 2050s and 2080s with scenarios RCP 4.5 (Left) and RCP 8.5 (right) and baseline period (1989-2018) Myitkyina Station

The average monthly maximum temperature trends show the similar result with the above station according to the figure 5.13. The simulated maximum temperature is projected to be peak in April in 2050s and 2080s under both of RCP 4.5 and RCP 8.5. The maximum temperature is slightly increased about 4°C for EC-EARTH, HadGEM2-ES and MICRO5 models while MPI-ESM-MR shows constantly increase trends as the highest temperature from April to October compared with baseline period in RCP 4.5 and it is significantly increased about 3.5°C in 2050s and 4°C in 2080s in RCP8.5. The temperature changes in all periods for RCP 4.5 shows insignificantly. The overall look is that the monthly maximum temperature will be significantly increased in all periods under both scenarios.

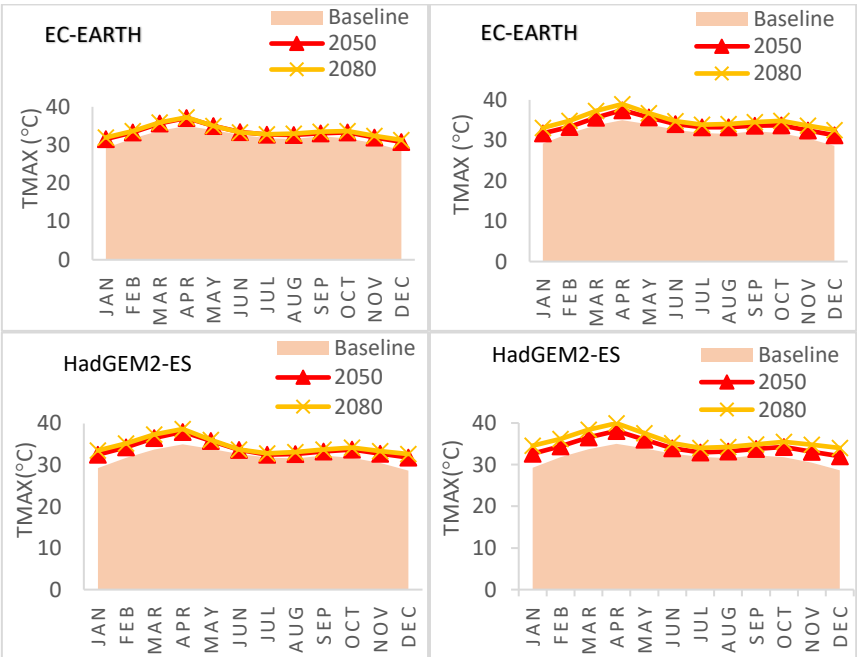

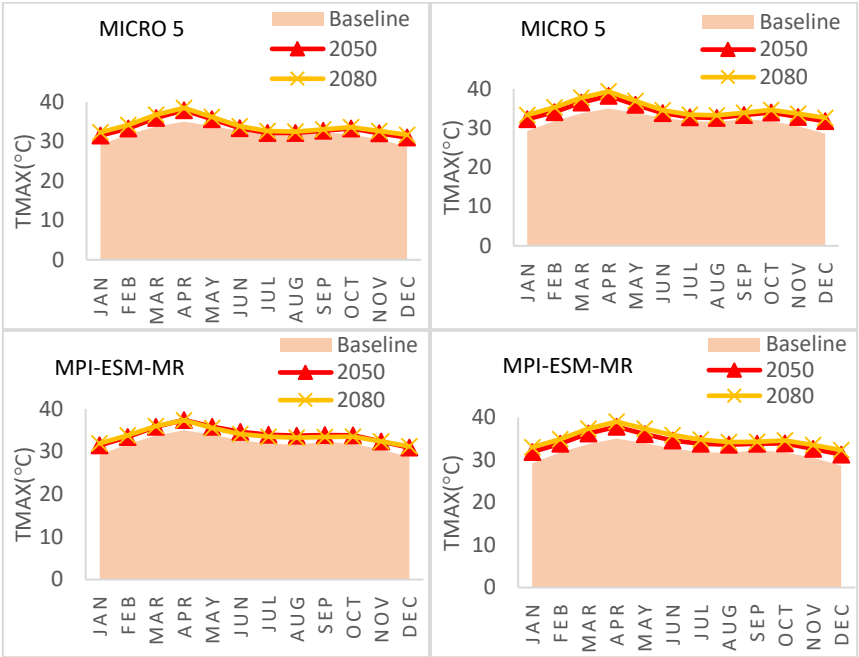

Figure 5.14: Projected future monthly maximum temperature for the periods of 2050s and 2080s with scenarios RCP 4.5 (Left) and RCP 8.5 (right) and baseline period (1989-2018) Bamo Station

According to the figure 5.14, it can be seen clearly, the maximum temperature is intended to increase until 40°C under both of the scenarios for all models. This station has the similar result with above station which shows highest projected temperature in April and significantly increased about 3°C for all GCMs in two periods under RCP 4.5 which shows insignificantly changes trends. It is slightly increased about 2.5°C in 2050s and 6°C in 2080s compared to baseline period under RCP 8.5. For the remaining months, the temperature is slightly increased than baseline period for all models respectively. In this station, it shows clearly that temperature projection under RCP 8.5 is slightly higher than RCP 4.5 for two periods.

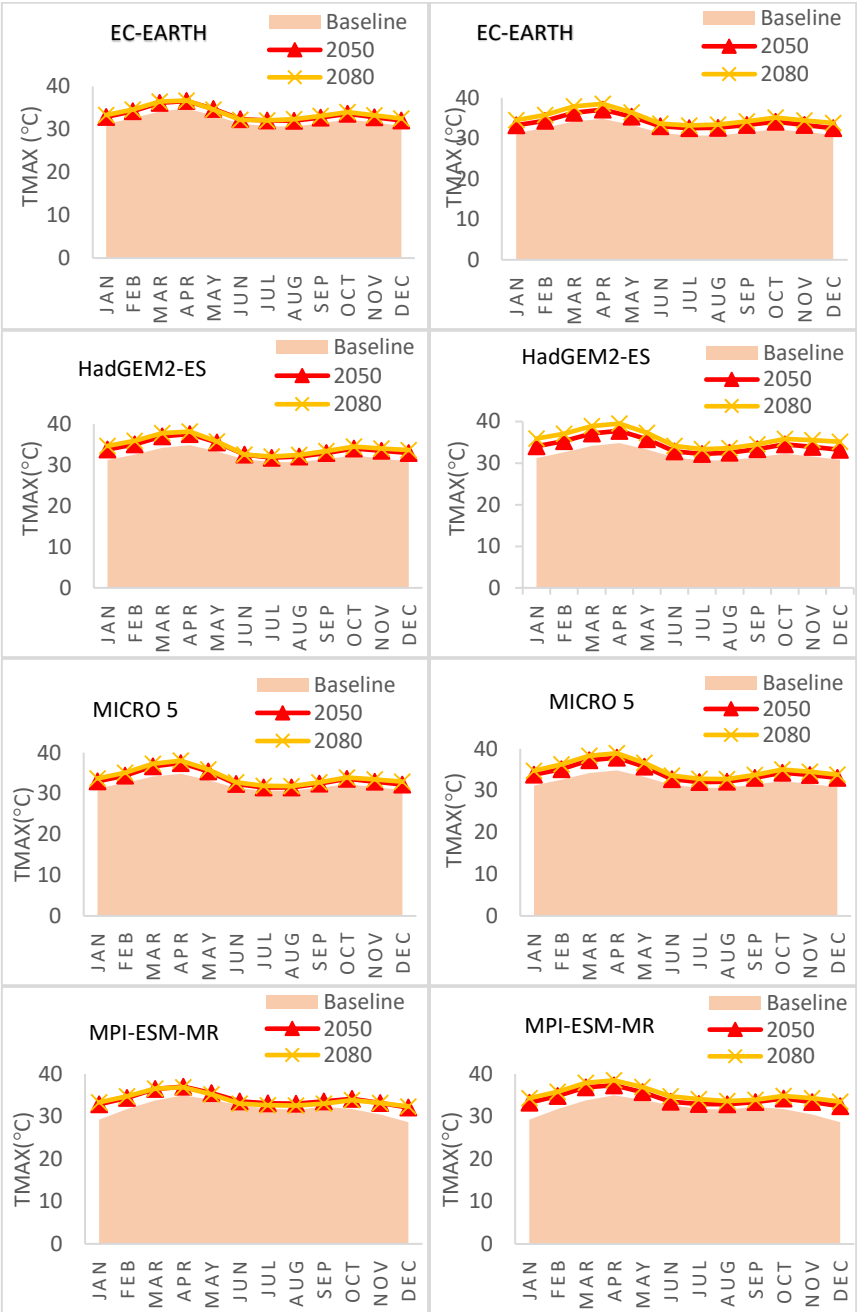

Figure 5.15: Projected future monthly maximum temperature for the periods of,2050s and 2080s with scenarios RCP 4.5 (Left) and RCP 8.5 (right) and baseline period (1989-2018) Katha Station

Moderate temperature change for all two periods (>1 ºC) appears under RCP4.5 for all models and (>4ºC) appears under RCP8.5 for MICRO 5 and MPI-ESM-MR models while it significantly changes about (>2 ºC) in 2080 under RCP 8.5 for EC-EARTH and HadGEM2-ES models. An overall look is that maximum temperature is intended to be increased until 40 ºC for all periods under both scenarios.

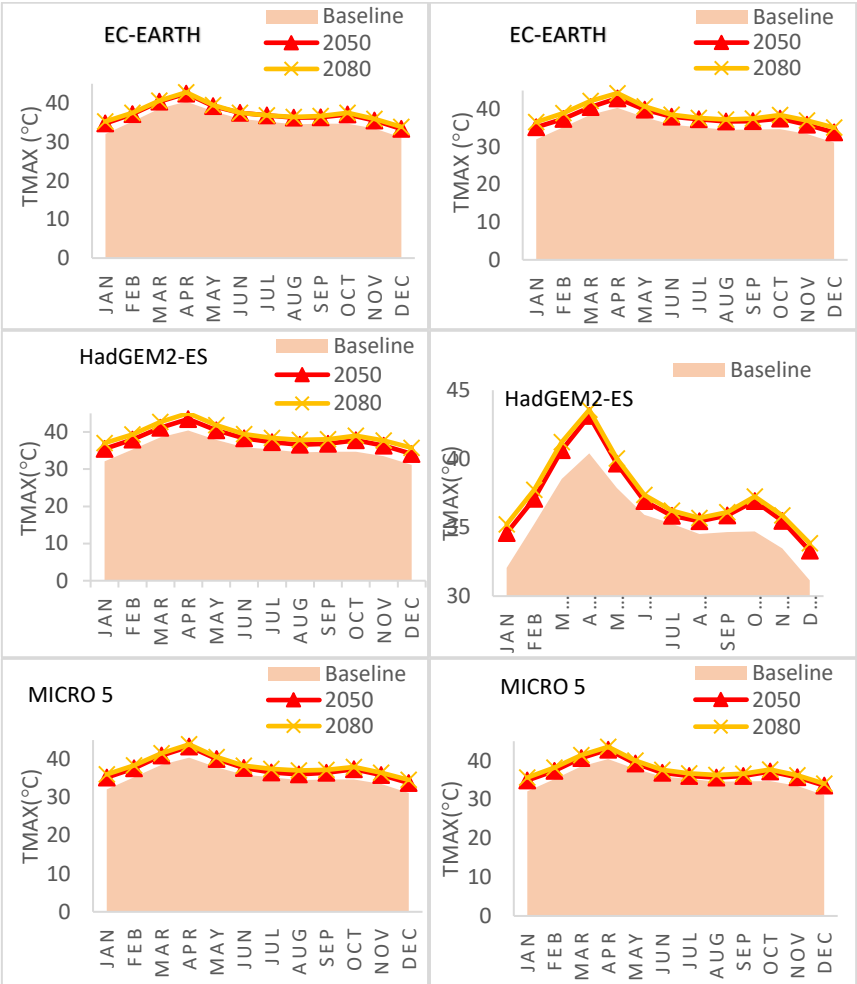

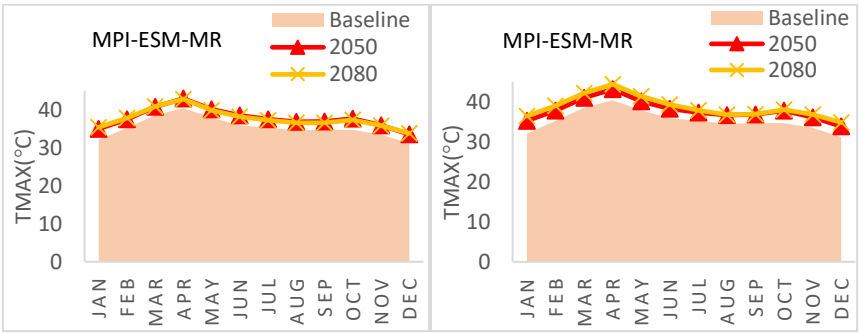

Figure 5.16: Projected future monthly maximum temperature for the periods of 2050s and 2080s with scenarios RCP 4.5 (Left) and RCP 8.5 (right) and baseline period (1989-2018) Mandalay Station

the maximum temperature is observed to be at peak in April under both RCPs for all two periods as shown in figure 5.16. It is projected to be at about 42.9ºC (2050s), and 42.8 ºC (2080s) in April under RCP4.5 and at 43.1ºC (2050s), and 44.4ºC (2080s) under RCP8.5 for four GCMs. Projections of all the GCMs under both scenarios indicate an increase in Tmin in each month for all three future periods under both scenarios. By comparing with the temperature changes in RCPs, EC-EARTH, HadGEM2-ES and MPI-ESM-MR shows moderated changes in three periods while MICRO5 changes insignificantly under RCP 4.5. Under RCP 8.5 MICRO5 shows insignificant changes in 2030 and moderated changes in 2050s and 2080d while the remaining GCMs shows about (>2ºC) increased significantly for three periods.

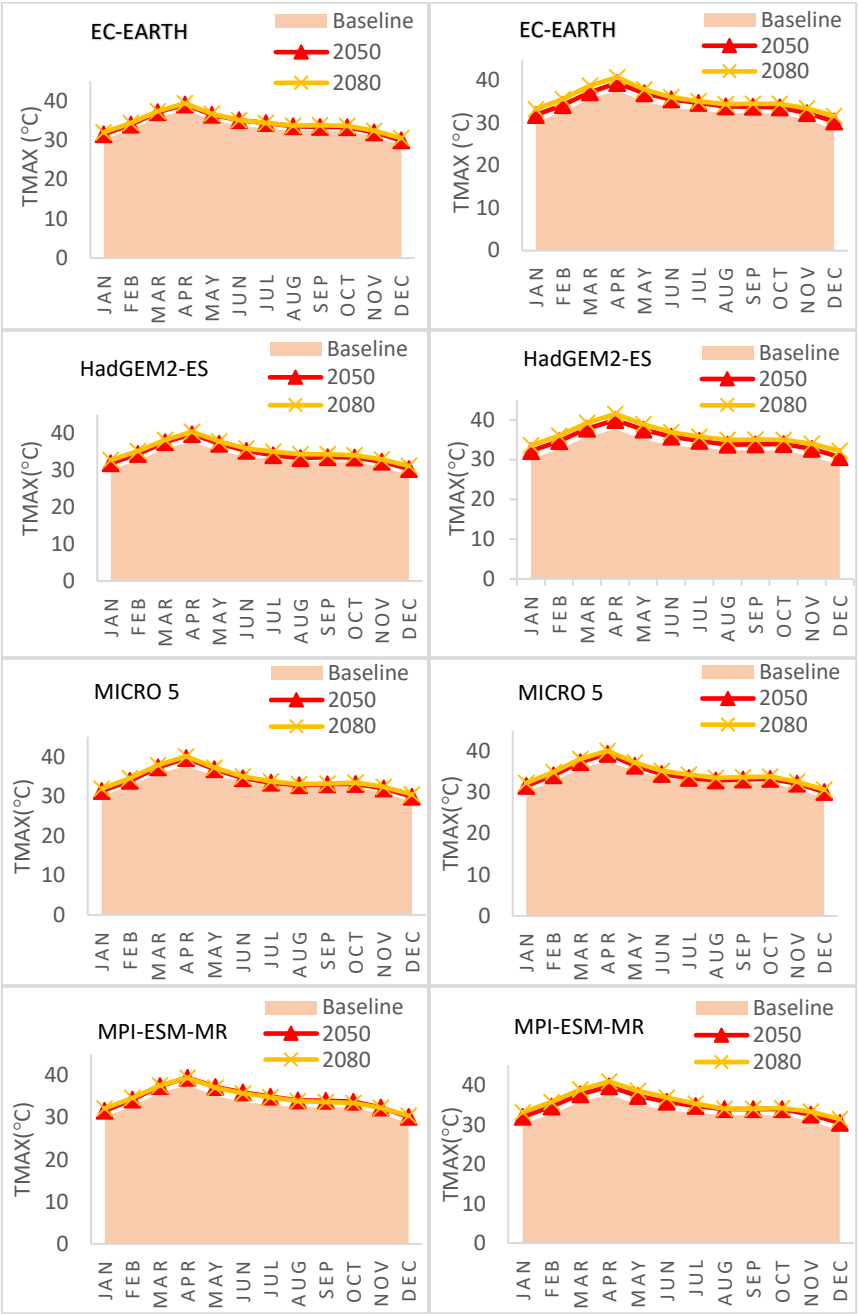

Figure 5.17: Projected future monthly minimum temperature for the periods of 2050s and 2080s with scenarios RCP 4.5 (Left) and RCP 8.5 (right) and baseline period (1989-2018) Sagaing Station.

According to the figure 5.17, moderate temperature change for all two periods (<1 ºC) appears in all periods under RCP4.5 and Under RCP 8.5, MPI-ESM-MR show moderated changes about (>2 ºC) while other models shows insignificantly changes. Although the observed Tmax is high in April for the whole basin, the temperature change for April is quite moderate.

CHAPTER 6. HYDROLOGICAL MODELLING FOR THE UPPER AYEYARWADDY RIVER BASIN

6.1. SWAT Model Setup

Of particular concern in this study is the Soil and Water Assessment Tool (SWAT) model, which is a widely used distributed hydrological model.

6.1.1 Watershed Delineation

To setup a SWAT model, the meteorological parameters of daily precipitation, maximum and minimum temperatures, solar radiation, relative humidity, and wind speed are compulsory. However, in this study, only daily precipitation and maximum and minimum temperatures during 1989-2018 at six meteorological stations were used because there is a lack of other meteorological parameters. There is no need to use the WXGEN weather generator because there is no missing data in this study area and only four hydrological stations were used. The stream flow data from 1989-2018 at these four stations was used in comparison with observed and simulated stream flow for calibration and validation. The outlet of the whole basin was selected at Sagaing station, where before the inlet is interrupted by the other river. The whole basin was divided into 13 sub-basins with a total basin area of 166,969 km^2. The DEM calculates good watershed characteristics such as elevations, longest flow path, reach etc. at sub-basin level. The figure below shows the sub-basins of the Upper Ayeyarwaddy River Basin.

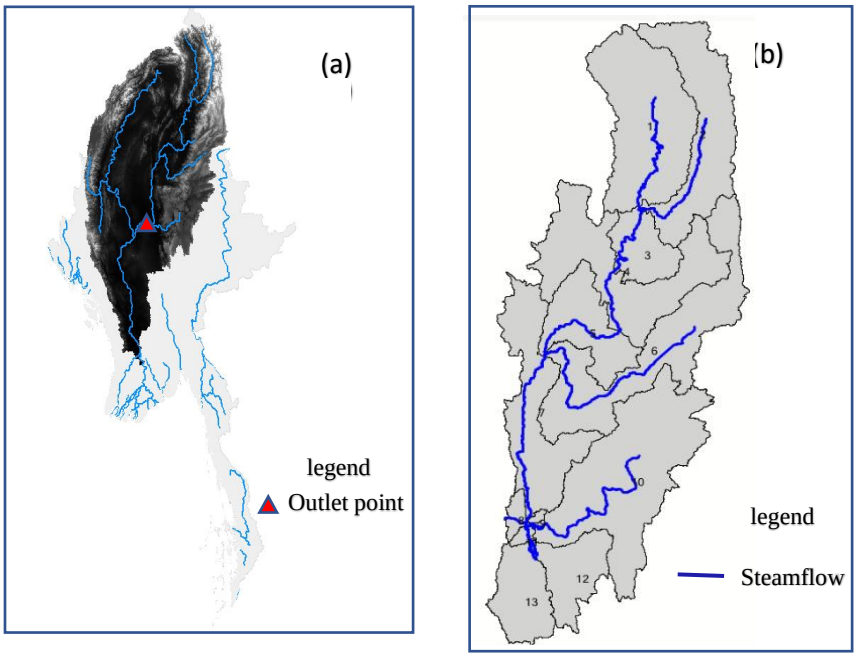

Figure 6.1: (a) Outlet and (b) Catchment grid of the Upper Ayeyarwaddy Basin

6.1.2 Definition of the Hydrological Response Unit (HRU)

The sub-basins were subdivided into HRUs (Hydrologic Response Unit) because each HRU predicts runoff separately. This study used a 5% threshold for land use, soil, and slope (SWAT has a limitation of 5-20%) to reduce the number of HRUs. The land use map and soil map (described in Figure 3.6) were loaded in ArcSWAT 2012 for land use and soil definition, With the combination of unique land use and soil, 71 HRUs for 13 sub-basins were generated within the Upper Ayeyarwaddy River Basin.

6.2 Result for Calibration and Validation

Before actual SWAT calibration and validation, various input parameters are required for statistical analysis. The model performance to simulate daily and monthly stream flows during the calibration and validation period is presented in the following tables and figures. The stream flows at the Myitkyina, Bamo, Katha and Sagaing stations were

analysed. In this study, the parameters controlling stream flow were tested and changed in accordance with the suggestions of Neitsch et al. (220a), Budhathoki (2006), Jha et al. (2007), and Schilling et al. (2008). A total of 22 sensitive parameters as described in Table 6.1 were analysed for sensitivity.

Table 6.1: Sensitive parameters of SWAT modelling for stream flow simulation in the Upper Ayeyarwaddy Basin

Parameters	Description of Parameter	Initial range	Fitted range
Ground water parameters			
GW_DELAY.gw	Time interval for recharge of the aquifer	517 ~ 519	527.0697
ALPHA_BF.gw	Baseline flow recession constant	0.82 ~ 0.98	0.885487
GWQMN.gw	Threshold water depth in the shallow aquifer for flow	1418 ~ 1809	1593
GW_REVAP.gw	Water depth in the aquifer for the occurrence of water rise to the unsaturated zone	0.06 ~ 0.0866	0.069
REVAPMN.gw	Water depth in the aquifer for the occurrence of water rise to the unsaturated zone	443 ~ 519	492
RCHRG_DP.gw	Deep aquifer percolation fraction.	1.17 ~1.53	1.24
Surface Parameters			
CN2.mgt	Initial SCS CN II value	12.27 ~ 20.68	19.06
SURLAT.bsn	Surface runoff log coefficient	10.1 ~ 11.99	11.72
OV_N.rte	Manning's coefficient for overland flow	5.02 ~ 8.6	8.48
CH_N2.rte	Manning's "n" value for the main channel	0.22 ~ 0.26	0.239
CH_K2.rte	Channel effective hydraulic conductivity	161 ~ 234	216.36
HRU_SLP.hru	Average slope steepness	9.21 ~9.41	9.34
SLSUBBSN.hru	Average slope length.	77.87 ~92.46	84.33
Soil parameters			

SOL_AWC.sol	Soil water storage	0.41 ~ 0.57	0.56
SOL_K.sol	Saturated soil hydraulic conductivity	-68.07 ~ 155.5	25.27
SOL_BD.sol	Moist bulk density.	1.165 ~1.58	1.44
ESCO.hru	Soil evaporation compensation factor	0.81 ~ 0.99	0.89
ESPO.hru	Plant uptake compensation factor	1.45 ~1.63	1.51

Each parameter was changed by one fixed value at a time, keeping other parameters constant. The two statistical indicators: R^2, and NSE were used for the model performance. The period of 1993-2005 of the streamflow data including 3 years warm-up was used for calibration and the validation was taken for 2006-2018 after good calibration results. Table 6.1 shows the parameter values using monthly stream flow data for comparison. Checking these sensitive parameters using monthly stream flow can be seen in Table 6.2 and Figures 6.2 and 6.3. Compared with the simulations of all the stations, the simulated and observed stream flows fitted well in most of the time except at Myitkyina station. As recommended by many researchers, R2 and NSE above 0.6 describes a perfect fit can be judged as satisfactory (Moriasi et al., 2007). In this section, R2 with the value of 0.66 indicate the satisfactory result at Myikyina station and value of 0.75 to 0.89 indicates good agreement of simulated flows at Bamo, Katha and Sagaing station during calibration and validation. NSE also indicates good agreement of the simulated flows with the observed flows ranging 0.66 to 0.75 during calibration and validation periods. Checking these parameters using monthly stream flow for calibration and validation can be seen in Table 6.2. However, some values of NSE (0.53 and 0.56) at Myitkyina station are boundary of its limitation and it shows a poor model performance in predicting stream flows. It may be due to error of stream

flow data during the calibration and validation periods. On the field, these two hydrological stations are operated with good equipment and well-trained staff now but there was weak system for collecting data in the past. Government could support good facilities and well practice for data collecting in these hydrological stations (DMH, 2009). It might be error in the observed data during 1993-2008 and it can influence model overestimation. Therefore, to improve on this model performance, detailed and long-term data will be needed for further analyses (Reungsang et al., 2010). However, overall evaluation of the SWAT demonstrated that the model has the capacity to predict stream flow within the Upper Ayeyarwaddy River Basin.

Table 6.2: SWAT performance to simulate stream flow using monthly data for the baseline period of 1993-2008

Station	Data	Calibration		Validation	
		R^2	NSE	R^2	NSE
Myitkyina	monthly	0.66	0.53	0.63	0.56
Bamo	monthly	0.80	0.75	0.85	0.75
Katha	monthly	0.79	0.75	0.89	0.69
Sagaing	monthly	0.75	0.69	0.72	0.66

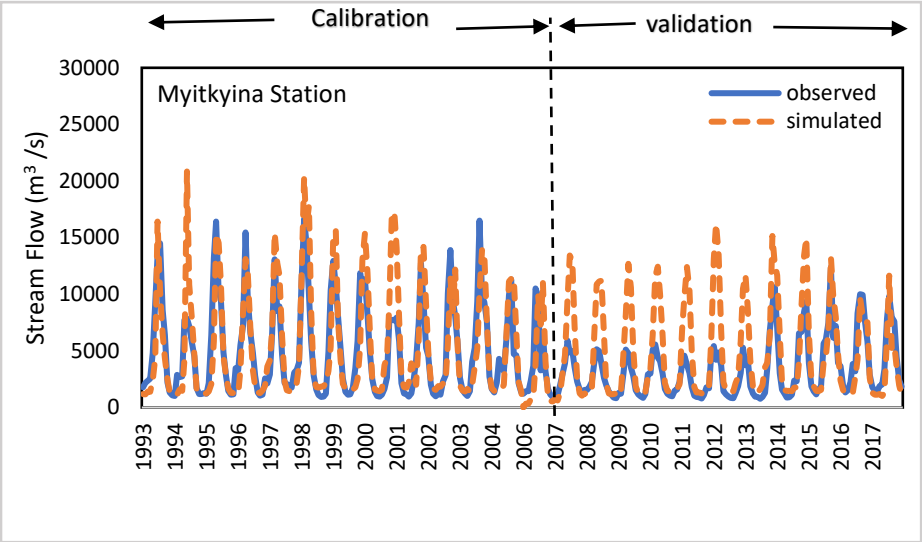

Figure 6.2 (a): Comparison between observed and simulated monthly stream flow at the Myitkyina station for the calibration and validation period

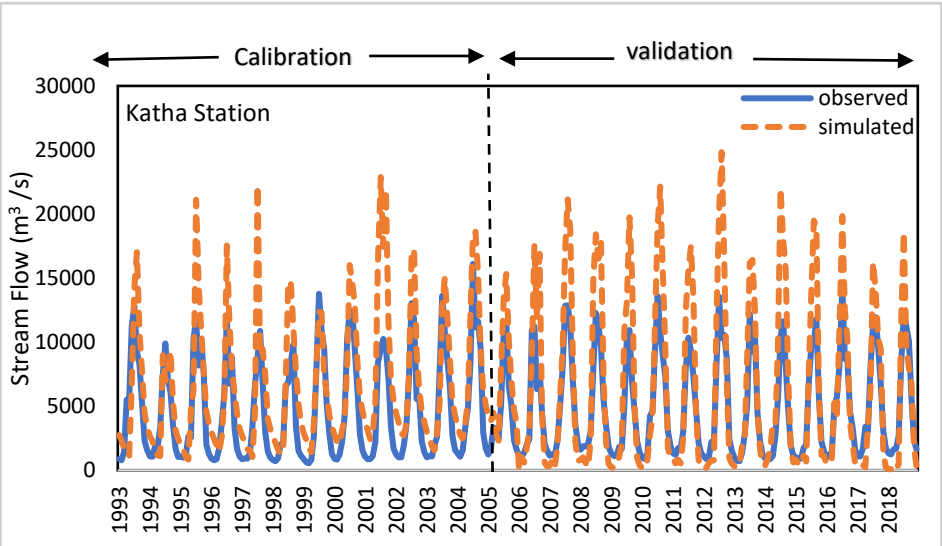

Figure 6.2 (b): Comparison between observed and simulated monthly stream flow at the Katha station for the calibration and validation period

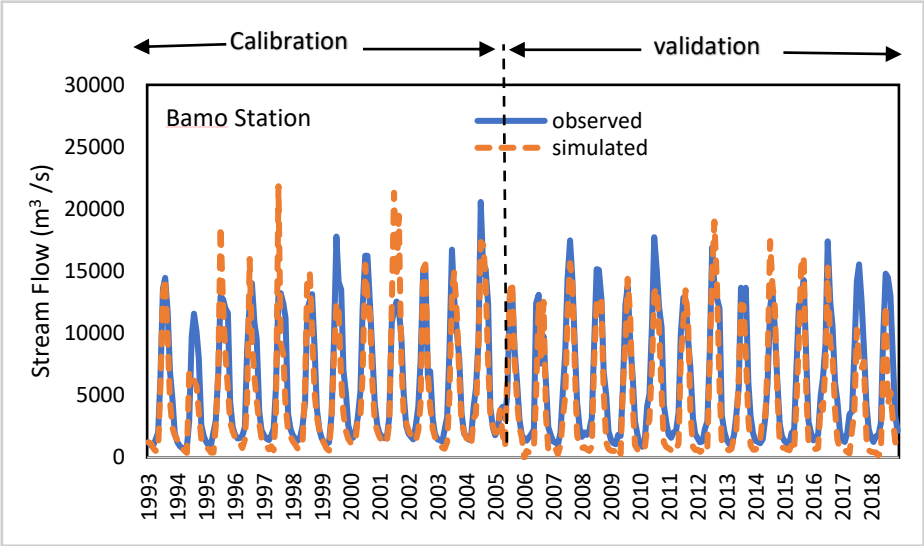

Figure 6.2 (c): Comparison between observed and simulated monthly stream flow at the Bamo station for the calibration and validation period

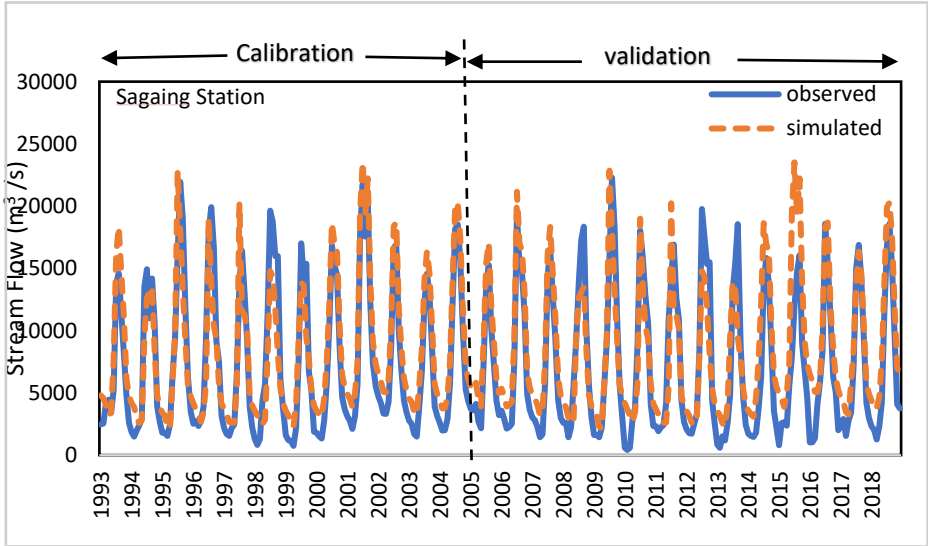

Figure 6.2 (d): Comparison between observed and simulated monthly stream flow at the Sagaing station for the calibration and validation period

CHAPTER 7. Impacts of Climate Changes on Hydrology

7.1 Impacts on Hydrology of the Upper Ayeyarwaddy River Basin

7.1.1 Changes in Average Monthly Stream Flow

The average monthly stream flow at the Myitkyina, Bamo, Katha and Sagaing stations for the baseline period and two future periods under two scenarios are described in Figure 7.1. Accordingly, the stream flow is projected to significantly decrease at Myitkyina station and increase in Bamo, Katha and Sagaing stations during two periods. The peak of stream flow is observed in August (the end of the rainy season) under both scenarios in all periods at the three stations, although the baseflow peaked in July. At the Myitkyina station, the baseline stream flow is higher than the simulated data of two scenarios for all the seasons. In the summer season, the baseline seasonal flow is a bit higher than the simulation at the rest of three stations in the month of January to April. Four months (September, October, November, and December) give same simulated stream flow with baseline at the Bamo station,

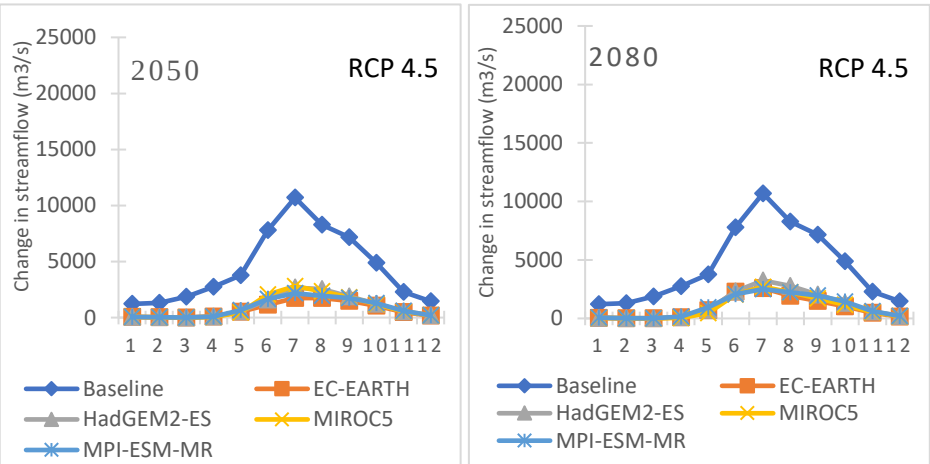

Figure 7.1(a). Simulated average monthly stream flow at Myitkyina station during the baseline period (1989-2018) and the two future periods under RCP4.5 scenario

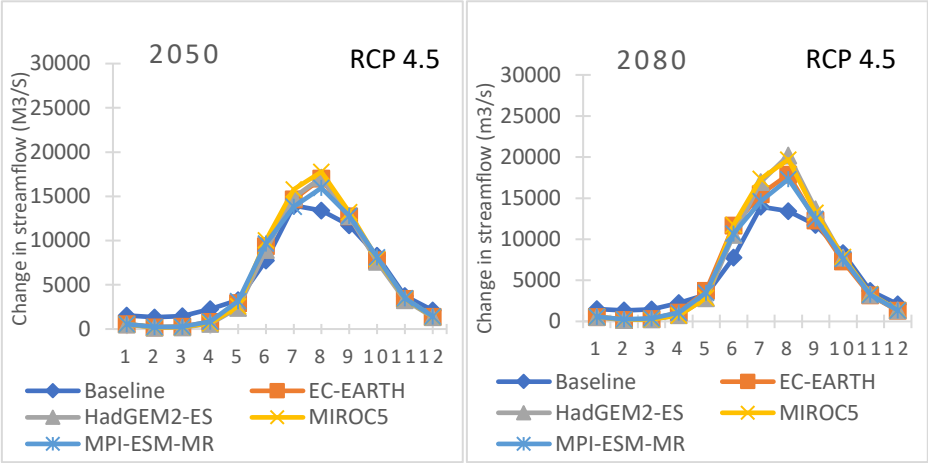

Figure 7.1(b). Simulated average monthly stream flow at Bamo station during the baseline period (1989-2018) and the two future periods under RCP4.5 scenario

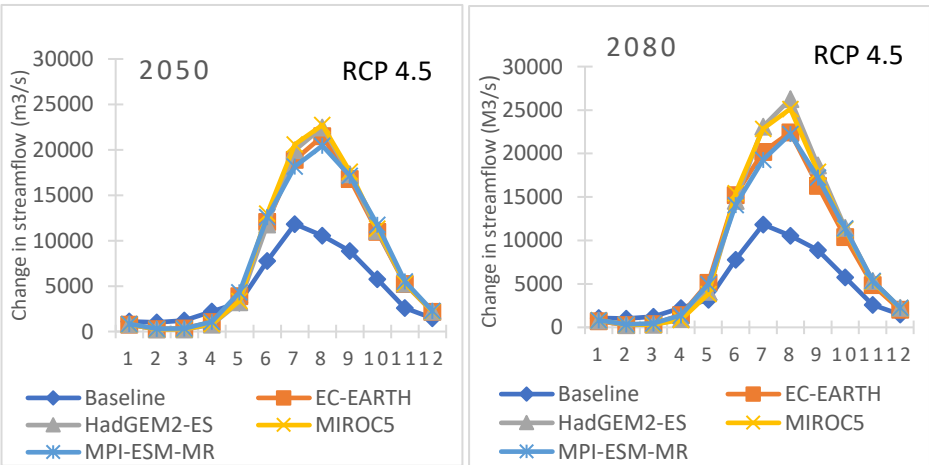

Figure 7.1(c). Simulated average monthly stream flow at Katha station during the baseline period (1989-2018) and the three future periods under RCP4.5 scenario

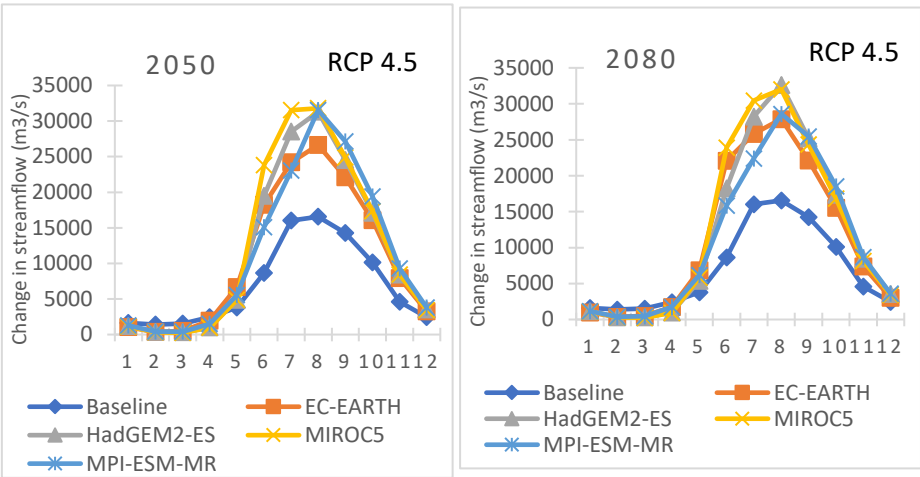

Figure 7.1(d). Simulated average monthly stream flow at Sagaing station during the baseline period (1989-2018) and the three future periods under RCP4.5 scenario

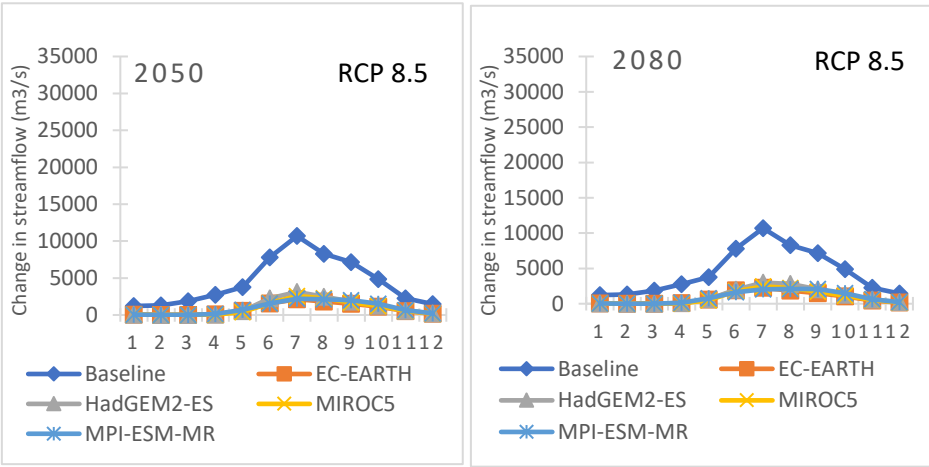

Figure 7.1(e). Simulated average monthly stream flow at Myitkyina station during the baseline period (1989-2018) and the three future periods under RCP8.5 scenario

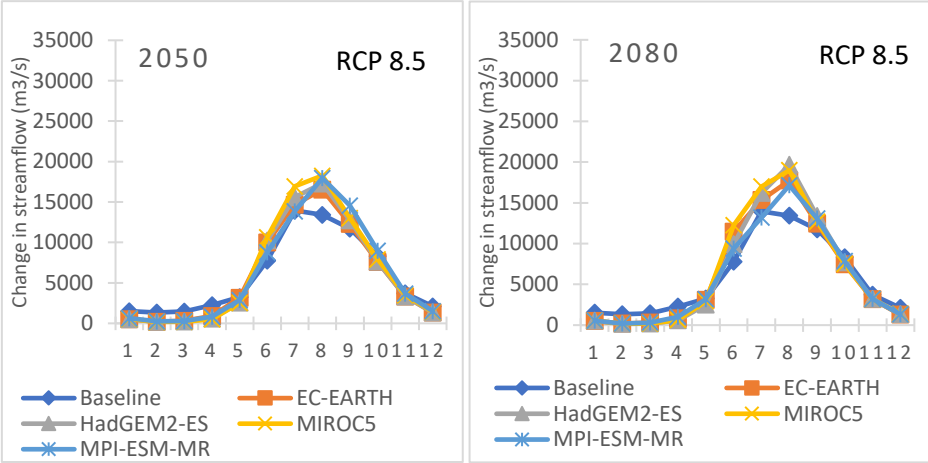

Figure 7.1(f). Simulated average monthly stream flow at Bamo station during the baseline period (1989-2018) and the three future periods under RCP8.5 scenario

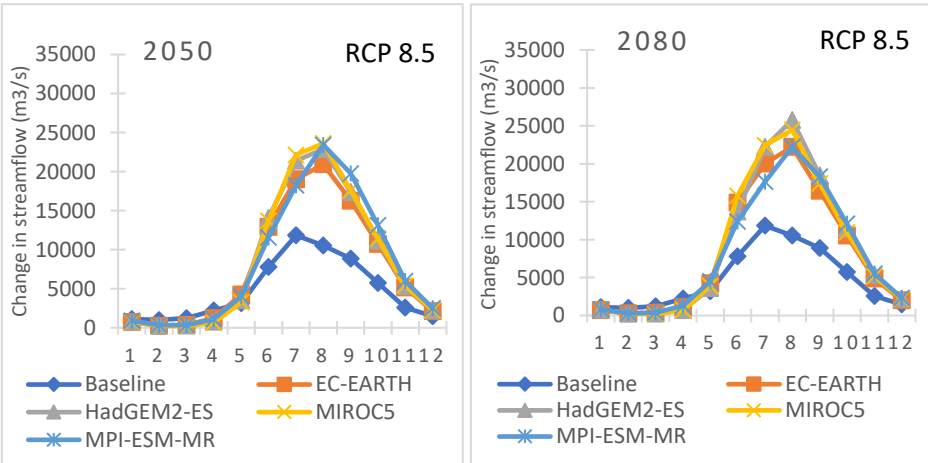

Figure 7.1(g). Simulated average monthly stream flow at Katha station during the baseline period (1989-2018) and the three future periods under RCP8.5 scenario

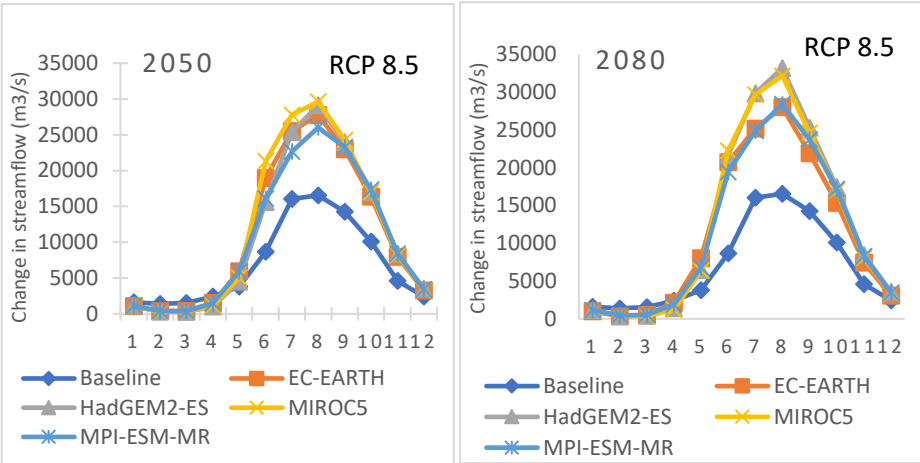

Figure 7.1(h). Simulated average monthly stream flow at Sagaing station during the baseline period (1989-2018) and the three future periods under RCP8.5 scenario

From the results of Figure 7.1, Myitkyina area shows declining stream flow changes for all seasons under both scenarios while inclining stream flow changes at the rest of three stations for all months. It may be resulted in two factors: climate change and man-made activities. The Upper Ayeyarwaddy River begins from the mountainous area above Bamo station. Because of temperature increasing in summer (approximately 0.9˚C), there is water shortage problem at origin point of the Upper Ayeyearwaddy River locating in the valley. There has been a general decrease in streamflow because of dam effect. This decrease has been more intense in the most regulated river basins because they provide water to different economic sectors. Dam regulation and water transfers between basins have also decreased streamflow and exacerbated droughts in downstream regions. The migrated people are moving upper side of the city and making agricultural production. They use mostly surface water more than ground water because ground water is difficult in mountainous area. The local people use surface water for irrigation and domestic.

7.1.2 Projected Changes in Annual and Seasonal Stream Flow

Table 7.1 shows percentage changes of stream flow at the four stations: Myitkyina, Bamo, Katha and Sagaing stations with respect to the baseline period of 1989-2018. All GCMs are CMIP5 models, but their projections cannot be similar. GCM projections can be varied according to atmospheric conditions, station elevation, geology of study area and current weather. Generally, the high resolution GCM can project the best results, but it cannot be confirmed. Therefore, my research can suggest the climate modellers not to use one or two GCMs for their research. Using more GCMs is a good practice for climate studies. Table 7.2 and 7.3 shows increases or decreases in annual average stream flow, summer seasonal stream flow, rainy seasonal stream flow, and winter seasonal stream flow for the future climate in scenarios RCP4.5 and 8.5 at the four stations. The average change in stream flow has predicted the increase and decrease in stream flow for future periods and scenarios when averaging the change from all GCMs. Changes in average stream flows , annual seasonal stream flow for all periods in the century are expected to increase for all scenarios at the Katha and Sagaing station, but there is a decreasing trend of flow changes at the Myitkiyna and Bamo stations with the 89% of largest decreased value being .

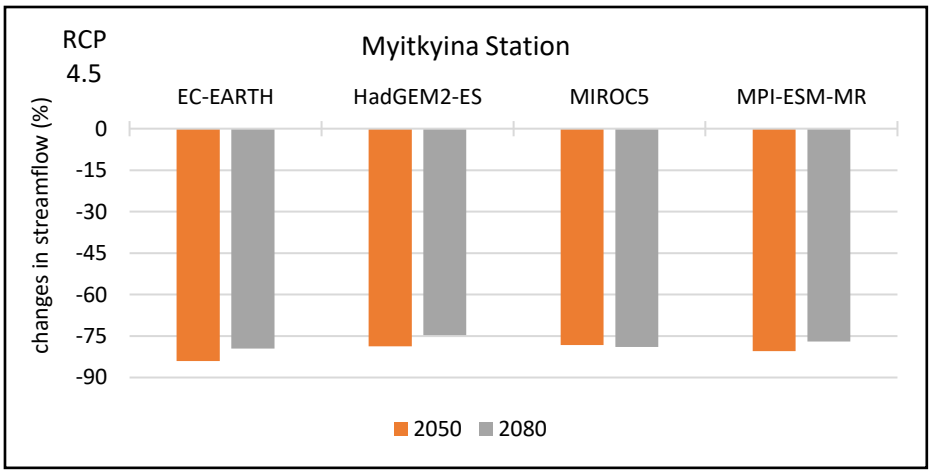

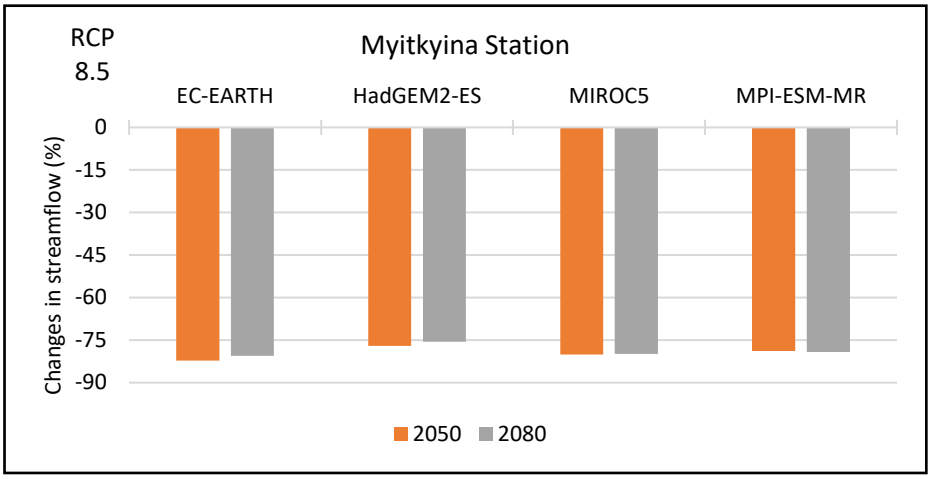

Figure 7.2(a). Percentage changes in annual average stream flow due to various GCMs for future periods and scenarios with respect to the baseline period 1989-2018 at Myitkyina station

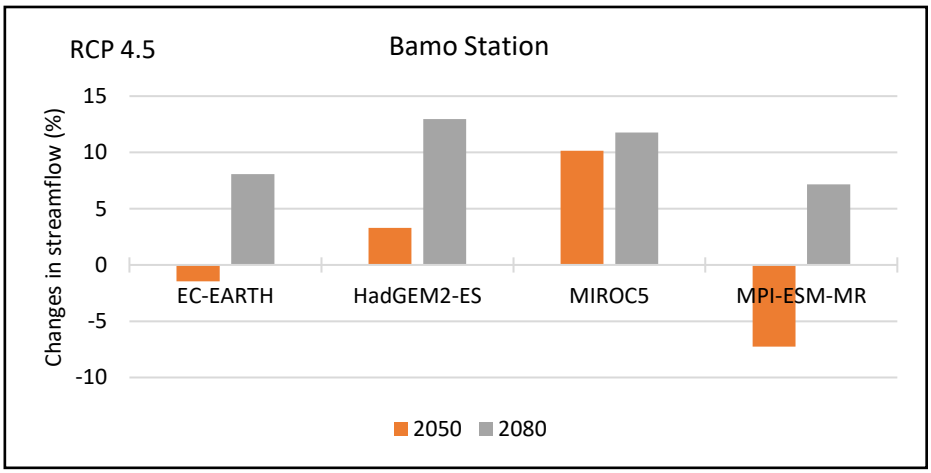

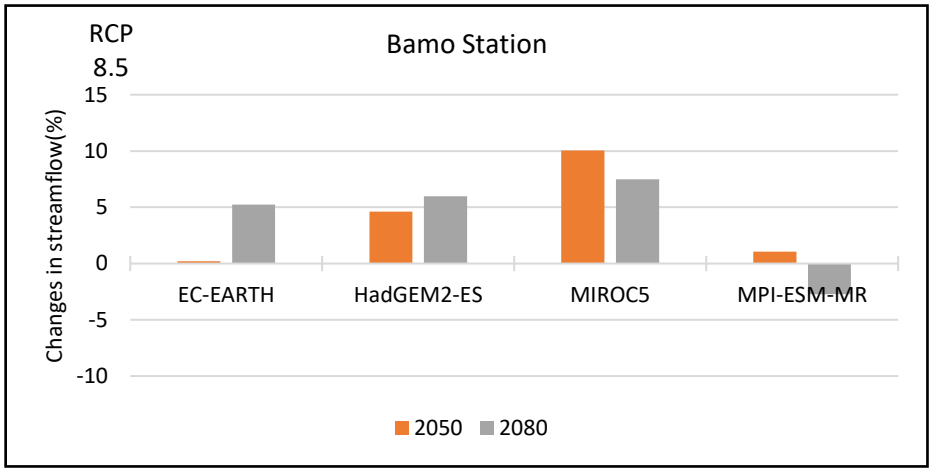

Figure 7.2(b). Percentage changes in annual average stream flow due to various GCMs for future periods and scenarios with respect to the baseline period 1989-2018 at Bamo station

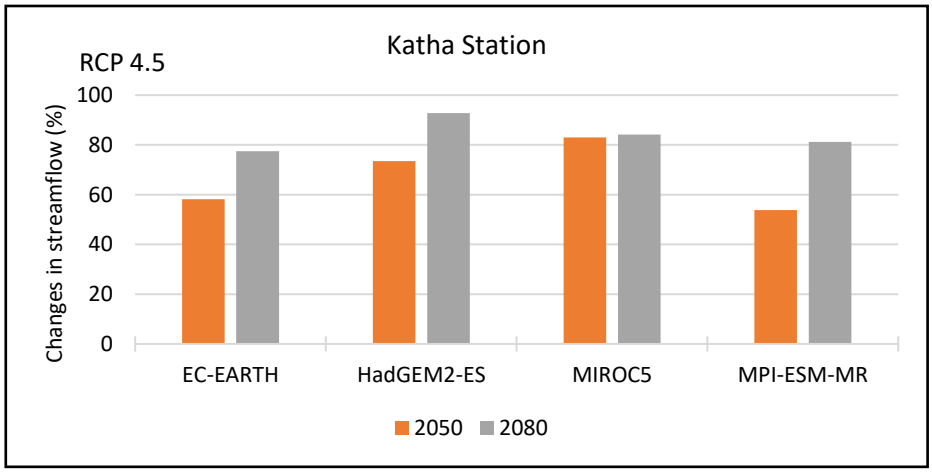

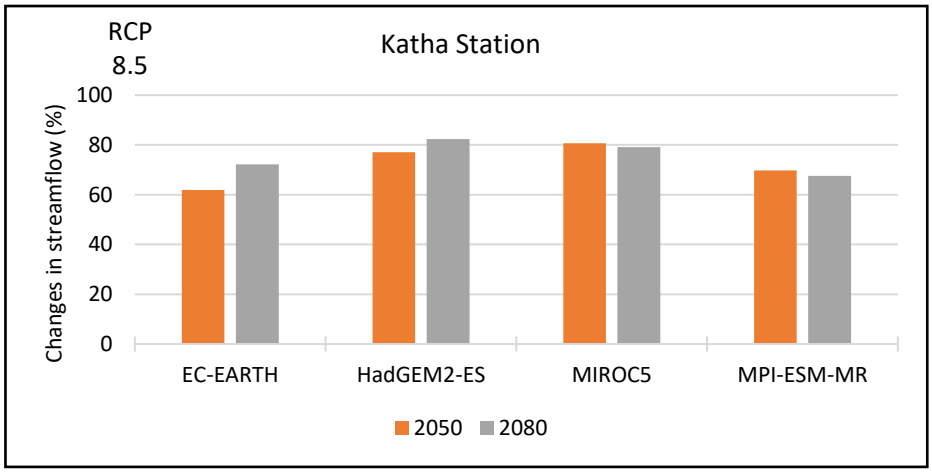

Figure 7.2(c). Percentage changes in annual average stream flow due to various GCMs for future periods and scenarios with respect to the baseline period 1989-2018 Katha station

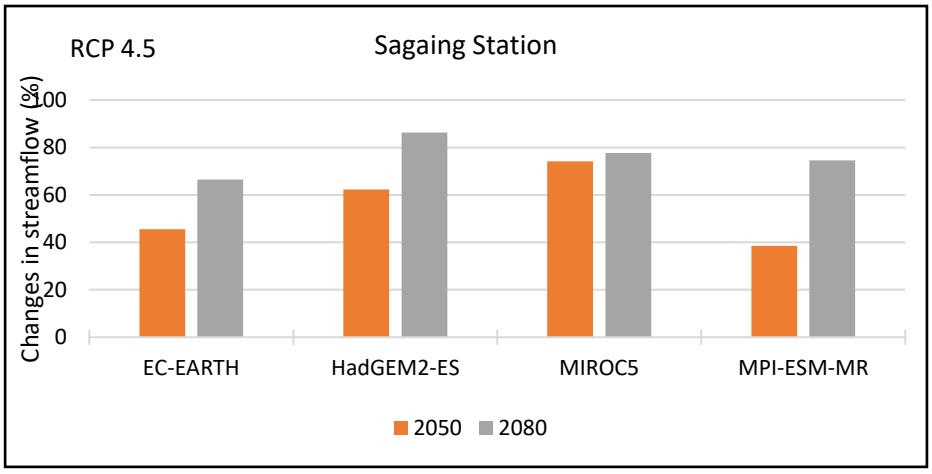

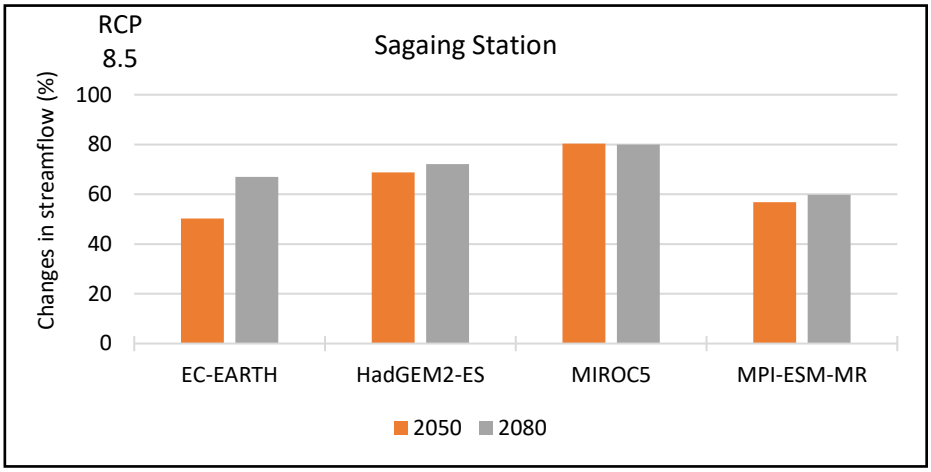

Figure 7.2(d). Percentage changes in annual average stream flow due to various GCMs for future periods and scenarios with respect to the baseline period 1989-2018 Sagaing station

In this section, the impact of the expected climate change under RCP4.5 and 8.5 scenarios was examined by comparing different GCMs during the reference period (1990-2009) and a future period (2010-2099). The change in seasonal and annual stream flow as projected by four GCMs under RCP4.5 and 8.5 scenarios during two future periods with respect to the baseline period is shown in Figures 7.2 and 7.3. The results indicate that there is likely to be a chance of increase/decrease in seasonal as well as annual stream flow in all two future periods as shown by the majority of the four GCMs and their average. Due to the predicted increase in rainy season precipitation, stream flow is expected to increase at the Bamo, Katha and Sagaing stations for all two periods under both scenarios as projected by the four GCM models with the exception of decreasing rainy seasonal flow at the Myitkyina station for RCP4.5 and RCP8.5. Due to the combination of reduced summer precipitation, increased temperature and consequent increased evaporation, stream flow is expected to decrease in the models at the Myitkyina station under both scenarios with the largest decreasing flow being 89% . The greatest increase in change of winter flow can be seen in the HadGEM2 model for all periods under both scenarios at the Katha and Sagaing stations and it has changes which keep decreasing flow at Myitkyina and Bamo stations for all two periods under the two scenarios, and MIROC5 also reduce stream flow at

the Myitkyina and Bamo station. The greatest decreasing winter flow is 80 % under both scenarios at the Myitkyina station. The risk of extremely decreased annual and seasonal stream flow is expected for all models in all periods under both scenarios occurring at the Myitkyina station. The EC-EARTH, HadGEM2-ES, MICRO5 and MPI-ESM-MR models show a significant increase in annual stream flow changes at the three stations under RCP4.5 and 8.5 scenarios and in rainy and winter seasonal flow changes at the Katha and Sagaing station. According to the results in Figure 7.2 and 7.3, the maximum increase in stream flow (95%) occurred in the 2050s and 2080s under the RCP4.5 and 8.5 scenario using HadGEM2-ES at the Katha station. The highest decrease in flow (80%) is observed in the 2050s and (95%) 2080s by EC-EARTH under both scenarios. The maximum increase in flow during the 2050s (95%), is predicted by using HadGEM2-ES and by using MIROC5 GCM under RCP4.5 and RCP8.5 also experienced this in the 2050s and 2080s (80%) and using EC-EARTH GCM under both scenarios experienced in the 2050s (60%) and 2080s (79%) while 50% increase in 2050s and 80% in 2080s by MPI-ESM-MR. From these results, it can be seen that the highest increase in stream flow (80%) during the 2050s and 95% during 2080s under RCP 4.5 and RCP8.5 scenarios is predicted only by HadGEM2-ES for the Katha station. EC-EARTH predicts the highest decrease in stream flow of 85% and 70% during the 2050s and 2080s under the both scenario at Myitkyina Station. Figure 7.2 and 7.3 confirms a dominant influence of change in annual and seasonal flow over the Upper Ayeyarwady River Basin. These results show that average annual stream flow is relatively sensitive to increased annual precipitation for the whole basin area. In this study, the projections of GCMs are different from each other, creating uncertainty, and the main source of this climate sensitivity is caused by cloud feedback (Hoose et al., 2009). Therefore, many researchers support the use of various GCMs to project future global climate data in the study area. In this study, the greatest GCM projection varies seasonally and annually at each of the two stations. It can be seen that at the Myitkyina station under RCP4.5, the projection of all GMS shows the lowest annual and seasonal stream flow change for the 2050s and 2080s. All GCMs are interactively coupled with aerosol models to represent their direct 77 and indirect effects with a new cloud

microphysics scheme but their projections are different due to cloud concentration (Zeng et al., 2014)

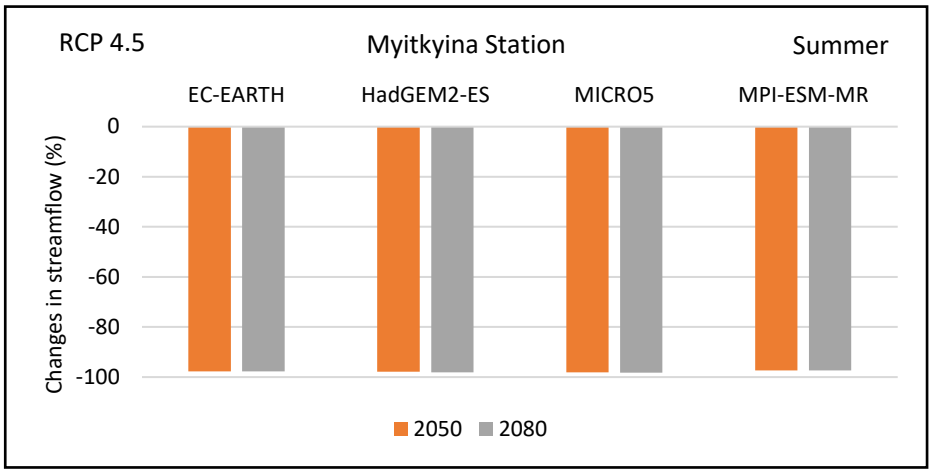

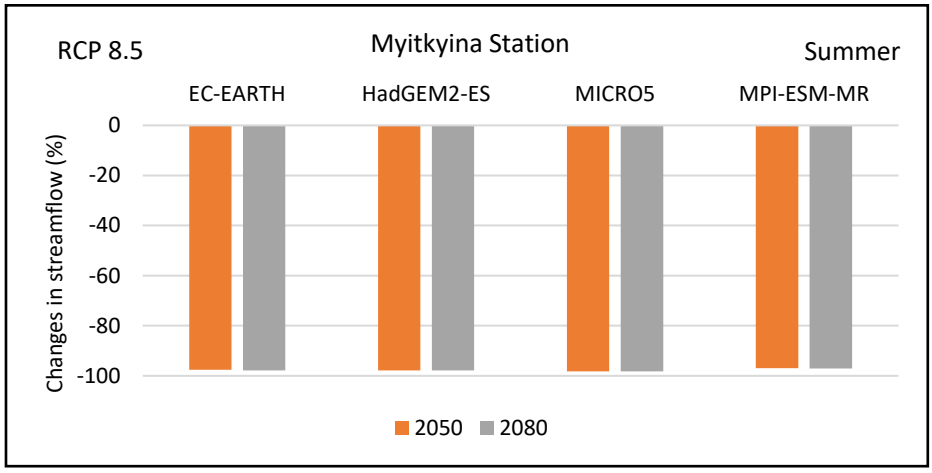

Figure 7.3(a). Percentage changes in seasonal (summer) average stream flow due to various GCMs for future periods and scenarios with respect to the baseline period 1989-2018 at Myitkyina station

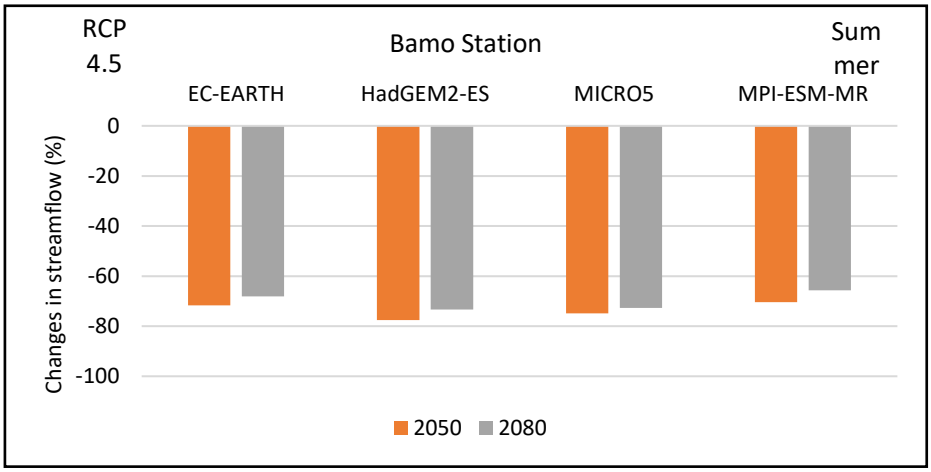

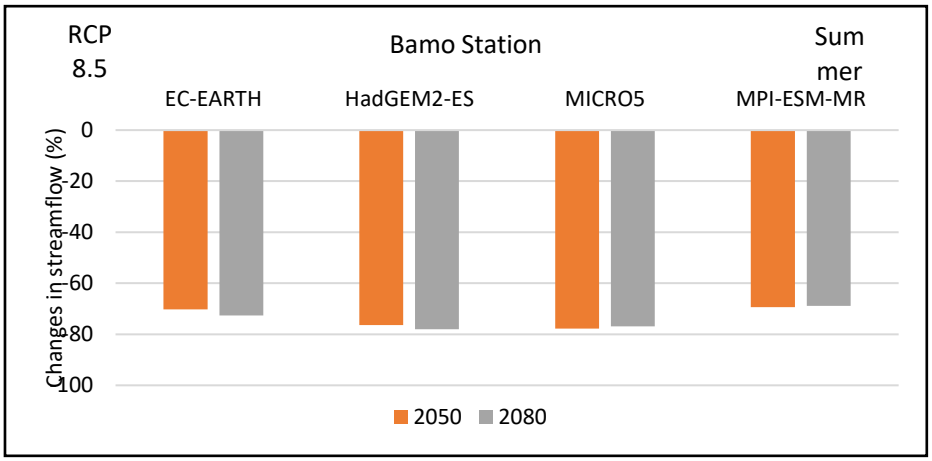

Figure 7.3(b). Percentage changes in seasonal (summer) average stream flow due to various GCMs for future periods and scenarios with respect to the baseline period 1989-2018 at Bamo station

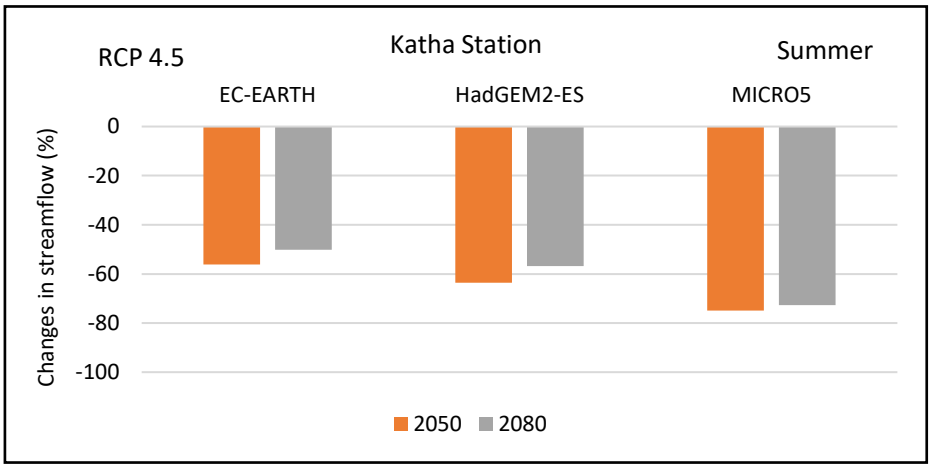

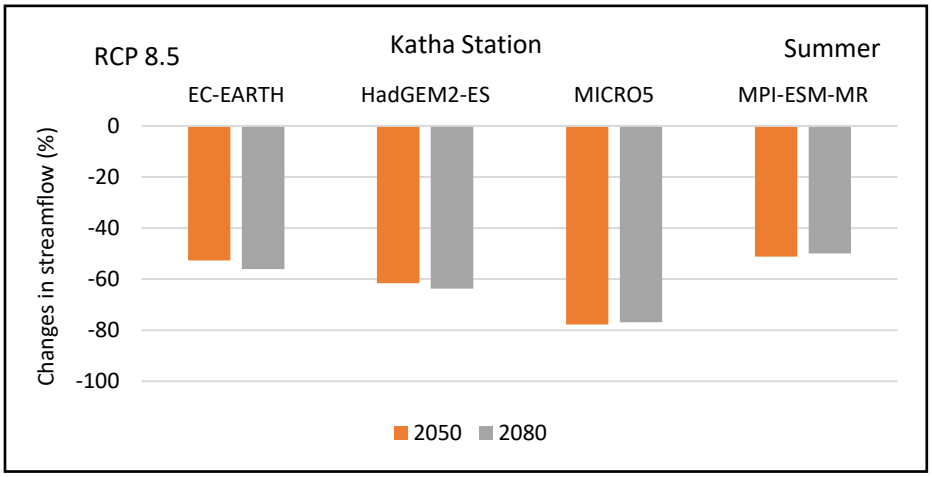

Figure 7.3(c). Percentage changes in seasonal (summer) average stream flow due to various GCMs for future periods and scenarios with respect to the baseline period 1989-2018 at Katha station

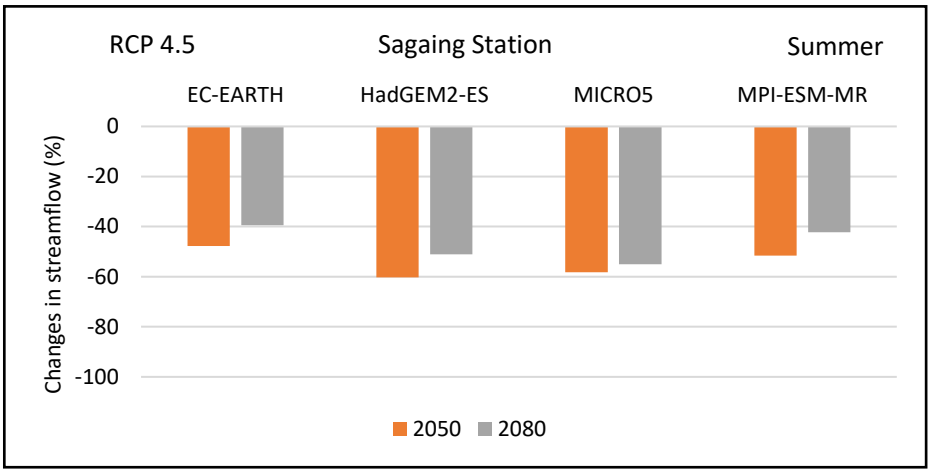

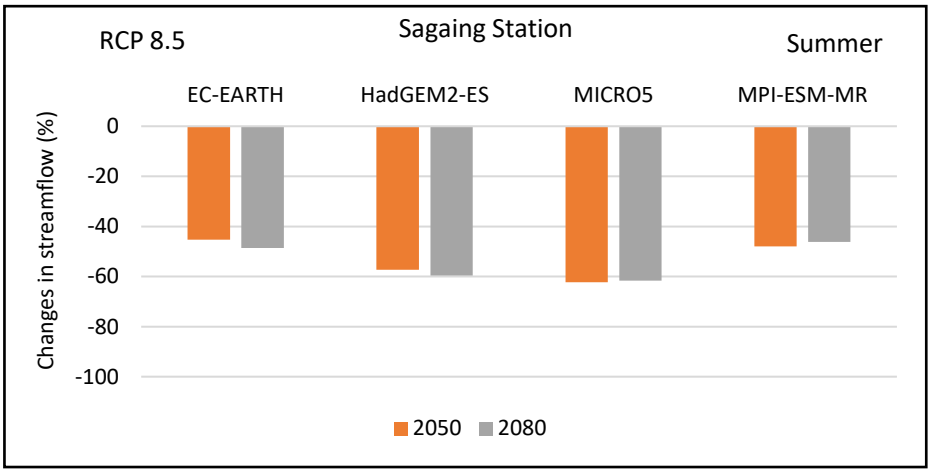

Figure 7.3(d). Percentage changes in seasonal (summer) average stream flow due to various GCMs for future periods and scenarios with respect to the baseline period 1989-2018 at Sagaing station

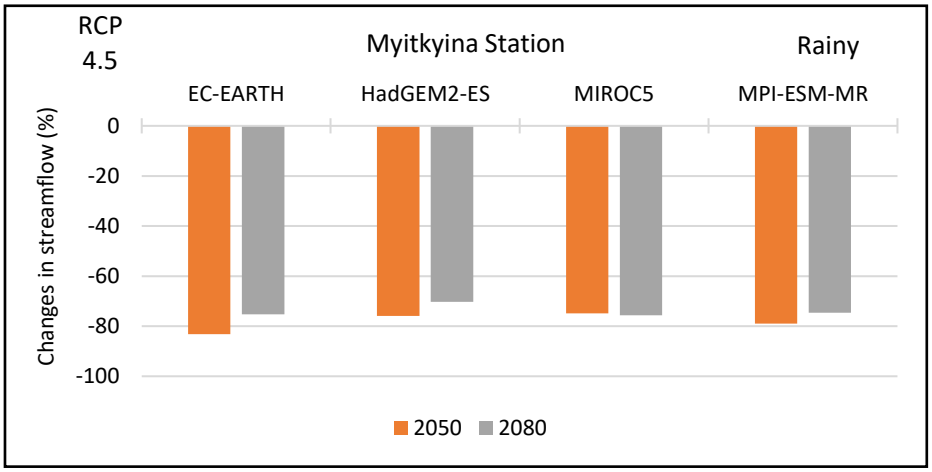

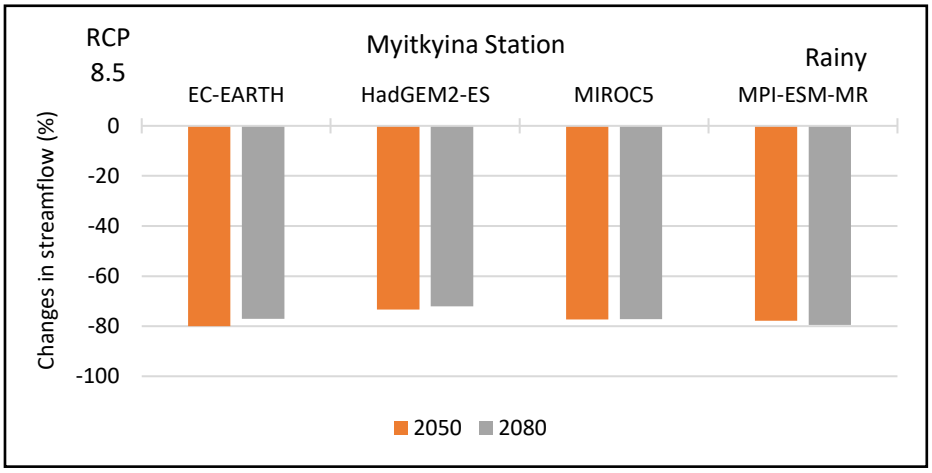

Figure 7.3(e). Percentage changes in seasonal (rainy) average stream flow due to various GCMs for future periods and scenarios with respect to the baseline period 1989-2018 at Myitkyina

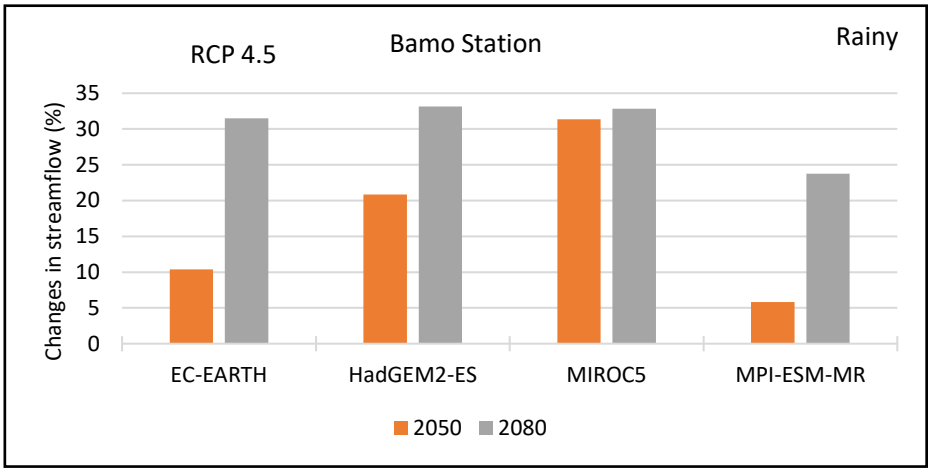

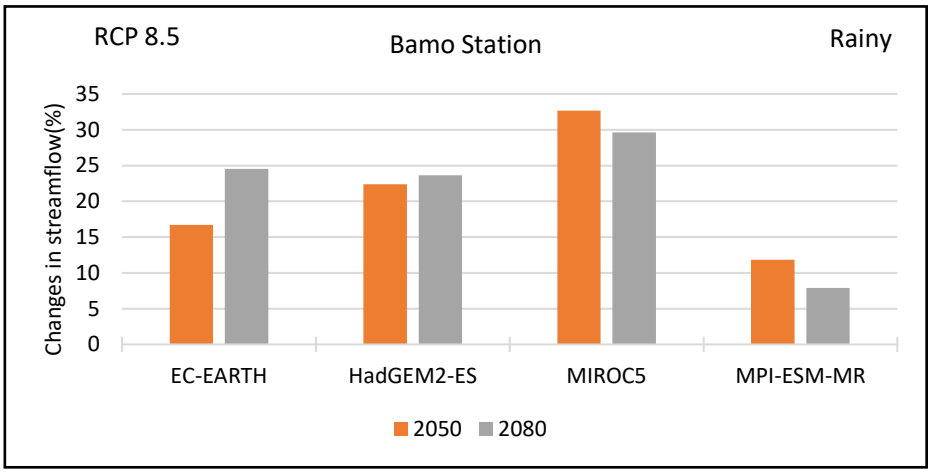

Figure 7.3(f). Percentage changes in seasonal (rainy) average stream flow due to various GCMs for future periods and scenarios with respect to the baseline period 1989-2018 at Bamo station

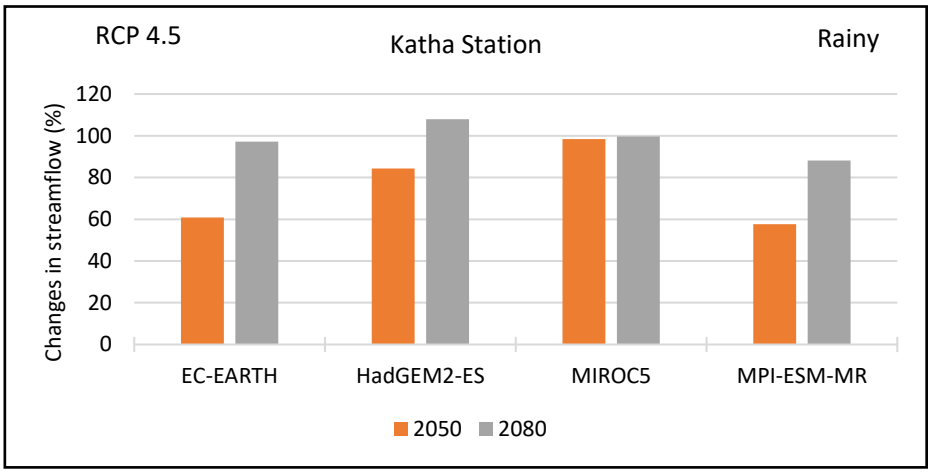

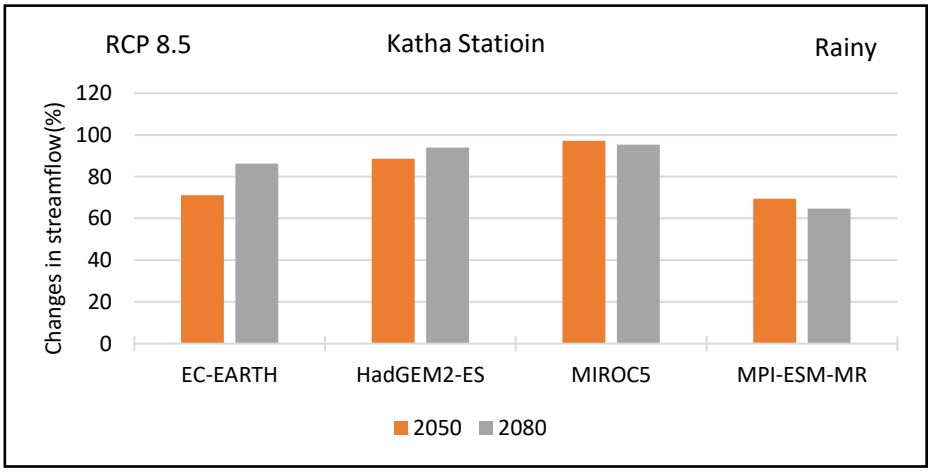

Figure 7.3(g). Percentage changes in seasonal (rainy) average stream flow due to various GCMs for future periods and scenarios with respect to the baseline period 1989-2018 at Katha station

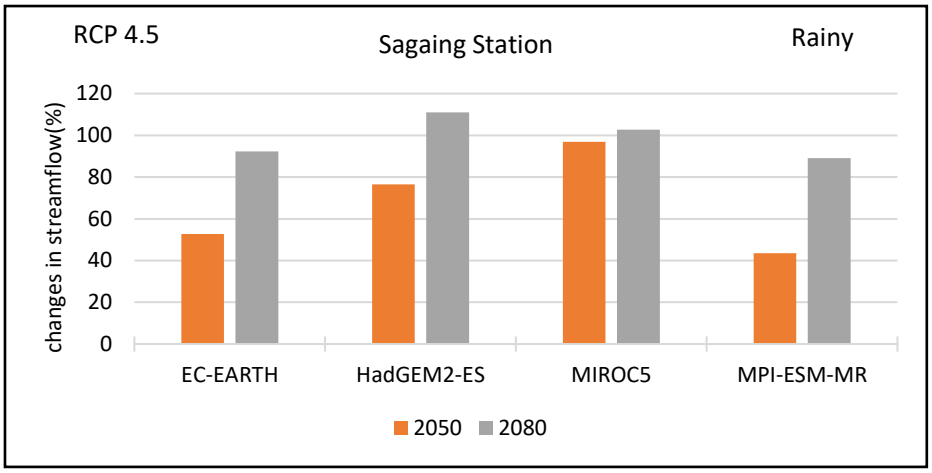

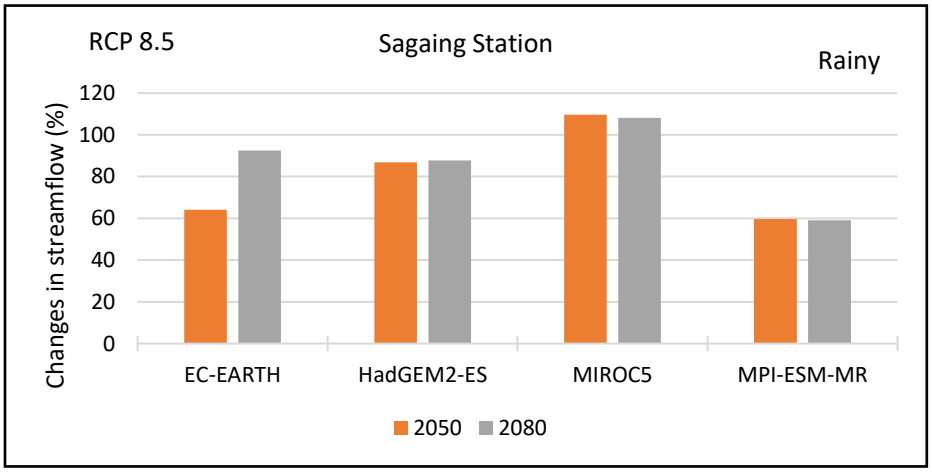

Figure 7.3(h). Percentage changes in seasonal (rainy) average stream flow due to various GCMs for future periods and scenarios with respect to the baseline period 1989-2018 at Sagaing station

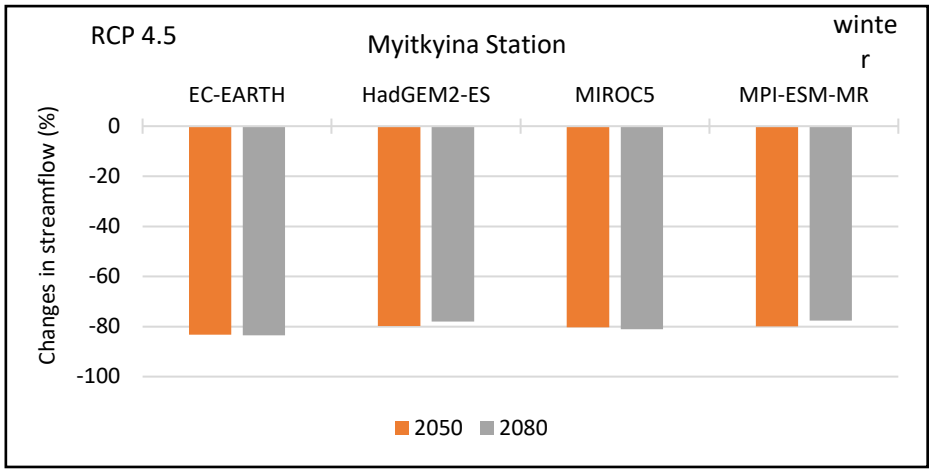

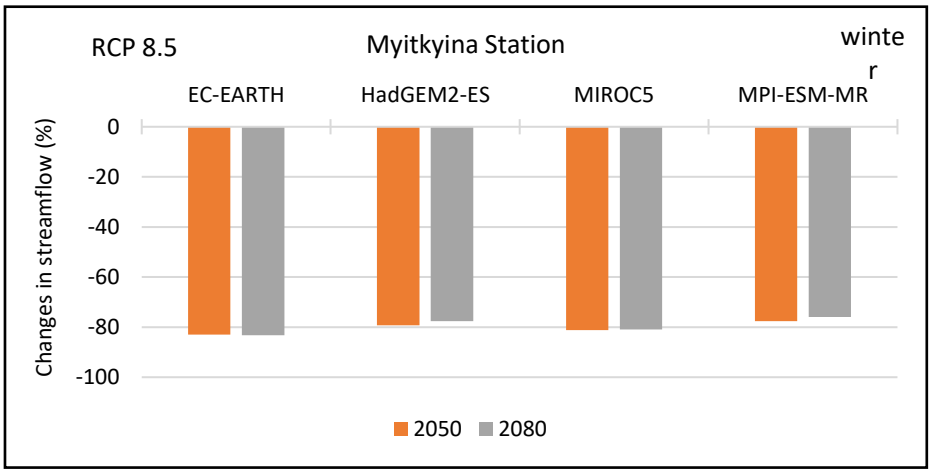

Figure 7.3(i). Percentage changes in seasonal (winter) average stream flow due to various GCMs for future periods and scenarios with respect to the baseline period 1989-2018 at Myitkyina station

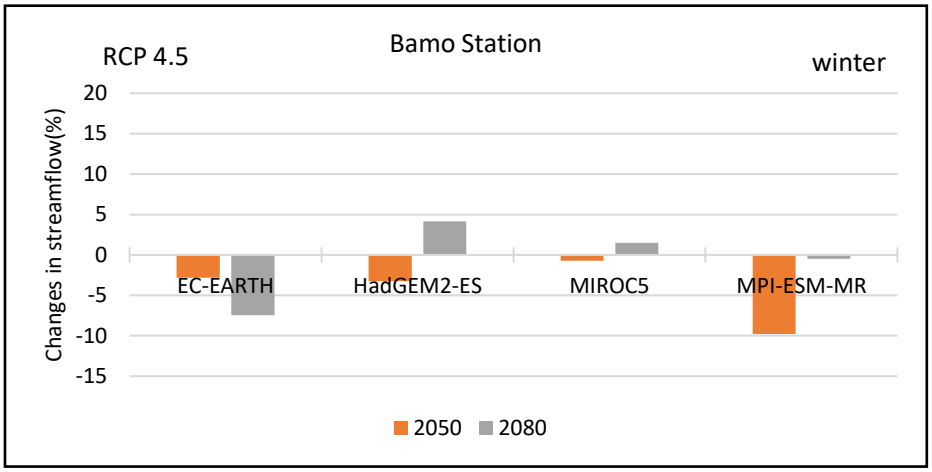

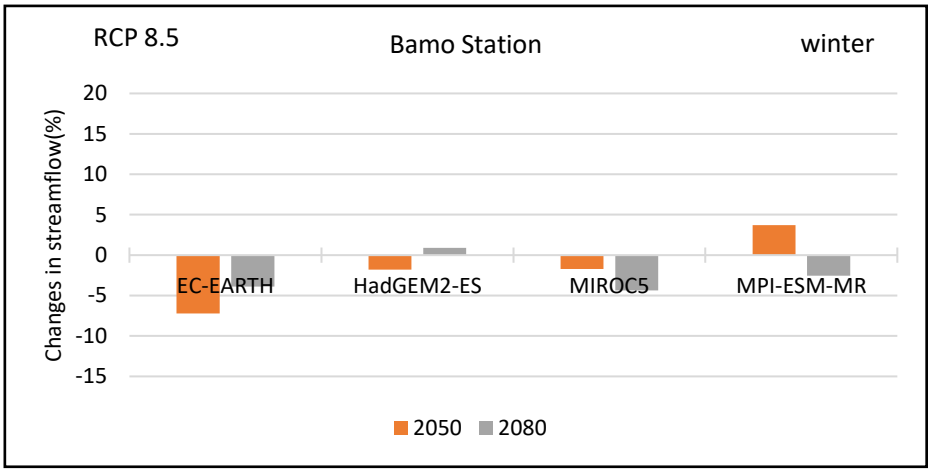

Figure 7.3(j). Percentage changes in seasonal (winter) average stream flow due to various GCMs for future periods and scenarios with respect to the baseline period 1989-2018 at Bamo station

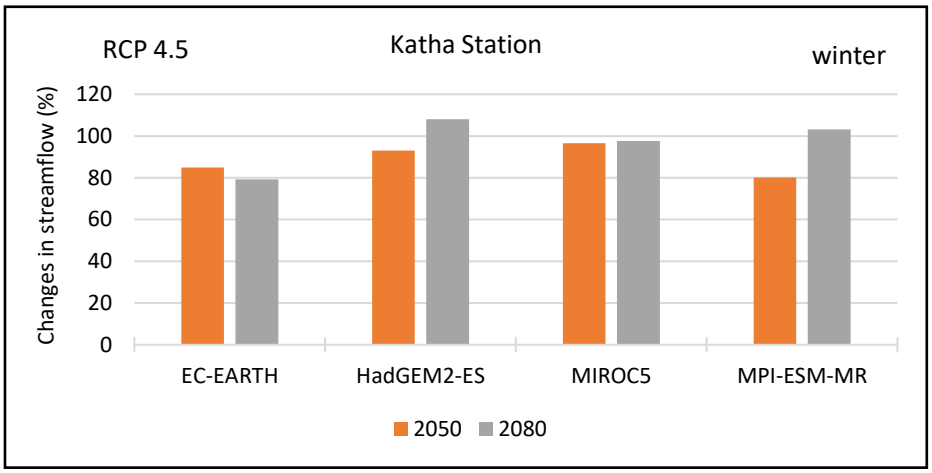

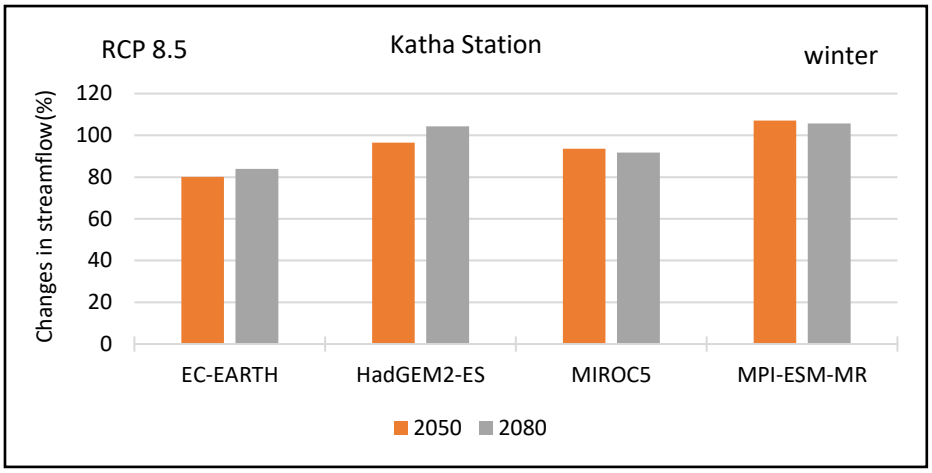

Figure 7.3(k). Percentage changes in seasonal (winter) average stream flow due to various GCMs for future periods and scenarios with respect to the baseline period 1989-2018 at Katha station

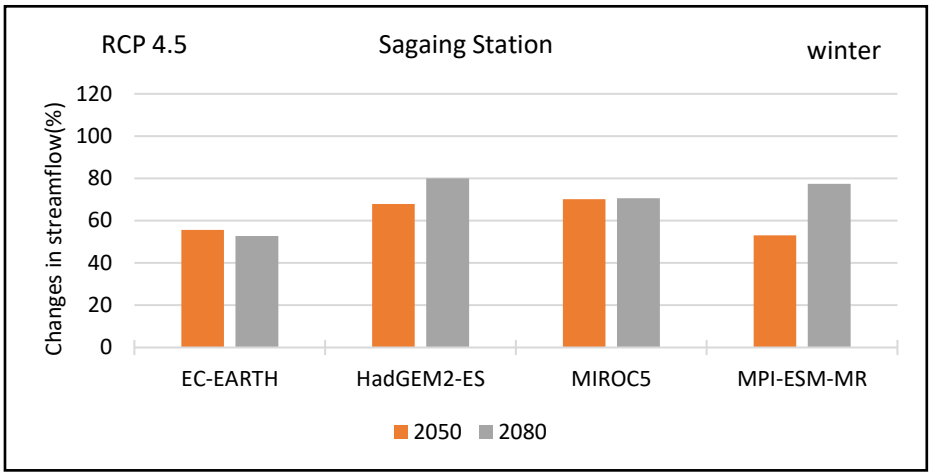

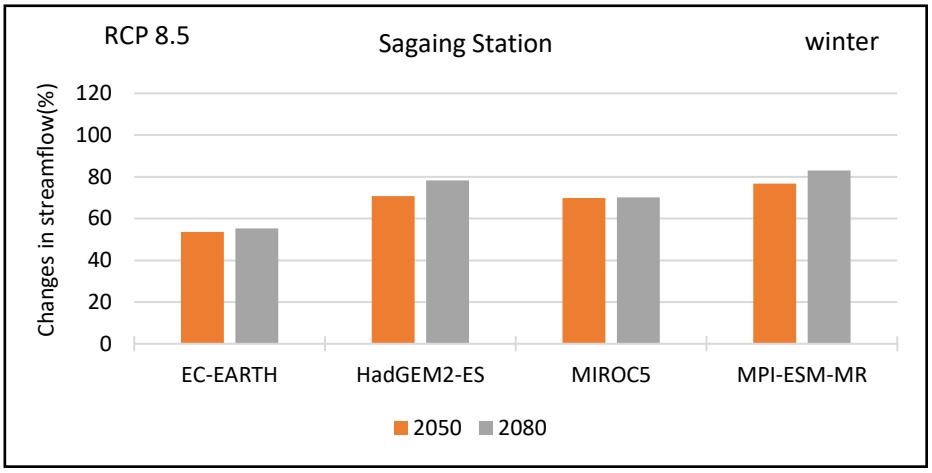

Figure 7.3(l). Percentage changes in seasonal (winter) average stream flow due to various GCMs for future periods and scenarios with respect to the baseline period 1989-2018 at Sagaing station

7.2 Uncertainty in Stream Flow Projections

7.2.1 Uncertainty in Annual Streamflow Projections under two scenarios

This section aims to outline the range of uncertainty arising from the difference in projection of various GCMs under two emission scenarios. The uncertainty range is estimated as cluster plots. All GCMs under each of the two scenarios indicate increases in stream flow change in annual projections at the four stations as shown in the figures below. The average annual stream flow projection changes due to four GCMs under both scenarios for two periods relative to the baseline at the four stations are presented in Figure 7.4. By checking the highest changes in stream flow projection, the HadGEM2-ES model shows the highest projection for stream flow changes in the 2050s and 2080s under both scenarios. On the other hand, the EC-EARTH, MICRO5 and MPI-ESM-MR models also similar projected stream flow changes in all periods under both scenarios. By comparing all GCMs, all their projections are very different in all periods. The uncertainty range for all GCMs at the all stations under RCP4.5 and 8.5 is presented in Figure 7.4. The uncertainty is observed in the HadGEM2-ES model at the highest level (42%) for the 2050s and 2050s at the Bago stations while the other models are observed below 35%. The stream flow projection changes of other GCMs are not very high. Because of GCM uncertainties, many researches stated to use various kinds of GCMs for the climate change and water resources researches. At the Bamo station, the changes in average annual stream flow projection due to four GCMs under RCP4.5 and 8.5 for the 2050s, and 2080s relative to the baseline period are shown by checking for uncertainties in Figure 7.4 (b) which shows the uncertainties of all GCMs projections in all periods under RCP 4.5 and 8.5 at the Bamo station. It is proven that the HadGEM2-ES and MICRO5 models can project the maximum level of stream flow changes in all three periods under both scenarios except 2080s period of RCP4.5 and RCP 8.5 scenario. The percentage changes for uncertainty using all GCMs in Bamo station shows the highest level compared with the other stations.

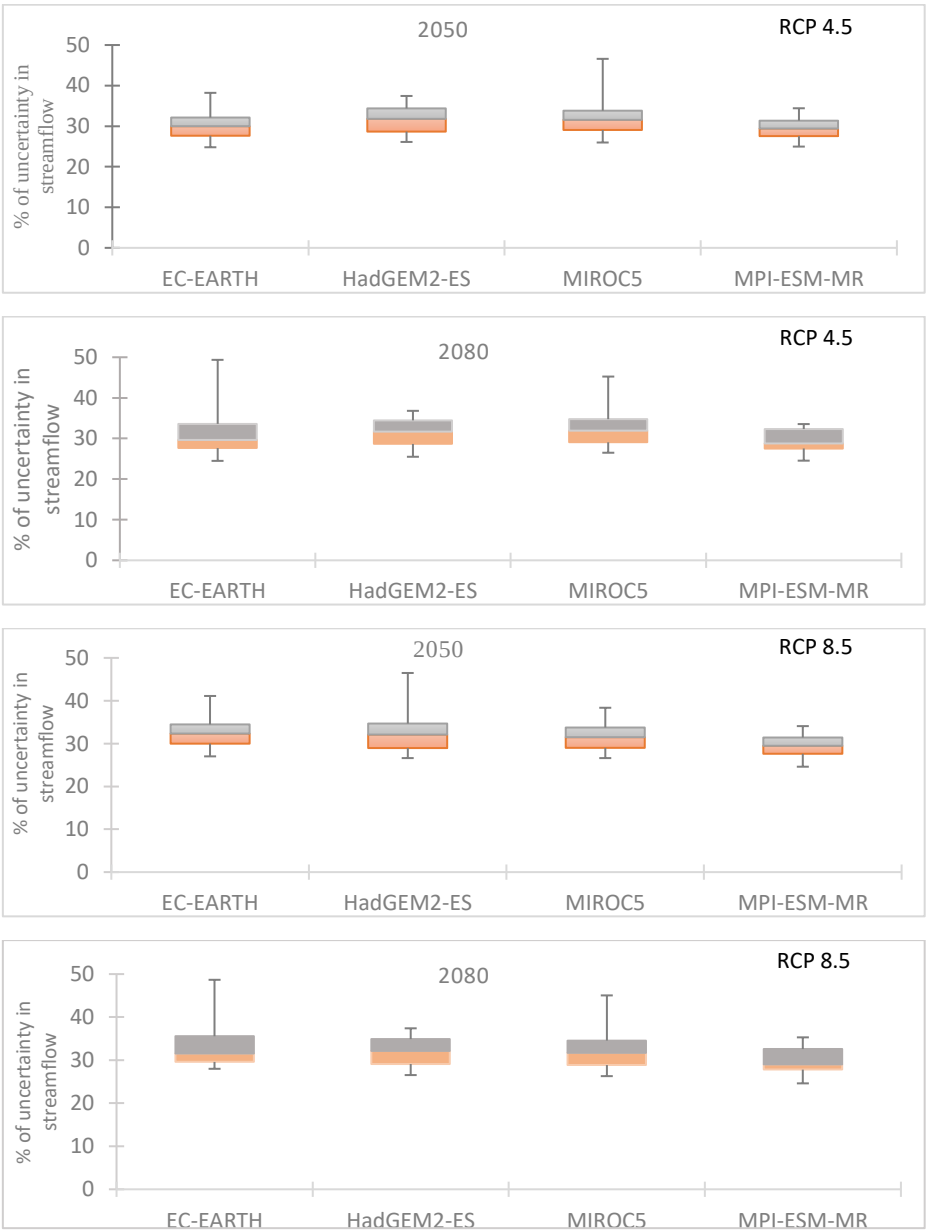

Figure 7.4(a). Percentage Changes in annual stream flow at the Myitkyina station under RCP4.5 and RCP 8.5 for the two future periods relative to the baseline period (1989-2018)

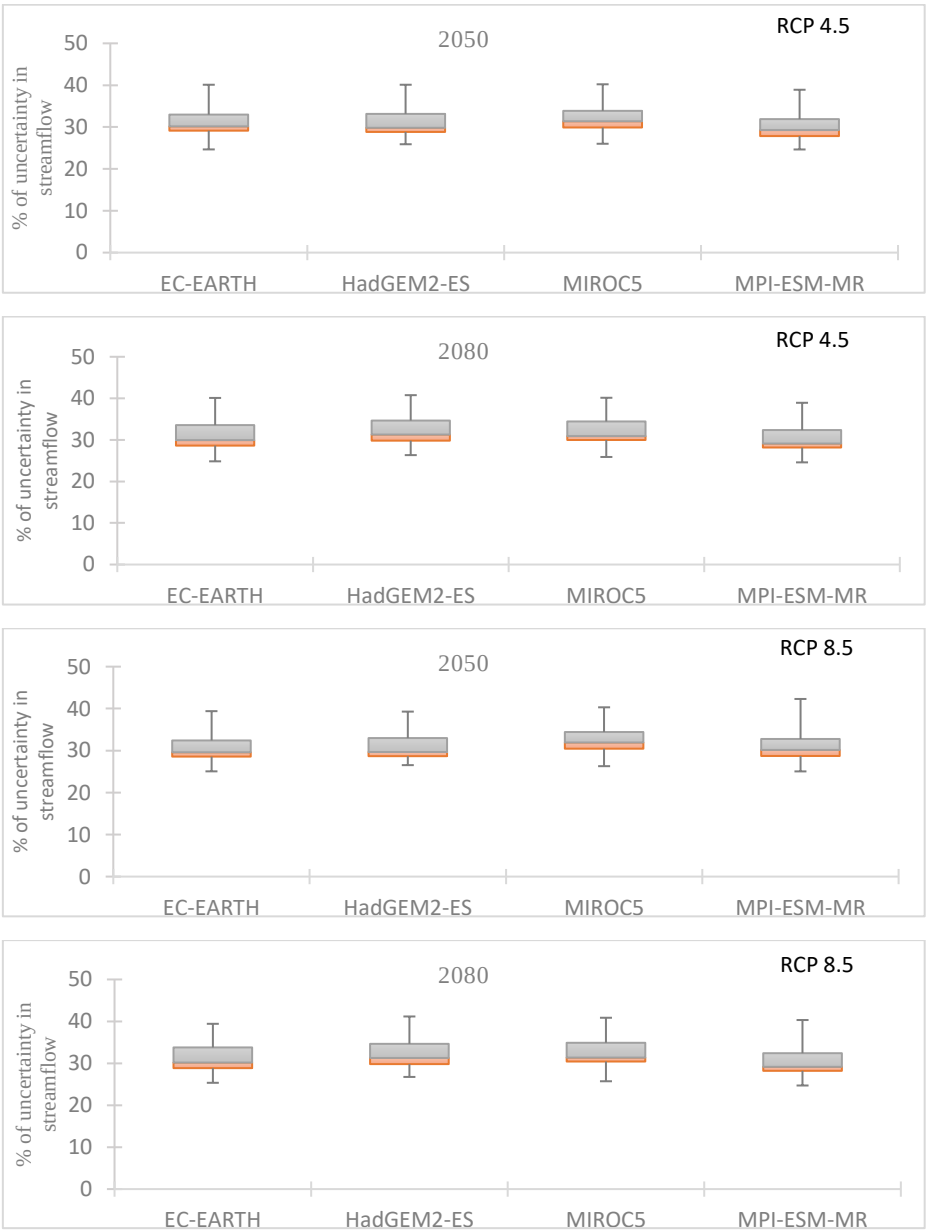

Figure 7.4(b). Percentage Changes in annual stream flow at the Bamo station under RCP4.5 and RCP 8.5 for the two future periods relative to the baseline period (1989-2018)

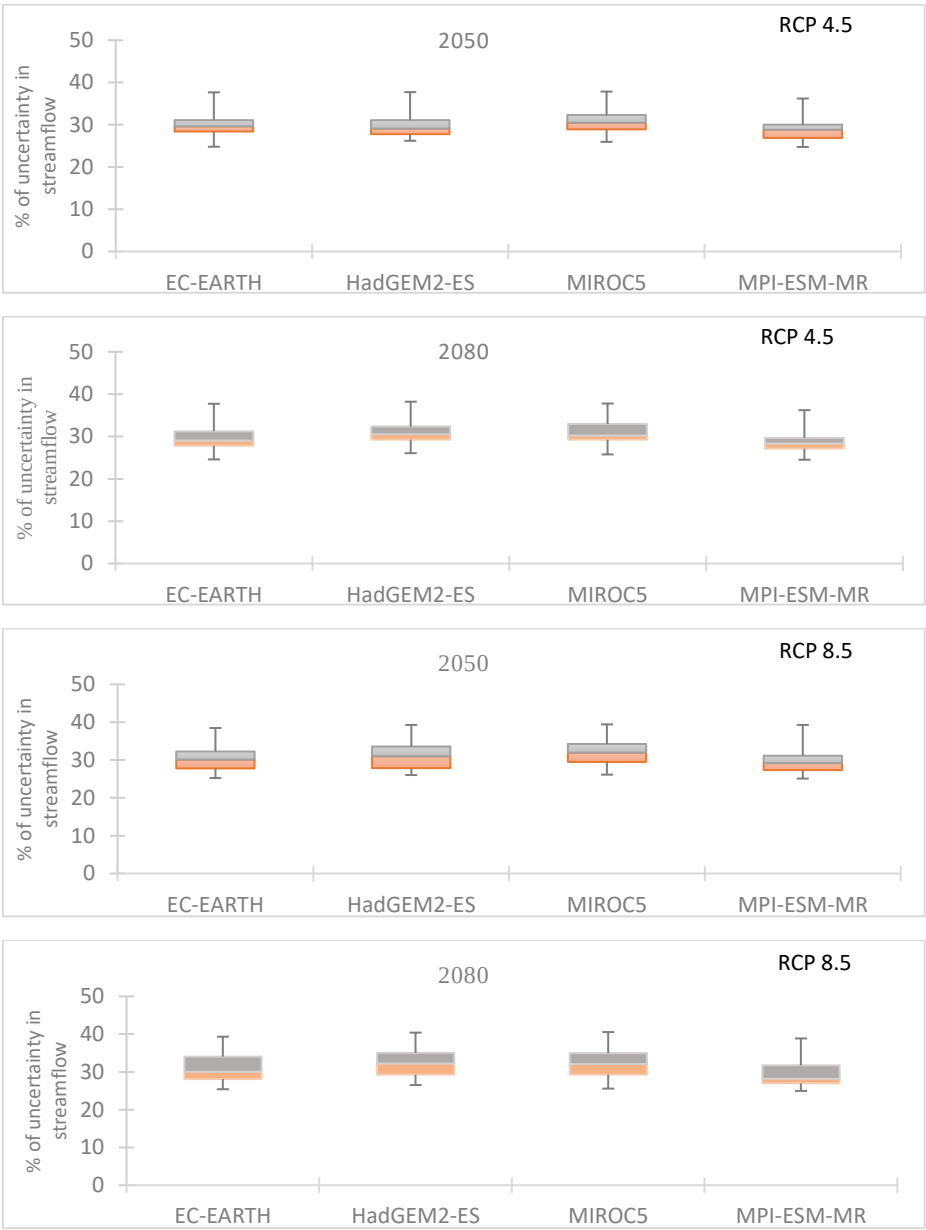

Figure 7.4(c). Percentage Changes in annual stream flow at the Katha station under RCP4.5 and RCP 8.5 for the two future periods relative to the baseline period (1989-2018)

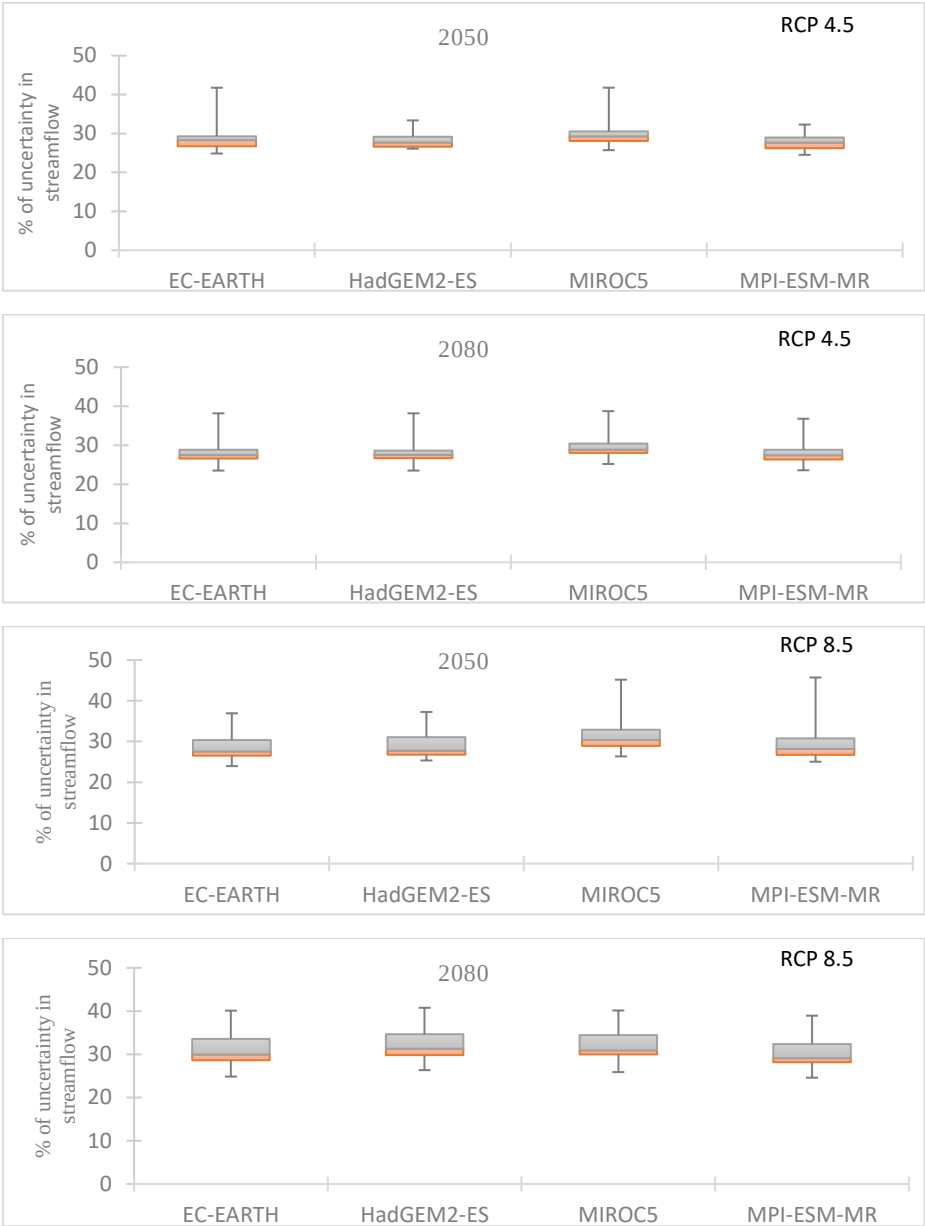

Figure 7.4(d). Percentage Changes in annual stream flow at the Sagaing station under RCP4.5 and RCP 8.5 for the two future periods relative to the baseline period (1989-2018)

7.2.3 Uncertainty in Seasonal Streamflow Projections Under Two Scenarios

The range of changes for uncertainty in seasonal and annual projections under the two scenarios RCP4.5 and RCP8.5 from their respective GCMs for the four stations are shown in Figure 7.5. According to these results, for the summer season, stream flow projection for all three periods indicates a highest uncertainty for projection changes of 50% in the 2050s, and 59 % in the 2080s at Myitkyina station, 39% in the 2050s, and 45 % in the 2080s at Bamo station, 38% in the 2050s, and 41 % in the 2080s at Katha station and 39% in the 2050s, and 47 % in the 2080s at Sagaing station from the baseline period although the average change in stream flow. The summer is at the highest level compared with other seasonal changes. Rainy seasonal flow shows an increased change in two periods approximately 30% at the all stations under both scenarios. The rainy season is at the lowest level of uncertainties. The winter seasonal flow projection deviates from the baseline period shows over 40% increase changes is observed in the Bamo station under both scenarios while the projection changes for the other stations show below 40%. From the results of these figures, there are uncertainty projections for annual and summer low stream flow changes for Myitkyina station and summer and winter low stream flow at Bamo station.

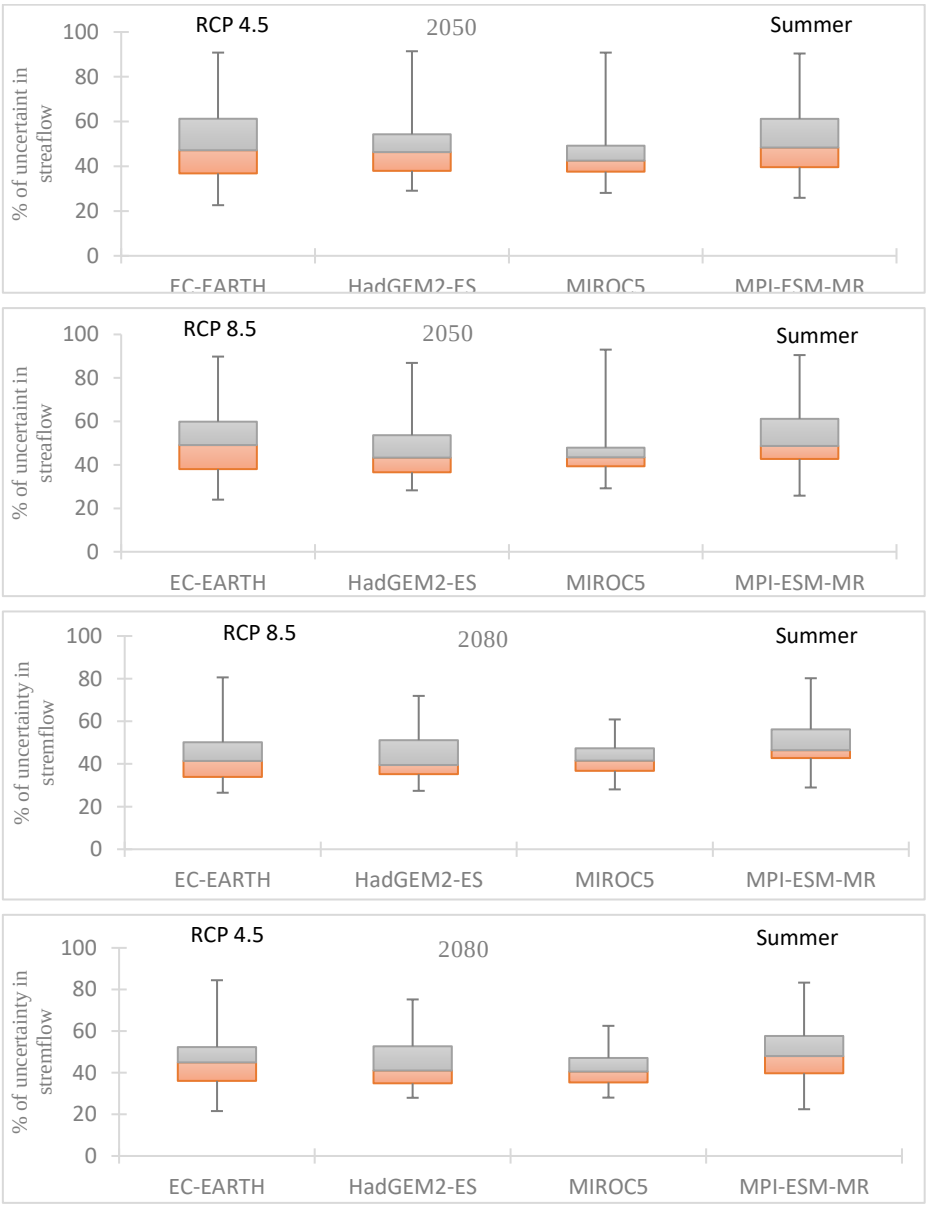

Figure 7.5(a). Percentage of uncertainty in seasonal (summer) stream flow at the Myitkyina station under RCP4.5 and RCP 8.5 for the two future periods relative to the baseline period (1989-2018)

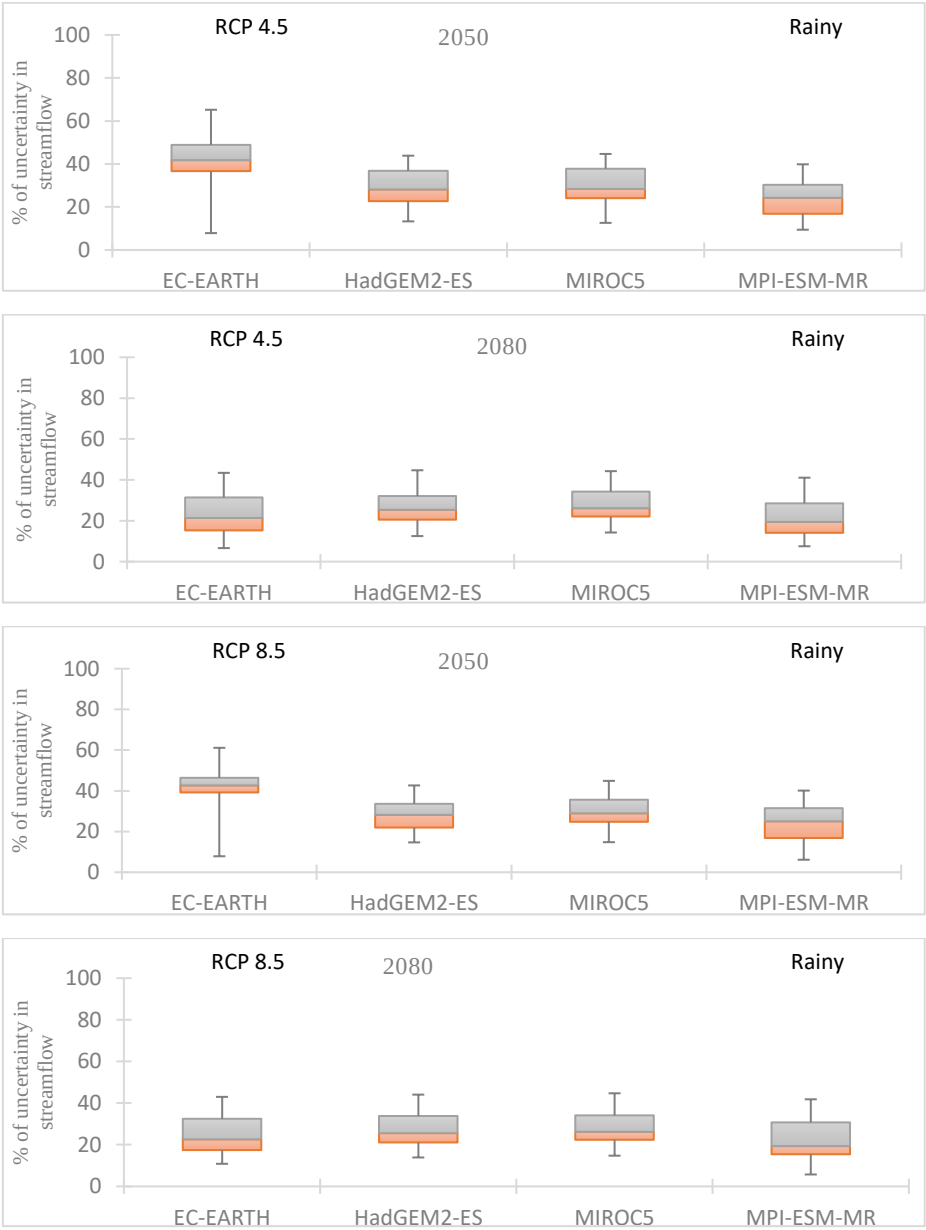

Figure 7.5(b). Percentage of uncertainty in seasonal (rainy) stream flow at the Myitkyina station under RCP4.5 and RCP 8.5 for the two future periods relative to the baseline period (1989-2018)

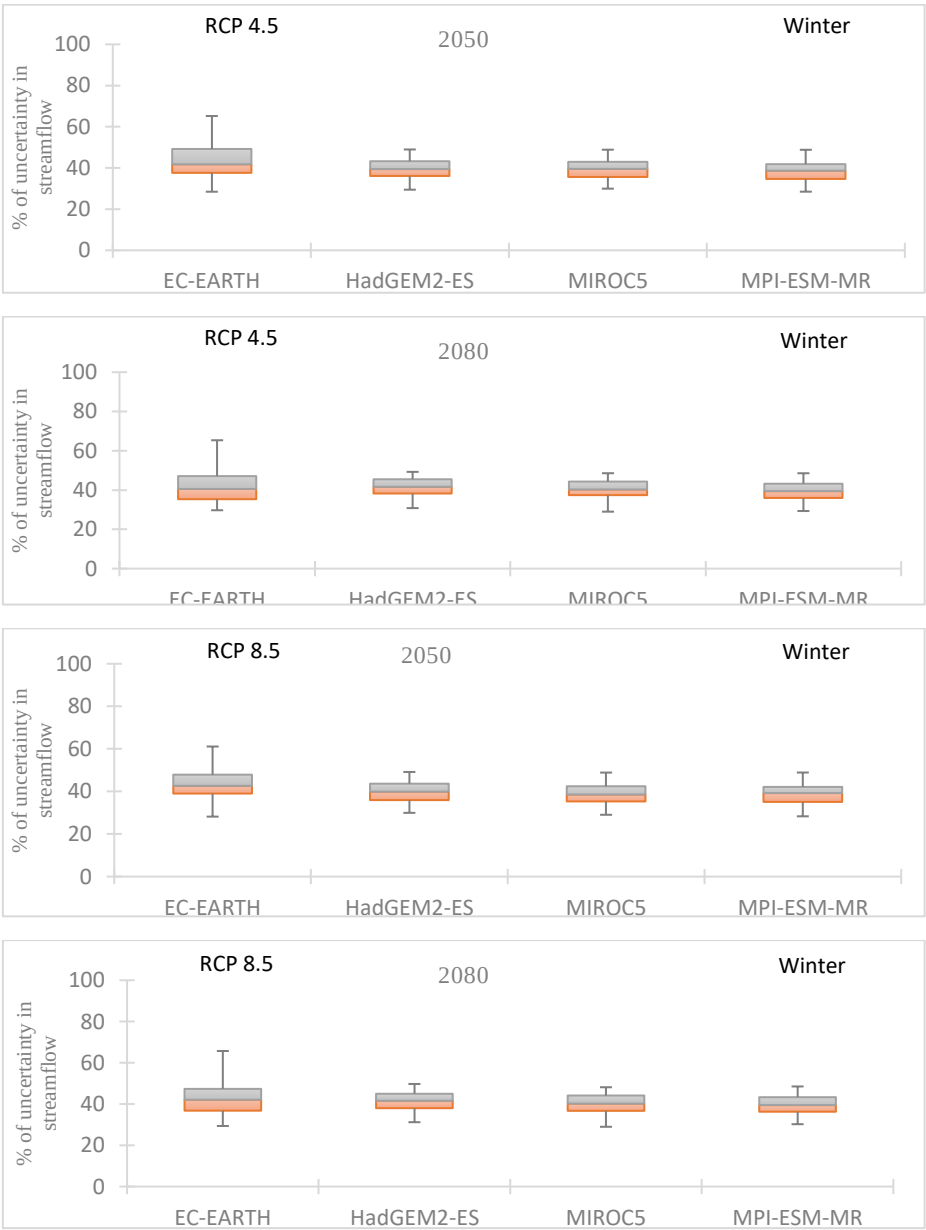

Figure 7.5 (c). Percentages of uncertainty in seasonal (winter) streamflow at the Myitkyina station under RCP4.5d and RCP 8.5 for the two future periods relative to the baseline period (1989-2018)

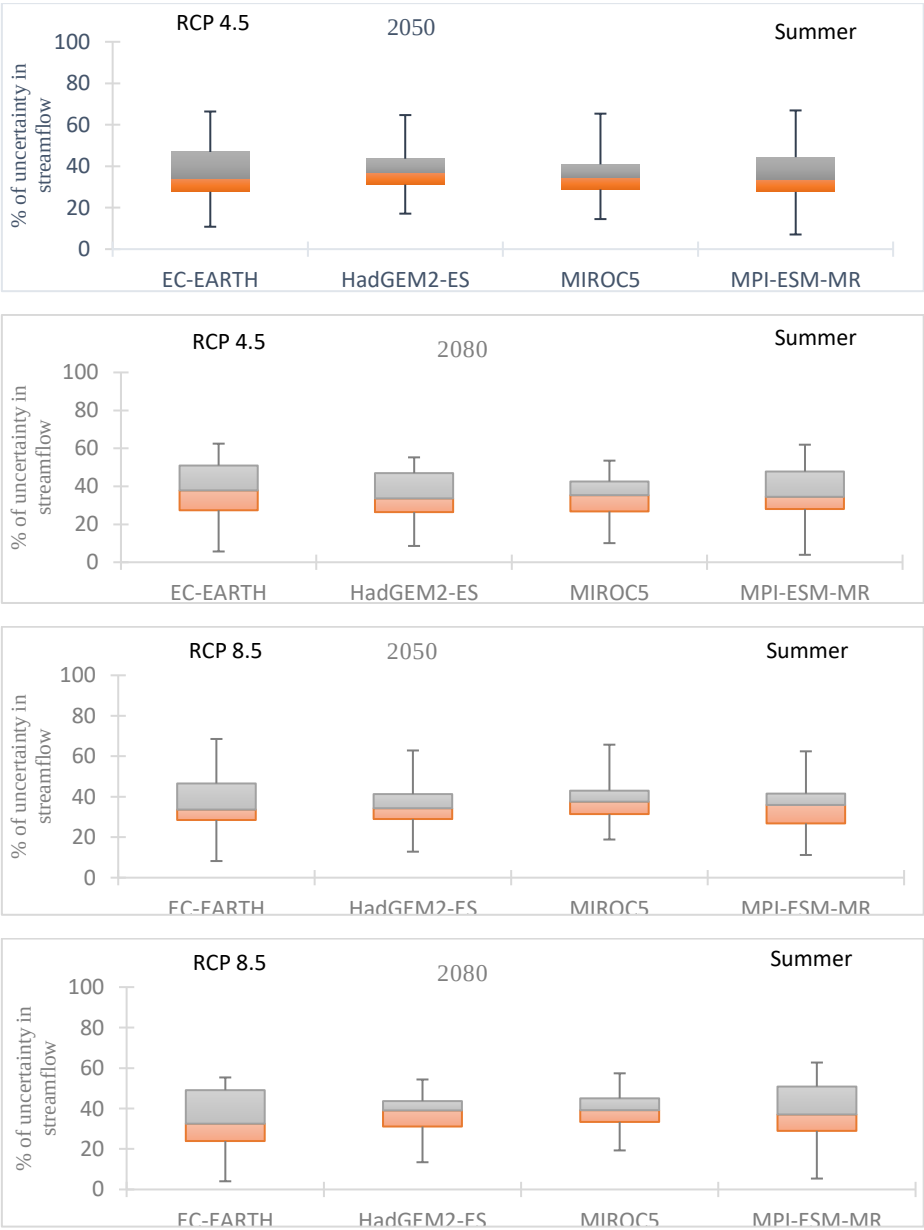

Figure 7.5(d). Percentage of uncertainty in seasonal (summer) stream flow at the Bamo station under RCP4.5 and RCP 8.5 for the two future periods relative to the baseline period (1989-2018)

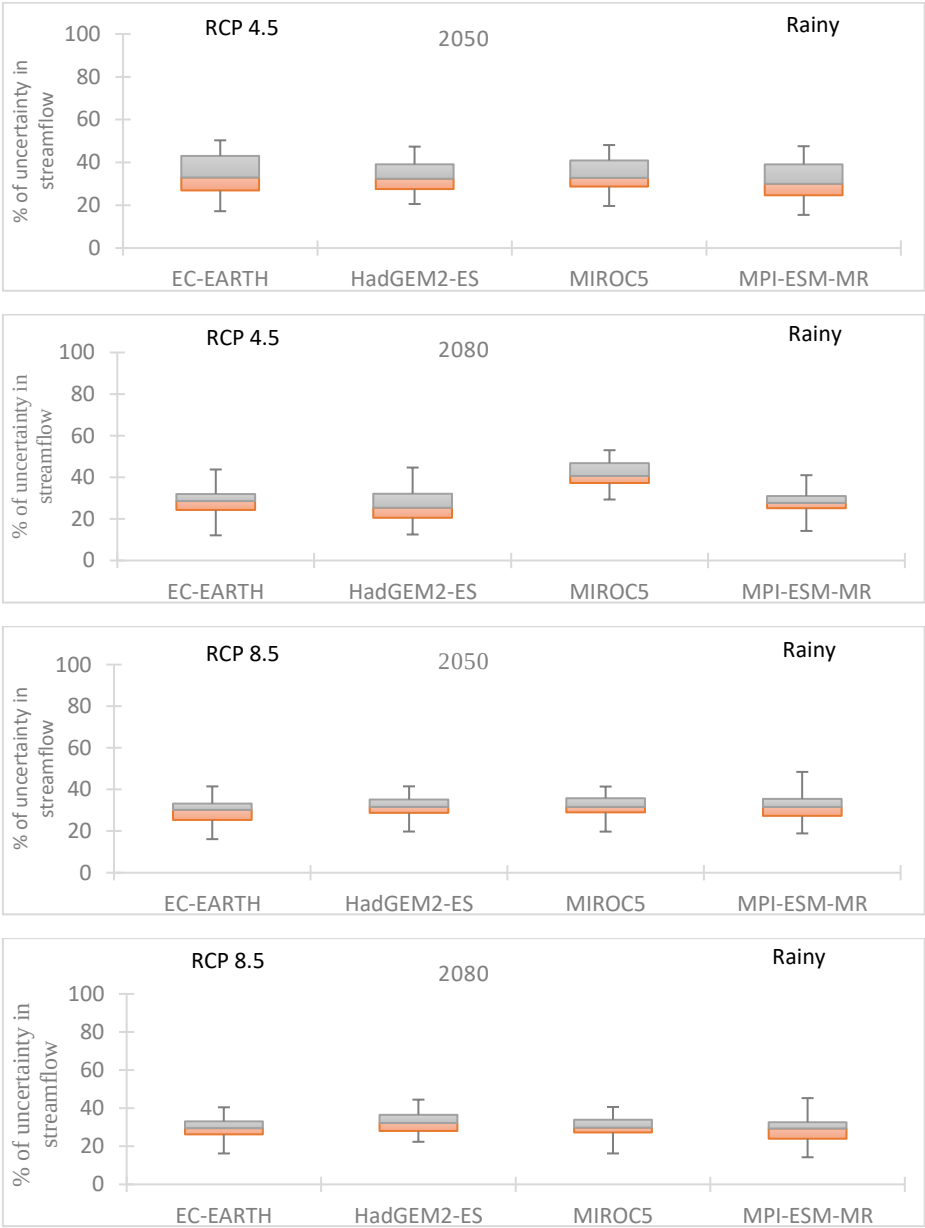

Figure 7.5(e). Percentage of uncertainty in seasonal (rainy) stream flow at the Bamo station under RCP4.5 and RCP 8.5 for the two future periods relative to the baseline period (1989-2018)

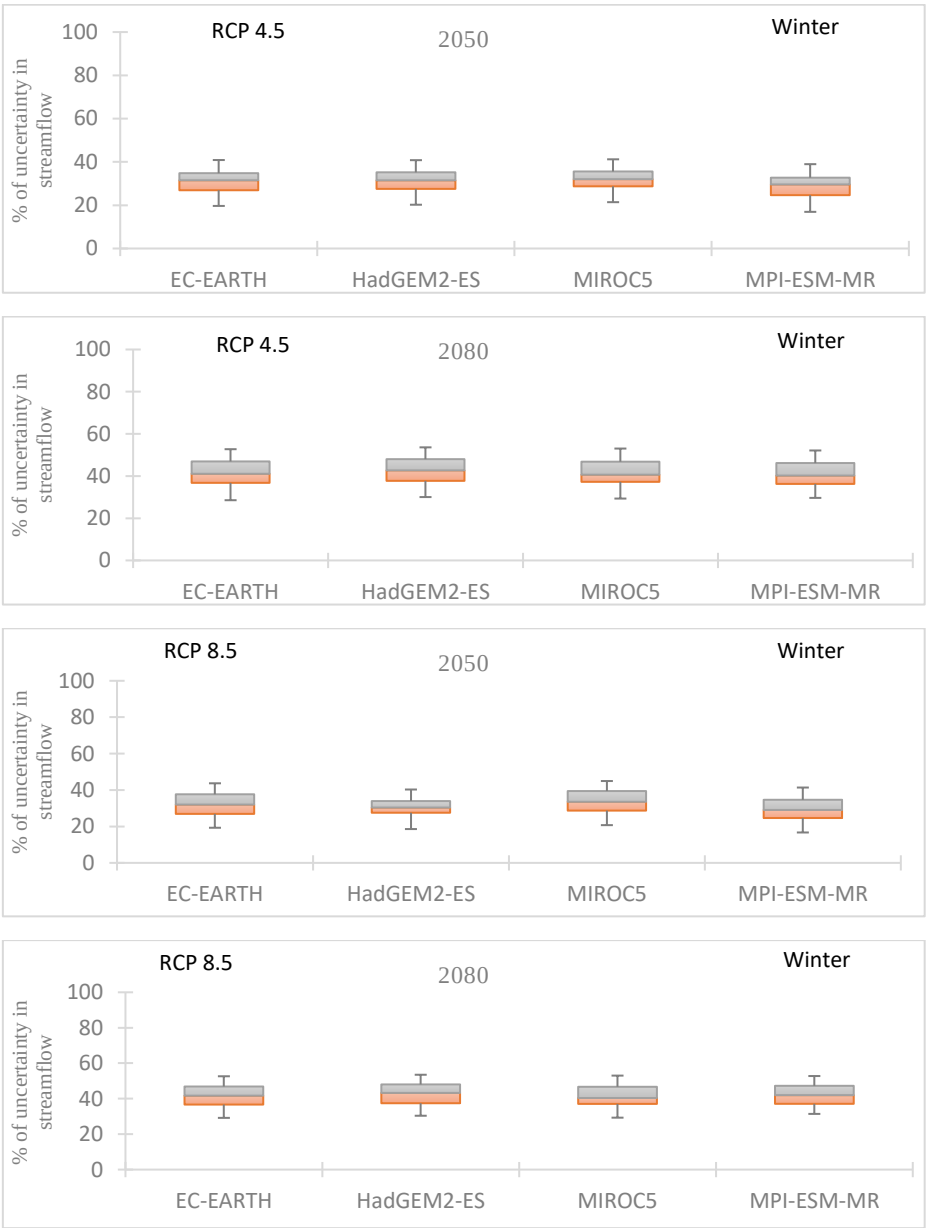

Figure 7.5(f). Percentage of uncertainty in seasonal (winter) stream flow at the Bamo station under RCP4.5 and RCP 8.5 for the two future periods relative to the baseline period (1989-2018)

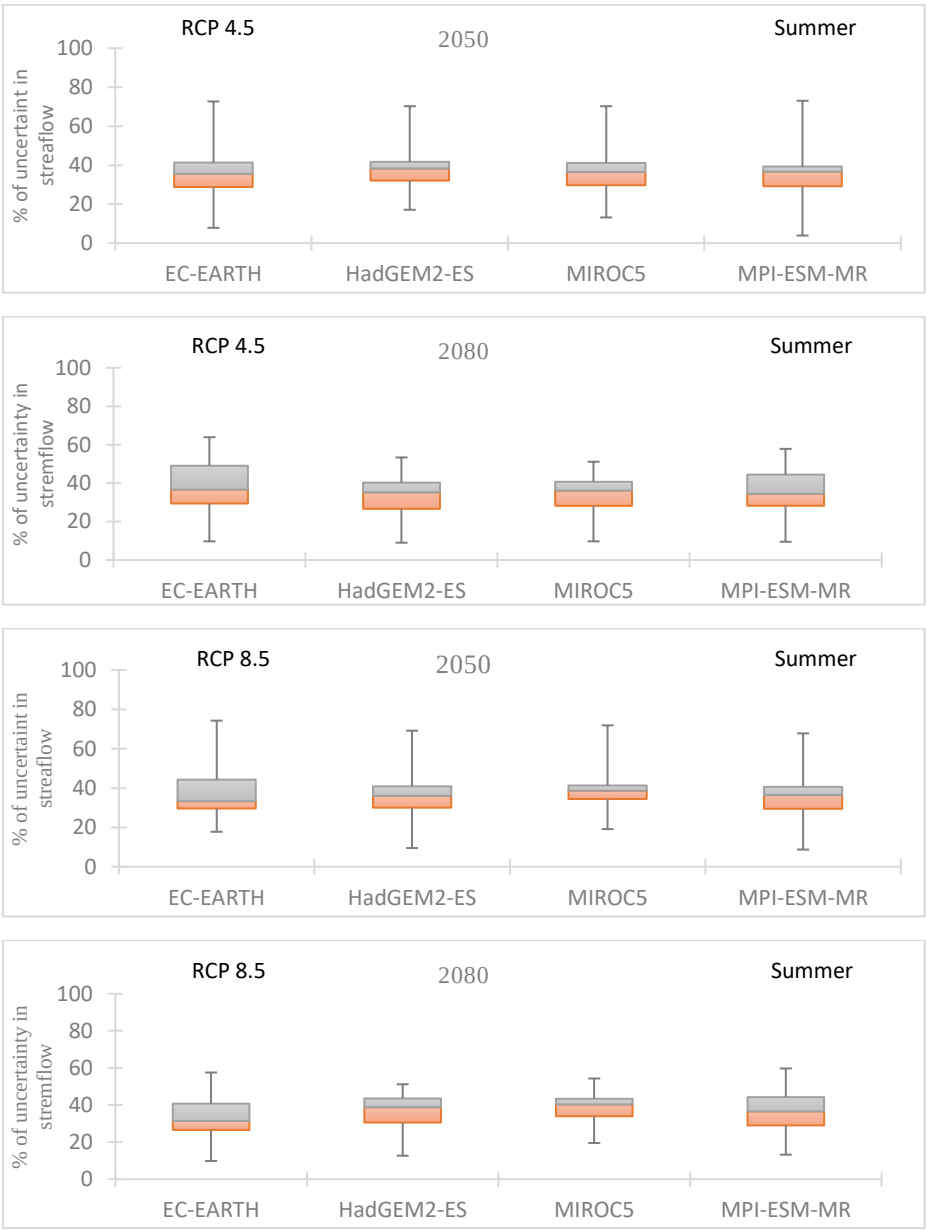

Figure 7.5(g). Percentage of uncertainty in seasonal (summer) stream flow at the Katha station under RCP4.5 and RCP 8.5 for the two future periods relative to the baseline period (1989-2018)

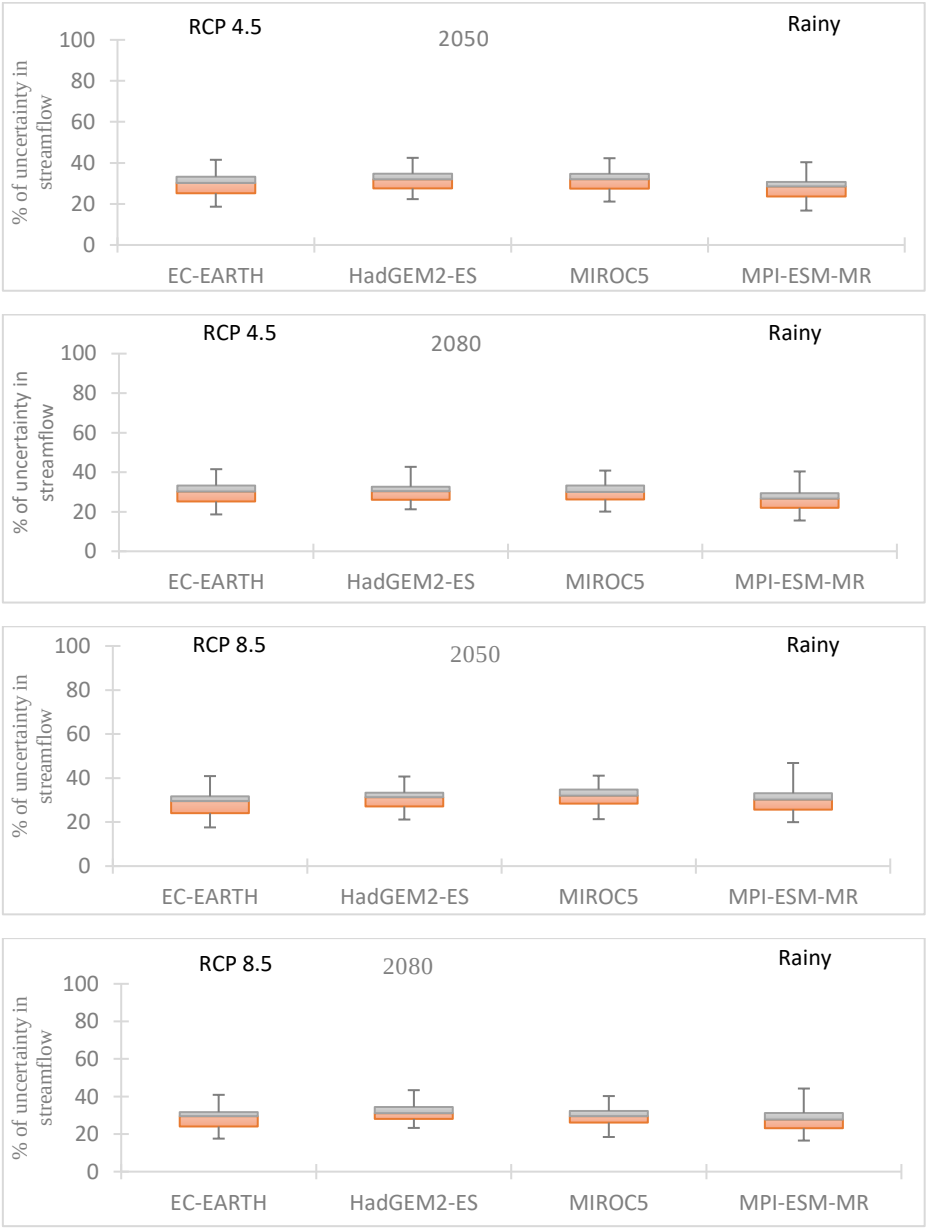

Figure 7.5(h). Percentage of uncertainty in seasonal (rainy) stream flow at the Katha station under RCP4.5 and RCP 8.5 for the two future periods relative to the baseline period (1989-2018)

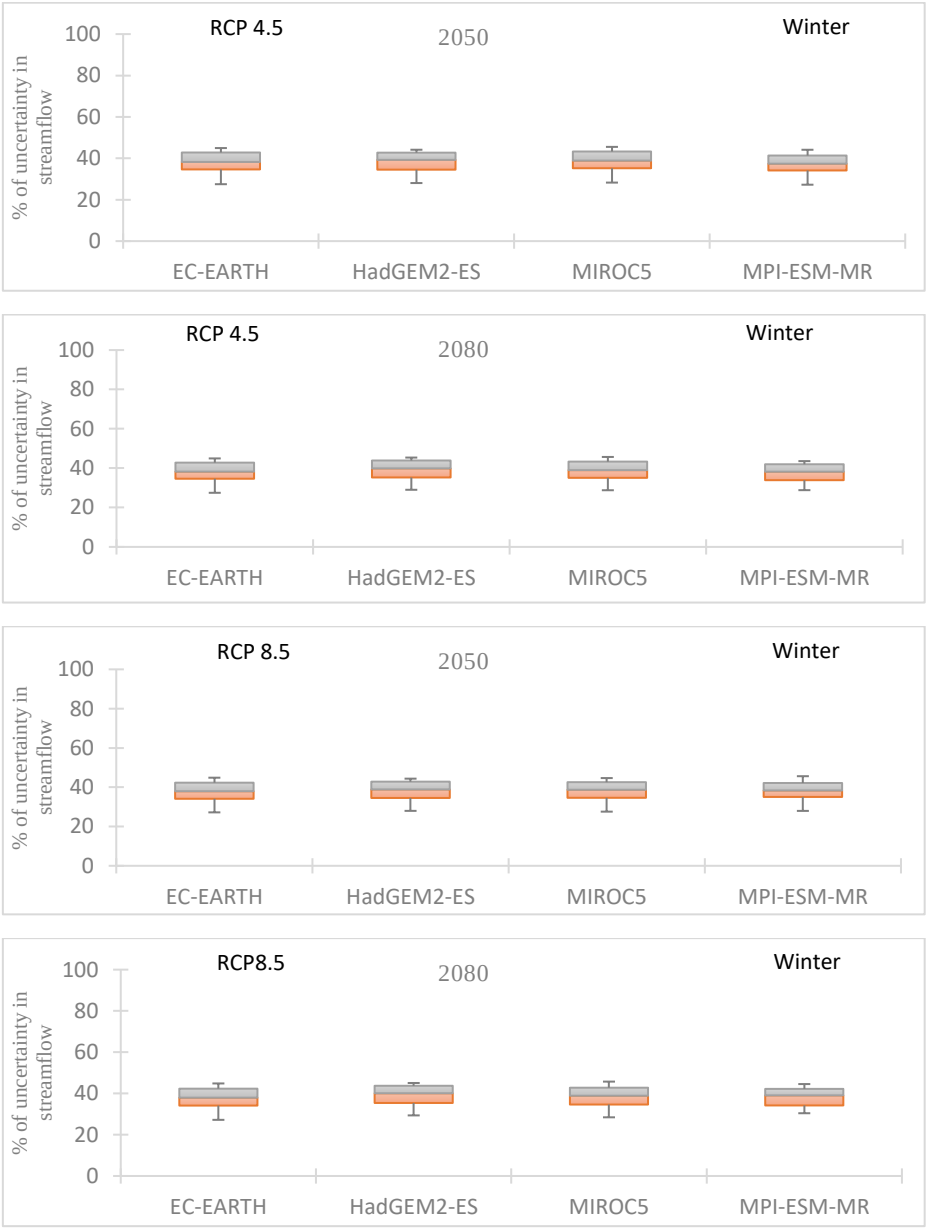

Figure 7.5(i). Percentage of uncertainty in seasonal (winter) stream flow at the Katha station under RCP4.5 and RCP 8.5 for the two future periods relative to the baseline period (1989-2018)

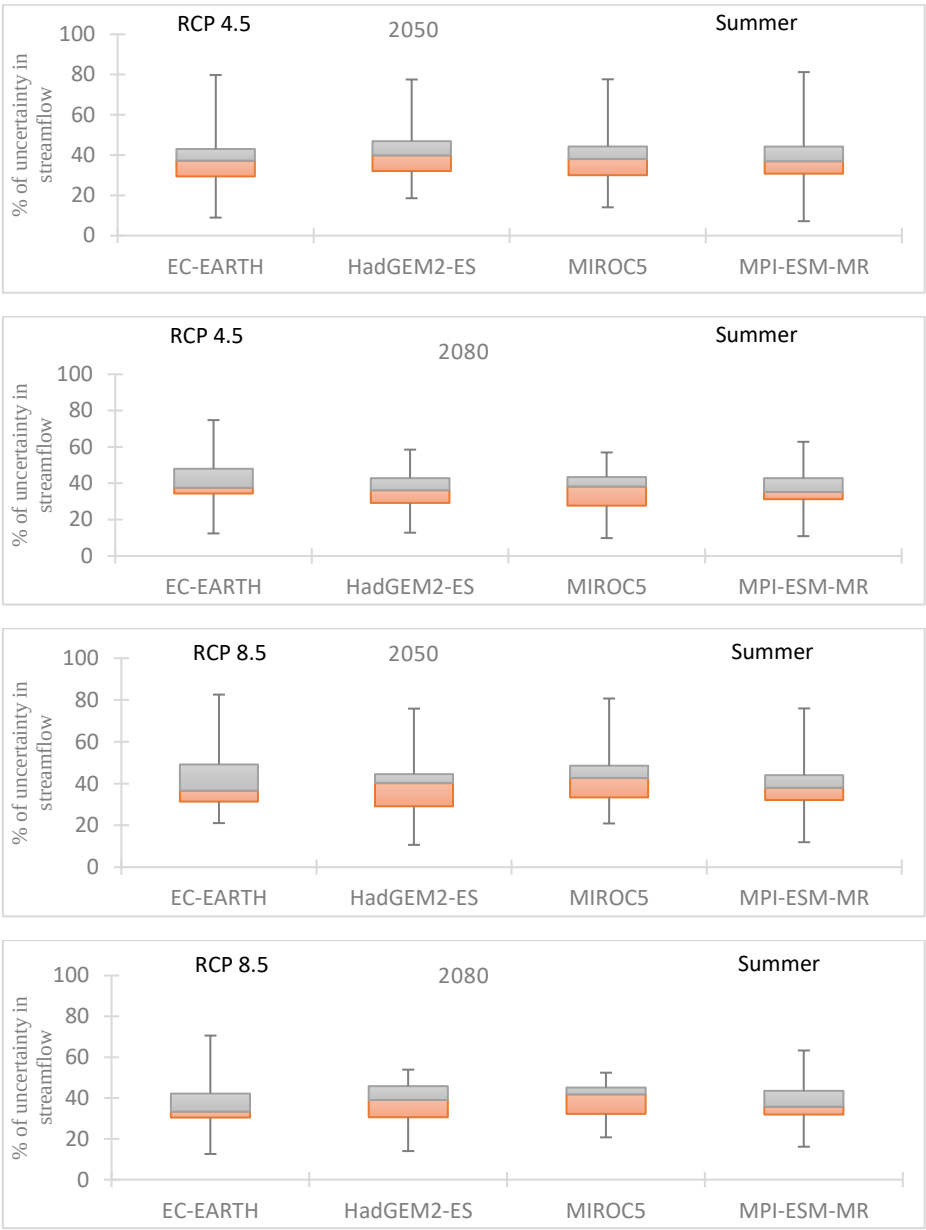

Figure 7.5(j). Percentage of uncertainty in seasonal (summer) stream flow at the Sagaing station under RCP4.5 and RCP 8.5 for the two future periods relative to the baseline period (1989-2018)

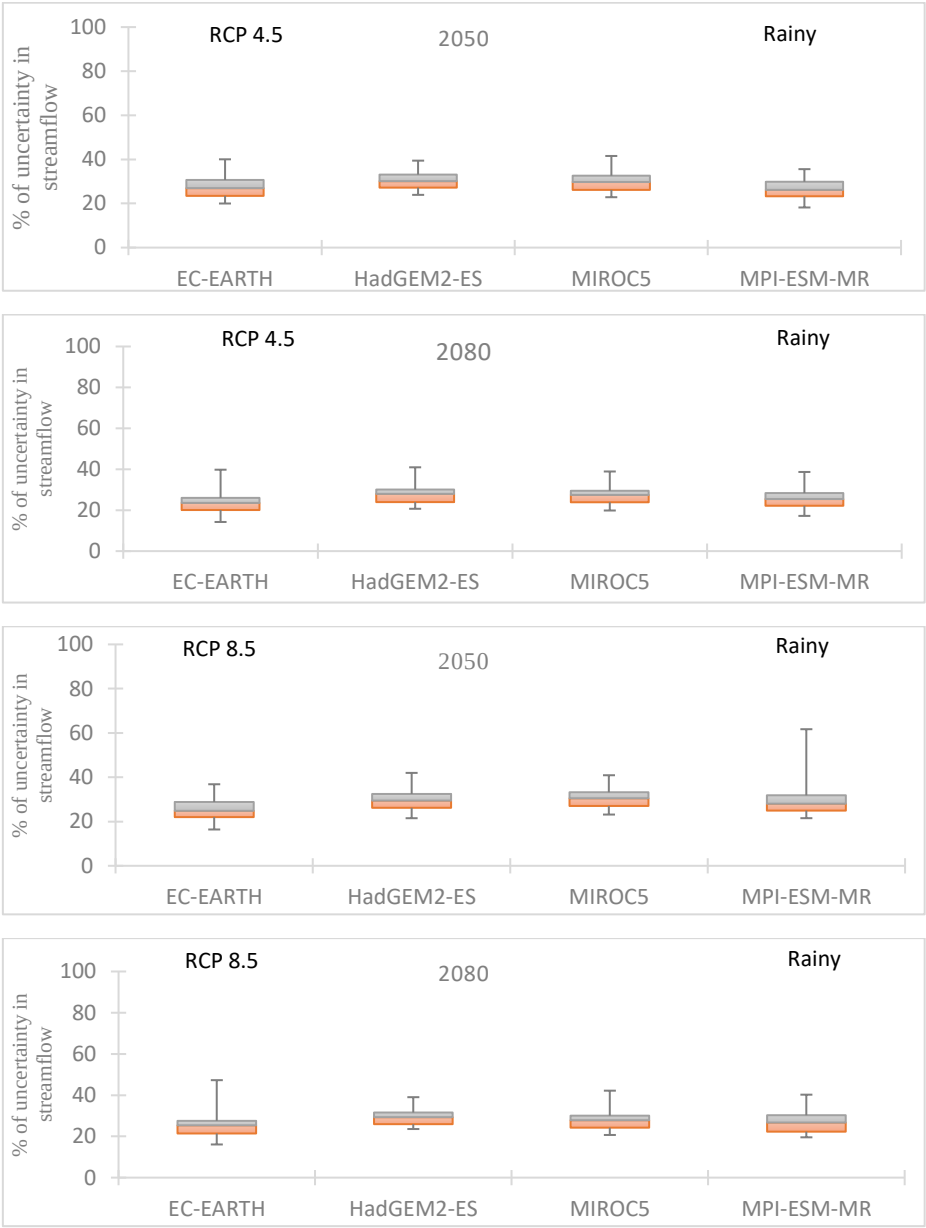

Figure 7.5(k). Percentage of uncertainty in seasonal (rainy) stream flow at the Sagaing station under RCP4.5 and RCP 8.5 for the two future periods relative to the baseline period (1989-2018)

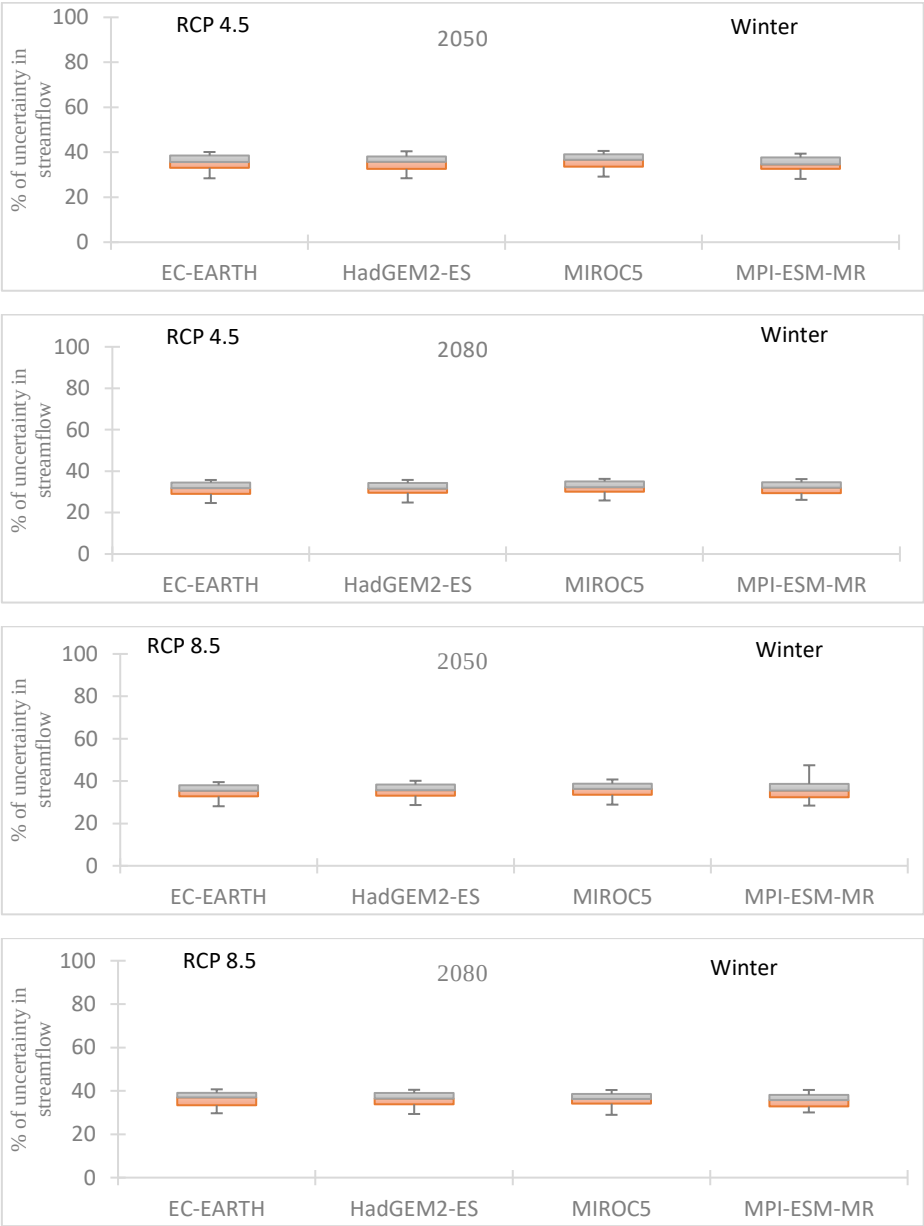

Figure 7.5(l). Percentage of uncertainty in seasonal (winter) stream flow at the Sagaing station under RCP4.5 and RCP 8.5 for the two future periods relative to the baseline period (1989-2018)

The results in this study indicate uncertainty in future projections indicated by four GCMs and two emission scenarios. Uncertainty of projection using a choice of downscaling and hydrological models was not considered in this study. The uncertainty of the annual and seasonal stream flow projection changes for these two scenarios was estimated. This study uses different resolutions of 4 CMIP5 GCMs. All these GCMs have good resolutions and their simulations can perform well (relative to the other GCMs) when compared to the historical climate of the Asia region (Miao et al., 2014). It is clear that all the models are very relatively good in reproducing the general patterns of precipitation over the whole area of the Upper Ayeyarwaddy River Basin. After SWAT modelling using these GCM bias corrected data of the future period 2021 - 2080, these projections of four GCMs are different from each other, creating uncertainty of the annual and seasonal stream flow changes in the whole basin. In addition, it is found that different models show varying abilities in stream flow simulations. The results provided a clear solution that at station, the highest projection of annual stream flow changes (over 40%) is observed in HadGEM2-ES and MICRO5 GCM, followed by 36% of EC-EARTH and 39 % of MPI-ESM-MR under both scenarios at Bamo station while the changes for all GCMS of the other stations are observed below 35%. EC-EARTH and MPI-ESM-MR simulates the least projection of stream flow changes in the future. This study using four GCMs gives a big advancement to quantify the uncertainties in stream flow projections under a future climate. Floods are frequently seen in the downstream area. Heavy rains always move towards the Upper Ayeyarwaddy River channel from the surrounding mountainous area. Therefore, more stream flows can be observed at Bamo station, with the combined effects of River geology and tidal flow patterns (described in Section 7.1). Decreasing stream flow changes can be seen in the Myitkyina area. Another human made activity is locating Myit Sone Dam in the upstream of Myitkyina city. The government function of hydropower is to supply sufficient elasticity for national development. Sometimes this dam release storage water if the storage water reaches at the maximum capacity affecting floods in the downstream area. The affecting of tidal flow joins with the storm water in Myitkyina area and it can be seen increasing stream flow changes in downstream area.

CHAPTER 8. Summary, Conclusions and Recommendations

8.1 Summary

In this study, statistical downscaling (LARS-WG) was applied to analyse the future changes in maximum and minimum temperature and precipitation in the Upper Ayeyarwaddy River Basin under RCP4.5 and 8.5 scenarios. Downscaling of these meteorological parameters was very important in order to study the impacts of climate change on the hydrological cycle of the basin. All the four GCMs used are part of CMIP5. The selection of GCMs for the study area was a challenge, and they were evaluated using LARS-WG as a decision support tool. The performance indicators R2 and RMSE were employed for the evaluation. The statistical downscaling method (LARS-WG) simulated temperature and precipitation projections from four GCMs for two RCP scenarios. Two future periods were considered: 2021-2050 (2050s), and 2051-2080 (2080s). LARS-WG was first validated for each of the four stations used in this study. The simulated data by LARS-WG for maximum and minimum temperature and precipitation at all four stations showed good agreement with the observed data in terms of R2 and RMSE. It can be seen for both maximum and minimum temperatures that the monthly and seasonal values are more reliable. The monthly, seasonal and annual changes are projected for the future with respect to the baseline period (1989-2018). Both the temperature and precipitation are projected to undergo changes in the future in the Upper Ayeyarwaddy River Basin for RCP4.5 and RCP8.5 climate change scenarios. Average annual Tmax and Tmin are projected to increase in both parts of the Upper Ayeyarwaddy River Basin under both scenarios in all two future periods. The rise in maximum and minimum temperatures projected by RCP4.5 and RCP 8.5 are closer. According to the LARS-WG , the near future (2050s) and mid future (2080) are expected to be the most affected period as far as rise in temperature and precipitation are concerned. These temperature changes are small but will also influence the stream flow in the basin and water availability during the dry seasons. Therefore, it can be ascertained that the projections of multiple GCMs and RCP scenarios are important for climate change studies. As in the baseline data, April is expected to be the hottest month in the basin up to 2080 under both scenarios. The mean temperature is projected to be

as high as 38.8 ºC under RCP4.5 and 39.6 ºC under RCP8.5 in the basin. Both periods are projected to be the hottest under both scenarios. For precipitation, the wettest month will keep shifting over the two periods and is in contrast to the baseline months of observed data. June and July are the wettest months with the 2050s and 2080s being the wettest period as per the projections. The simulated annual precipitation in all two periods is more than the observed annual precipitation under both scenarios. It can be concluded that future temperature and precipitation over the Upper Ayeyarwaddy River Basin will increase, and the use of a multi-model multi-scenario approach is a prerequisite for studying climate change impacts on a regional scale.

The SWAT model showed satisfactory performance in simulating the stream flow measured at the Myitkyina, Bamo, Katha and Sagaing stations during calibration (1993-2005) and validation (2006-2018) periods. The values of statistical indicators R^2 and NSE are well under the acceptable limit of $R^2 > 0.6$ and NSE > 0.5 (guidelines of Santhi et al., 2001 and Van Liew et al., 2007) during calibration as well as validation. The performance of the calibrated SWAT model was also analysed using the baseline period for observed and simulated data. The good agreement between observed and simulated monthly values indicates that the calibrated model with a set of optimised parameters could be applied to examine the responses of stream flow to climate change in the Upper Ayeyarwaddy River Basin. The results show that the SWAT model performs well for the Upper Ayeyarwaddy River Basin. This ensures that the model can certainly be extended to study the outcomes of climate change on stream flow of the Upper Ayeyarwaddy River Basin and its tributaries.

The majority of the GCMs projected an increase in stream flow for two future periods in the Upper Ayeyarwaddy River Basin due to the results of stream flow changes of all GCMs relative to the baseline period at the Bamo, Katha and Sagaing stations while Myitkyina is projected an decrease flow. GCMs cannot agree on whether stream flow changes will be positive or negative. All GCMs indicate a positive change in the two periods under both scenarios at the Bamo, Katha and Sagaing station. However, at the Myitkyina station, GCMs show decreasing changes. All the GCMs insignificantly changes (approximately 90% increasing) under both scenarios in the future period at

the Katha and Sagaing station but at the Bamo station, the maximum stream flow changes (+10%) in 2050s and (+13%) in 2080s are observed in MICRO5 under for the future period. The average value of all GCMs indicates a positive change in rainy and winter seasons as well as for annual stream flow changes at the Katha and Sagaing stations under both scenarios for all periods. At the Myitkyina station, a negative change is observed in the both seasonal and annual for all periods under both scenarios. At the Bamo station, a negative change is observed in the winter season with the remainder showing positive changes for all periods under both scenarios. The changes for Bamo station clearly indicate the uncertainties of GCMs. Under climate change scenarios, all seasonal and annual stream flows can show changes ranging from -80% to almost +90% at both stations for the period 2021-2080.

The uncertainty of the annual and seasonal stream flow projection changes for these two scenarios was estimated followed by four GCMs. All these GCMs have good resolutions and their simulations can perform well (relative to the other GCMs) and it is clear that all the models are very relatively good in reproducing the general patterns of precipitation over the whole area of the Upper Ayeyarwaddy River Basin. After SWAT modelling using these selected GCM data from LARS-WG statistical downscaling method , these projections of four GCMs are different from each other, creating uncertainty of the annual and seasonal stream flow changes in the whole basin. According to the results, the uncertainty level of all GCMs are insignificantly changes for all stations. However, in winter season, the Bamo station is observed the highest uncertainties level (over 40%) while other stations are observed under 35%.

8.2 Conclusions

In this study, the projected impacts of climate change on the stream flow changes of the Upper Ayeyarwaddy River Basin in Myanmar were assessed. It is observed that the future average monthly precipitation projected by four GCMs models changes in significantly compared to the precipitation of the baselined period from January to April at Myitkyina station. For the remaining months, EC-EARTH, HadGEM2-ES and MICRO5 show the upward trends while MPI-ESM-MR changes insignificantly. The results clearly show that July is the most having the highest precipitation in the year.

The future precipitation projected at the Bamo station is observed that June is the month having the highest precipitation and all GCMs are slightly increased compared with the baseline period. However, the precipitation changes insignificantly from January to May compared to the baseline period at Katha station. The trend for EC-EARTH changes insignificantly while the remaining models are significantly increased. The similar results are found for the other stations. Overall, the highest average monthly precipitation (approximately 40 mm) occurs in July during the future. The average annual precipitation is projected to be until 43% increasing in the future period. Average annual temperature is projected to rise in the entire basin under both scenarios. April is observed to be the hottest month with mean temperature of 39 ºC for the whole basin. The projections of all GMS under the two scenarios indicate an increase in both annual maximum and minimum temperature for all future periods. From all the case, the minimum temperature will increase in the range from 2°C to 2.5°C in 2050s , 3°C to 4°C in 2080s and the maximum temperature will increase in the range from 2.5°C to 3.5°C in 2050s ,4°C to 6°C in 2080s.

The performance of the SWAT model during calibration and validation is satisfactory at the monthly scales to analyze the stream flow changes due to the impacts of climate change in the future. R^2 and NSE values of monthly stream flows for all stations are above 0.6 and 0.5 which are the perfect value to achieve the best fit between the simulated and measured flow at the monitoring for future streamflow projection as recommended by many researchers.

Under the climate change scenarios, the average stream flow changes at the Myitkyina station is projected to decrease at the maximum rate of 85% while the other stations are projected to be higher in the future. The seasonal stream flow changes in summer season (varying -40 % to -99%) are projected for all stations and in the rainy season (varying +10% to +115%) are projected to be higher in comparison to the other seasons during 2021 -2080. In the winter season (varying +40% to 100%) are projected at Katha and Sagaing station while Bamo station is projected both increasing and decreasing due to the uncertainties of GCMs.

Uncertainty in climate change impact analysis has been widely recognised. Analysing it becomes an important task particularly when impact analysis results are used for adaptation purposes. In this study, the impact of climate change on stream flow in the Upper Ayeyarwaddy River Basin for 2050s, and 2080s under RCP4.5 and RCP8.5 scenarios were investigated by using four GCMs. To understand the impacts of climate change on water resources, it is important to examine the uncertainty of climate change impacts on water resources. Exploration within climate change hydrological impact assessments has often focused on GCM uncertainty and emission scenarios. Chen et al., (2011) extracted from these results that the choice of GCM is the major contributor to uncertainty. Maurer (2007) investigated that uncertainty in future emission scenarios plays an important role in the degree of climate impact on water resources in the watershed. To address this issue, this study analysed future climate projections by using four GCMs for RCP 4.5 and 8.5 scenarios. In this study, the range of uncertainty for annual streamflow is 30 % to 43 % in the whole basin for the future period of 2021-2080. The highest range of uncertainty for summer stream flow changes is projected roughly above 56% under both scenarios for the future period in the whole basin. Large extreme change increases can be projected approaching +45% for winter season flow at Bamo station under both scenarios. The rainy season is affected by a low flow change projection of generally 30% under both scenarios in the future period of 2021-2080.

climate change affected both low-flow and high-flow rates. The greater streamflow caused by precipitation increases while the streamflow reductions caused by temperature increases. In this study, high flow commonly occur in rainy season and low flows occur in summer and winter seasons, respectively. The greatest impacts on flow classes also would commonly occur in these seasons. Climate change effects on hydrology will impact water uses and water management. Therefore, our results may help anticipate climate change effects and adaptive measures to take advantage of positive effects such as adapting to life in a changing climate which involves adjusting to actual or expected future climate to reduce our vulnerability to the harmful effects of climate change like sea-level encroachment, more intense extreme weather events or food insecurity. It also encompasses making the most of any potential beneficial opportunities associated with climate change. and to mitigate the negative effective. In

reality, there are many factors to change independently in adaptation to climate change in near future such as land use and agricultural practices and it must be considered in adaptation studies. Therefore, the policy makers and water engineers can use suitable adaptation strategies due to the impacts of climate change for the Upper Ayeyarwaddy River Basin because the study results and findings are also beneficial to future climate adaptation measures. And the future researchers may consider to analyse the climate change impacts on river erosion and soil erosion In addition this study can provide national development plans to reduce the vulnerability of argue for effective linkages between climate change issues and development planning, incorporating climate change impact and risk assessment into long term national development strategies.

Moreover, climate change conditions in Myanmar are getting worse with the increased rate of GHG emissions levels in the atmosphere and increasing in frequency and intensity of rainfall lead to floods and increasing in water scarcity and drought according to the comparison between observed and simulated data and therefore, it is necessary to control and reduce flood potentials in the wet season and the severity of drought in the dry season. The greenhouse gas emissions rate in Myanmar cannot reduce and the level of gas will keep going up and reach the RCP4.5 and RCP8.5 conditions. Therefore, stronger efforts and finding ways to reduce and to mitigate carbon dioxide emissions should be undertaken to lower global warming and climate change in the atmosphere.

8.3 Recommendations

The main contribution of this research is that it must be considered climate changes during water resources planning and managements In addition, because of changes in temperature, precipitation and stream flow, water management planners must consider the climate change scenarios for watershed study. This study can also be adapted for other watershed management projects which have climate change impacts on water resources. Nonetheless, there are limitations to this study. This study considered the data from RCP4.5 and 8.5 scenarios. It is based on the reason that some CMIP5 GCMs cannot produce RCP6 scenario yet and are still under processing. Another limitation is that uncertainty quantifying was considered due to emission scenarios and GCM

structures because these two factors are strongly influenced on uncertainty more than others. . In addition, it is suggested to consider the uncertainty due to SWAT parameters. Even though the results obtained by this study presented some limitations, they should be adjusted and then can be used modelling for other watersheds where the same problem occurs. Although climate change is potentially affecting on water resources, land use change also influences on it. Therefore, land use change also effects the accuracy of the results and updating data of land use in the study area is necessary for application in the future. In addition, many studies were carried out on sizeable river basins regulated by many large dams and reservoirs. The upper Ayeyarwaddy basin has seen major dam developments over recent years for hydropower and irrigation purposes with many planning phases. According to this study, it was found decease in the annual peak discharge under climate change when considering additional effects of future dams. Dam regulation and water transfers between basins have also decreased streamflows and exacerbated droughts in downstream regions. Other studies have chosen to ignore current and future dams altogether, instead focusing on the impacts of climate change as if the system were in its natural state. Therefore, it is suggested to identify interactions between changes in climate and streamflow due to dams or quantifying the respective contributions of natural factors and human activities to streamflow changes is important not only in theoretical perspective, but also in water resources management and soil and water conservation measures.

REFERENCES

Abbaspour, K.C., Yang, J., Maximov.I., Siber, R., Bogner, K., Mieleitner, J., Zobrist, J., Srinivasan, R. (2007). Modelling hydrology and water quality in the pre-alpine/ alpine Thur watershed using SWAT. Journal of Hydrology, 333 (2-4), 413-430.

Abrishamchi, A., Ebrahimian, A., Tajrishi, M., Marino, M. A. (2005). Case Study: Application of multicriteria decision making to urban water supply. Journal of Water Resources Planning and Management, 131(4), 326–335.

Ahmed, K.F., Wang, G., Silander, J., Wilson, A.M., Allen, J.M., Horton, R.M., Anyah, R. (2013). Statistical downscaling and bias correction of climate model outputs for climate change impact assessment in the U.S. northeast. Global and Planetary Change, 100, 320-332.

Akpınar, A., Kömürcü, M. İ., Kankal, M. (2011). Development of hydropower energy in Turkey: The case of Çoruh river basin. Renewable and Sustainable Energy Reviews, 15(2), 1201– 1209.

Arnell, N.W. (2004). Climate change and global water resources: SRES emissions and socio- economic scenarios. Global Environmental Change, 14, 31–52.

Arnold, J.G., Srinivasan, R., Muttiah, R.S., Williams, J.R. (1998). Large area hydrologic modelling and assessment Part I: model development. Journal of American Water Resources Association, 34 (1), 73-89.

Arnold, J.G., Moriasi, D.N., Gassman, P.W., Abbaspour, K.C., White, M.J., et al. (2012). SWAT: Model use, Calibration and Validation. Transactions of the ASABE, 55(4), 1491-1508.

Arora, V.K., Boer, G.J. (2001). Effects of simulated climate change on the hydrology of major river basins. Journal of Geophysical Research, 106, 3335-3348.

Aung, T.T., Mochida, Y., Than, M.M. (2013). Prediction of recovery pathways of cyclone- distributed mangroves in the mega delta of Myanmar. Forest Ecology and Management, 293, 103-113.

Balla, M.K., Awasthi, K.D., Singh, B.K., Sitaula, B.K., Pradhan, B.M. (2007). Land Use Changes and Geomorphometric Analyses in Galaundu andPokhare Khola Watersheds in Mid-hill Region of Nepal. International Journal of Ecology and Environmental Sciences, 33(2-3), 171-182.

Bates, B.C., Kundzewicz, Z.W., Wu, S., Palutikof, J.P., Eds. (2008).Climate change and water. IPCC Technical Paper VI.

Berg, P., Feldmann, H., Panitz, H.J. (2012). Bias correction of high resolution regional climate model data. Journal of Hydrology, 448-449, 80-92.

Beven, K.J. (1993). Prophecy, reality and uncertainty in distributed hydrological modelling. Advances in Water Resources, 16, 41-51.

Boe, J., Terray, L., Habets, F. and Martin, E. (2007). Statistical and dynamical downscaling of the Seine basin climate for hydro-meteorological studies. International Journal of Climatology, 27, 1643-1655.

Boyer, C., Chaumont, D., Chartier, I., Roy, A.G. (2010). Impact of climate change on the hydrology of St. Lawrence tributaries . Journal of Hydrology, 384, 65-83.

Bryan, E., Ringler, C., Okoba, B., Roncoli, C., Silvestri, S., Herrero, M.et al. (2013). Adapting agriculture to climate change in Kenya: Household strategies and determinants. Journal of Environmental Management, 114, 26-35.

Buytaert, W., Vuille, M., Dewulf, A., Urrutia, R., Karmalkar, A., Celleri, R. (2010). Uncertainties in climate change projection and regional downscaling in the tropical Andes: implications for water resources management. Hydrology and Earth System Sciences, 14, 1247-1258.

Cannon, A.J., Whitfield, P.H. (2001). Downscaling recent streamflow conditions in British Columbia, Canada using ensemble neural network models. Journal of Hydrology, 259, 136-151.

Chen, B., Zhang, X., Tao, J., Wu, J., et al. (2014). The impact of climate change and anthropogenic activities on alpine grassland over the Qinghai-Tibet Plateau. Agricultural and Forest Meteorology, 189-190, 11-18.

Cherkauer, K.A., Sinha, T. (2010). Hydrologic impacts of projected future climate change in the Lake Michigan region. Journal of Great Lakes Research, 36, 33-50.

Chiew, F.H.S., Kirono, D.G.C., Kent, D.M., Frost, A.J., Charles, S.P., Timbal, B., Nguyen, K.C., Fu, G. (2010). Comparison of runoff modelled using rainfall from

different downscaling methods for historical and future climates. Journal of Hydrology, 387, 10-23.

Chinvanno, S. (2004). Building Capacity of Mekong River Countries to Assess Impacts from Climate Change – Case Study Approach on Assessment of Community Vulnerability and Adaptation to Impact of Climate Change on Water Resources and Food Production. START.

Coats, R., Dettinger, M., Riverson, J., Reuter, J., Sahoo, G., et al. (2011). Projected 21st century trends in hydroclimatology of the Tahoe Basin. Journal of Quaternary International, 310.

Das, L., Lohar, D. (2005). Construction of climate change scenarios for a tropical monsoon region. Journal of Hydrology, 30, 39-52.

Dechmi, F., Burguete, J., Skhiri, A. (2012). SWAT application in intensive irrigation systems: Model modification, calibration and validation. Journal of Hydrology, 470-471, 227-238.

Deng, H., Luo, Y., Yao, Y., Liu, C. (2013). Spring and summer precipitation changes from 1880 to 2011 and the future projections from CMIP5 models in the Yangtze River Basin, China. Quaternary International, 304, 95–106.

Dowa, K., Connor, R.E., Yarnal, B., Carbone, G.J., Jocoy, C.L. (2007).Why worry? Community water system managers' perceptions of Climate vulnerability. Global Environmental Change, 17, 228–237.

Dunne, S.S., Lynch, P., McGrath, P., Semmler, T., Wang, S., et al. (2008). The impacts of climate change on hydrology in Ireland. Journal of Hydrology, 356, 28-45.

Dunning, D. J., Ross, Q. E., Merkhofer, M. W. (2000). Multiatribute utility analysis foraddressing Section 316(b) of the Clean Water Act. Environmental Science and Policy, 3, 7–14.

EPRI, (2009). Review of General Circulation Models and Downscaling Techniques, Climate Science Newsletter, October 2009, Electric Power Research Institute, California, USA.

Ercan, M.B., Goodall, J.L., Castronova, A.M., Humphrey, M., Beekwilder, N. (2014). Calibration of SWAT models using the cloud. Environmental Modelling & Software, 62, 188-196.

Fan, M., Shibata, H. (2015). Simulation of watershed hydrology and stream water quality under land use and climate change scenarios in Teshio River watershed, northern Japan. Journal of Ecological Indicators, 50, 79-89.

FAO (Food and Agriculture Organization of the United Nations) (1995). The Digital Soil Map of the World and Derived Soil Properties. CD-ROM, Version 3.5. Rome, Italy: FAO. http://www.fao.org/.

Feng, S., Hu, Q., Huang, W., Ho, C., et al. (2014). Projected climate regime shift under future global warming from multi-model, multi-scenario CMIP5 simulations. Journal of Global and Planetary Change, 112, 41-52.

Ficklin, D.L., Luo, Y., Luedeling, E. Zhang, M. (2009). Climate change sensitivity assessment of a highly agricultural watershed using SWAT. Journal of Hydrology, 374, 16-29.

Gardner, L.R. (2009). Assessing the effect of climate change on mean annual runoff. Journal of Hydrology, 379, 351-359.

Ghosh, S., Mujumdar, P.P. (2009). Climate change impact assessment: Uncertainty modelling with imprecise probability. Journal of Geological Research, 114, D18113, doi: 10.1029/2008JD011648, 2009.

Gosain, A.K., Rao, S., Basuary, D. (2006). Climate change impact assessment on hydrology of Indian river basins. Current Science, 90, No. 3: 346-353.

Gupta, H.V., Kling, H. (2011). On typical range, sensitivity, and normalization of Mean Squared Error and Nash-Sutcliffe Efficiency type metrics. International Journal of Water Resources Research, 47, W10601, doi :10.1029/2011WR010962.

Hansson, K., Danielson, M., Ekenberg, L. (2008). A framework for evaluation of flood management strategies. Journal of Environmental Management, 86, 465-480.

Hailemariam, K. (1999). Impact of climate change on the water resources of Awash River Basin, Ethiopia. Journal of Geological Research,12, 91-96.

Harpham, C., Wilby, R.L. (2005). Multisite downscaling of heavy daily precipitation occurrence and amount. Journal of Hydrology, 312, 235-255.

Hawkins, E., Osborne, T.M., Ho, C.K., Challinor, A.J. (2013). Calibration and bias correction of climate projections for crop modelling: An idealised case study over Europe. Agricultural and Forest Meteorology, 170, 19-31.

Hlaing, K., Haruyama, S., Aye, M. (2008). Using GIS-based Distributed Soil Loss Modeling and Morphometric Analysis to Prioritize Watershed for Soil Conservation in Bago River Basin of Lower Myanmar. Higher Education Press and Springer-Verlag.

Hoose, C., Kristjansson, J.E., Iversen, T. (2009). Constraining cloud droplet number concentration in GCMs suppresses the aerosol indirect effect. Geophysical Research Letters, 36.

Hwang, S.,Graham, W.D. (2014). Assessment of alternative methods for statistically downscaling daily GCM precipitation outputs to simulate regional streamflow. Journal of the American Water Resources Association, 1-23.

IPCC (2001). Third Assessment Report, Working Group-I Report. Cambridge University Press, Cambridge, UK.

ITC (2011). Report for mitigation of Bago Flood, Ministry of Agriculture and Irrigation. Republic of Union of Myanmar.

Jayakrishnan, R., Srinivasan, R., Santhi, C., Arnold, J.G. (2005). Advances in the application of the SWAT model for water resources management. Hydrological Process, 19(3), 749-762.

Keskinen, M., Chinvanno, S., Kummu, M., Nuorteva, P., Snidvongs, A., Varis, O., Västilä, K. et al. (2009). Water and Climate Change in the Lower Mekong basin. START.

D.N., Khoi, V.T.,Nhuyen, T.T.,Sam, P.T.,Nhi (2019). Evaluation on effects of climate and land-use changes on streamflow and water quality in the La Buong River Basin, southern Vietnam.

Koomen, E., Diogo, V., Dekkers, J., Rietveld, P. (2015). A utility-based suitability framework for integrated local-scale land-use modelling. Computers, Environment and Urban Systems, 50, 1-14.

Kim, J., Choi, J., Choi, C., Park, S. (2013). Impacts of changes in climate and land use/land cover under IPCC RCP scenarios on stream flow in the Hoeya River Basin, Korea. Science of the Total Environment, 452-453, 181-195.

Kusangaya, S., Warburton, M.L., Garderen, E.A.v., Jewitt, G.P.W. (2014). Impacts of climate change on water resources in southern Africa: A review. Physics and Chemistry of the Earth, 67-69, 47-54.

Lang, C., Fettweis, X., Erpicum, M. (2015). Stable climate and surface mass balance in Svalbard over 1979–2013 despite the Arctic warming. The Cryosphere, 9, 83-101.

Lioubimtseva, E., Henebry, G.M. (2009). Climate and environmental change in arid Central Asia: Impacts, vulnerability, and adaptations. Journal of Arid Environments, 73,963–977.

Liu, C., Hofstra, N. and Leemans, R. (2014). Preparing suitable climate scenario data to assess impacts on local food safety. Food Research International. .

Loo, Y.Y., Billa, L., Singh, A. (2014). Effect of climate change on seasonal monsoon in Asia and its impact on the variability of monsoon rainfall in Southeast Asia. Geoscience Frontiers, 21.

Mahmood, R., Babel, M.S. (2013). Evaluation of SDSM developed by annual and monthly sub- models for downscaling temperature and precipitation in the Jhelum basin, Pakistan and India. Theoretical and Applied Climatology, 113, 27-44.

Maneesha, K., Murty, V.S.N., Ravichandran, M., Yu, W., McPhaden, M.J. (2012). Upper ocean variability in the Bay of Bengal during the tropical cyclones Nargis and Laila. Progress in Oceanography, 106, 49-61.

Miao, C., Duan, Q., Sun, Q., Huang, Y., Kong, D. et al. (2014). Assessment of CMIP5 climate models and projected temperature changes over Northern Eurasia. Environmental Research Letters, 9, doi:10.1088/1748-9326/9/5/055007. .

Moriasi, D. N., Arnold, J. G., Liew, M. W. V., Bingner, R. L., Harmel, R. D., Veith, T. L. (2007). Model Evaluation Guidelines for Systematic Quantification of Accuracy in Watershed Simulations.

Nelson, B.W. (2001). Sediment dynamics in Rangoon River, Myanmar. Science of the Total Environment, 266, 15-21.

Nguyen, B.T. (2014). Effect of Land Use Change on Water Discharge in Vu Gia Watershed, Viet Nam using GIS and SWAT. Journal of Earth and Environmental Sciences, 3(2S), 80-91.

Piani, C., Weedon, G., Best, M., Gomes, S., Viterbo, P., et al. (2010). Statistical bias correction of global simulated daily precipitation and temperature for the application of hydrological models. Journal of Hydrology, 395, 199-215.

Reungsang, P., Kanwar, R.S., Srisuk, K. (2010). Application of SWAT Model in Simulating Stream Flow for the Chi River Subbasin II in Northeast Thailand. Trends Research in Science and Technology, 2 (1), 23-28.

Sangmanee, C., Chinvanno, S., Tanakitmethavut, J., Bunsomboonsakul, S., Thitiwate, J. (2011). Impact of Climate Change on Hydrological Regime of Khlong Krabi Yai Watershed, Krabi Province, Thailand. START.

Stratford, C., Acreman, M., Rees, G. Shilpakar, R. Wetland. Vulnerability Assessments of Phewa Lake, Pokhara, Nepal. Report of Centre for Ecology and Hydrology.

Strauch, M., Bernhofer, C., Koide, S., Volk, M., Lorz, C., Makeschin, F. (2012). Using precipitation data ensemble for uncertainty analysis in SWAT streamflow simulation. Journal of Hydrology, 414-415, 413-424.

Su, B., Zeng, X., Zhai, J., Wang, Y., Li, X. (2014). Projected precipitation and stream flow under SRES and RCP emission scenarios in the Songhuajiang River Basin, China. Journal of Hydrology, 18.

Thompson, J.R., Green, A.J., Kingston, D.G., Gosling, S.N. (2013). Assessment of uncertainty in river flow projections for the Mekong River using multiple GCMs and hydrological models. Journal of Hydrology, 486, 1-30.

Tongwen, W., Song, L., Li, W., Wang, Z., Zhang, H. et al., (2014). An overview of BCC climate system model development and application for climate change studies. Journal of Meteorological Research, 28(1), 34-56.

Varis, O., Kummu, M., Salmivaara, A. (2012). Ten major rivers in monsoon Asia-Pacific: An assessment of vulnerability. Applied Geography, 32, 441-454.

Verburg, P.H., Mastura, S.S.A., Veldkamp, W.S.A., Espaldon, R.L.V. (2000). Modeling the Spatial Dynamics of Regional Land Use: The CLUE-S Model.

Wang, C., Wanga, F., Wang, Q., Yang, D., Li, L., Xinlin Zhang., et al. (2013). Preparing for Myanmar's environment-friendly reform. Environmental Science, 25, 229-233.

Wang, S., McGrath, R., Semmler, T., Sweeney, C. (2006). The impact of climate change on discharge of Suir River Catchment (Ireland) under different climate change scenarios. Natural Hazards and Earth System Sciences, 6, 387-395.

Webb, E.L., Jachowski, N.R.A., Phelps, J., Friess, D.A., Than, M.M., Ziegler, A.D. (2014). Deforestation in the Ayeyarwaddy Delta and the conservation implications of an internationally engaged Myanmar. Global Environmental Change, 24, 321-333.

Willard, D.A., Phillips, T.L., Lesnikowska, A.D., DiMichele, W.A. (2007). Paleoecology of the Late Pennsylvanian-age Calhoun coal bed and implications for

long-term dynamics of wetland ecosystem. International Journal of Coal Geology, 69, 21–54.

Woo, M.k., Young, K.L. (2006). High Arctic wetlands: Their occurrence, Hydrological characteristics and sustainability. Journal of Hydrology, 320, 432–450.

Wu, Y., Liu, S. (2012). Automating calibration, sensitivity and uncertainty analysis of complex models using the R package Flexible Modelling Environment (FME): SWAT as an example. Environmental Modelling & Software, 31, 99-109.

Xiong, L.H., Yu, K.X., Zhang, H.G., Zhang, L.P. (2013). Annual runoff change in the headstream of Yangtze River and its relation to precipitation and air temperature. Hydrology Research, 44: 850.

Xu, H., Xu, C., Zhou, B., Singh, V.P. (2013). Modelling runoff response to land-use change using an integrated approach in Xiangjiang River basin, China. Hydrological Sciences Journal, 359, 390-396.

Xu, X., Scanlon, B.R., Schilling, K., Sun, A. (2013). Relative importance of climate and land surface changes on hydrologic changes in the US Midwest since the 1930s: Implication biofuel production. Journal of Hydrology, 497, 110-120.

Xu, Y.P., Zhang, X., Ran, Q., Tian, Y. (2013). Impact of climate change on hydrology of upper reaches of Qiantang River Basin, East China. Journal of Hydrology, 483, 51-60.

Yang, H., Sun, H., Jiao, L., Chen, X. (2010). Assessment on the Ecological Vulnerability of Wetland of China Irtysh river valley. 2nd Conference on Environmental Science and Information Application Technology.

Ye, L., Zhou, J., Zeng, X., Guo, J., Zhang, X. (2014). Multi-objective optimization for construction of prediction interval of hydrological models based on ensemble simulations. Journal of Hydrology, 519, 925-933.

You, Q., Min J., Fraedrich, K., Zhang, W., Kang, S., et al. (2014). Projected trends in mean, maximum, and minimum surface temperature in China from simulations. Global and Planetary Change, 112, 53-63.

Zeinivand, H., Smedt, F. (2008). Hydrological Modeling of Snow Accumulation and Melting on River Basin Scale. Water Resources Management, 23(11), 2271–2287.

Zeng, S., Riedi, J., Trepte, C.R., Winker, D.M., Hu, Y.-X. (2014). Study of global cloud droplet number concentration with A-Train satellites. Atmospheric, Chemistry and Physics, 14, 7125-7134.

Zhang, H., Huang, G.H., Wang, D., Zhang, X. (2011). Uncertainty assessment of climate change impacts on the hydrology of small prairie wetlands. Journal of Hydrology, 396, 94-103.

Zhang, P., Liu, Y., Pan, Y., Yu, Z. (2013). Land use pattern optimization based on CLUE-S and SWAT models for agricultural non-point source pollution control. Mathematical and Computer Modelling, 58, 588-595.

Zhang, P., Liu, R., Bao, Y., Wang, J. et al. (2014). Uncertainty of SWAT model at different DEM resolutions in a large mountainous watershed. Water Research, 53, 132-144.

Zhang, X., Xu, Y.P. ,Fu, G. (2014). Uncertainties in SWAT extreme flow simulation under climate change. Journal of Hydrology, 515, 205-222.

Zhang, X.C., Liu, W.Z., Chen, J. (2011). Trend and uncertainty analysis of simulated climate change impacts with multiple GCMs and emission scenarios. Agricultural and Forest Meteorology, 151, 1297-1304.

Zhang, Y., Sun, S., Seth, C., Manvendra, K., He, J. (2011). CCSM3 simulated regional effects of anthropogenic aerosols for two contrasting scenarios: rising Asian emissions and reduction of aerosols. International Journal of Climatology, 31, 95-114.

Zheng, H.W., Shen, G.Q., Wang, H., Hong, J. (2015). Simulating land use change in urban renewal areas: A case study in Hong Kong. Habitat International, 46, 23-24.

Zhou, F., Xu, Y., Chen, Y., Xu, C.Y., Gao, Y., Du, J. (2013). Hydrological response to urbanization at different spatio-temporal scales simulated by coupling of CLUE-S and the SWAT model in the Yangtze River Delta region. Journal of Hydrology, 485, 113-125.

Zokaib, S., Naser, G. (2011). Impacts of land uses on runoff and soil erosion A case study in Hilkot watershed Pakistan. International Journal of Sediment Research, 26, 343–352.

초 록

Ayeyarwady 강은 길이 2,170km, 총 면적 413,710km^2 에 이르는 미얀마에서 가장 큰 강이며 53,710,000 명의 인구가 밀접하게 연관되어 있는, 미얀마에서 경제적으로 가장 중요한 지역으로 여겨진다. 기후변화는 Ayeyarwady 강 유역 상류 수자원에 중요한 영향을 미치기 때문에 그러한 영향을 평가하고 그에 따른 수문학적 과정의 결과를 예측하는 것은 이 유역에서 상당히 중요하다. 본 연구에서는 토양과 수질평가 모델(SWAT)이 수치모의 모델로 사용되었다. SWAT 은 1989-2018 년 동안의 관측자료를 토대로 정밀하게 조정 및 검증된 뒤, 연구대상유역의 수문학적 과정에 미치는 기후변화의 영향평가를 위해 사용되었다. SWAT 은 1993-2005 년 동안의 자료를 토대로 매개변수를 조정하였으며 2006-2018 년의 자료를 바탕으로 모델의 활용성을 검증하였다. 수치모의 결과, Myitkyina 지점에서 R^2 값은 0.65(조정), 0.68(검증), Nash-Sutcliffe Efficiency (NSE)값은 0.43(조정), 0.55(검증), Bamo 지점에서 R^2 값은 0.71(조정), 0.64(검증), NSE 값은 0.71(조정), 0.64(검증), Katha 지점에서 R^2 값은 0.62(조정), 0.65(검증), NSE 값은 0.5(조정), 0.51(검증), 그리고 Sagaing 지점에서 R^2 값은 0.65(조정), 0.7(검증), NSE 값은 0.69(조정), 0.67(검증)으로 각각 나타났다. 위 결과를 분석해보면 한 개소의 지점을 제외하고는 SWAT 모델의 성능지표(R^2 와 NSE)는 만족할 만한 것으로 판단된다. Ayeyarwady River 유역 상류의 기후변화 자료는 CMIP5 로부터 취득하였다. 기후변화 시나리오는 EC-EARTH, HadGEM2-ES, MICROC5, 그리고 MPI-ESM-MR 의 네 개의 서로 다른 GCMs(General Circulation Models)로부터 다운스케일링되었으며 medium stabilization scenarios (RCP4.5)와 high emissions scenario (RCP8.5)와 같은 두 개의 Representative Concentration Pathway(RCP)가 활용되었다. 본 연구에서는

SDSM, ASD, delta change 등 다양한 통계적 다운스케일링 기법들 중, 비교적 월 기상변수들을 잘 재현한다는 점에서 Semenov and Stratonovitch 가 제시한 LARS-WG 를 활용하였다. LARS-WG 는 확률분포를 도시하기 위한 매개변수군을 추정하기 위해 어떤 특정한 지역에서 취득한 1989-2015 년 동안의 기상자료들(일별 강우, 기온)에 대해 검증되었으며, 도시된 확률분포는 합성 기상시계열자료를 생성하기 위해 사용되었다. 네 개의 GCMs 을 투영한 결과, RCP 4.5 와 8.5 시나리오에서 미래의 모든 세 계절에 대해 연간 Tmax 와 Tmin 모두 기준치보다 증가하는 양상을 보였다. 장마철은 모든 두 기간의 어떤 계절보다 미래에 가장 큰 강수량이 기록될 것으로 전망되었다.

연구대상지역에 미치는 기후변화 영향평가는 가까운 미래인 2050 년도(2021-2050 년)와 먼 미래인 2080 년도(2051-2080 년)를 대상으로 수행되었다. Katha, Sagaing 지점에서 네 개의 GCMs 을 활용한 연평균 유량은 2050 년도에 약 70%, 2080 년도에 약 80%의 증가추세를 보였으며, Myitkyina 지점에서는 연간, 계절별 유량 모두 80%의 가장 급격한 감소를 보였다. 연간 유량 최대 증가치는 EC-EARTH, HadGEM2-ES, 그리고 MICRO5 를 통해 2050 년도 9%, 2080 년도 15%로 산정되었으며 최대 감소치는 RCP4.5, 8.5 조건에서 MPI-ESM-MR 을 통해 Bamo 지점에서 2080 년도 15%로 산정되었다. 모든 지점에서 계절별 평균 유량에 대해서는, 모든 두 시나리오 조건에서 여름철 유량이 한 세기동안 약 80% 감소할 것으로 전망되었다. 장마철과 겨울철 유량에 대해서는, Katha, Sagaing 지점에서 2050 년도에 84%, 2080 년도에 107%로, Bamo 지점에서 2050 년도에 30%, 2080 년도에 40%로 꾸준하게 증가할 것으로 예측되었다.

모든 시나리오 상에서, 모든 지점의 미래기간에 대한 연간, 그리고 계절별 유량의 변화에 대한 불확실도의 범위는 약 30%에서 45% 사이에 분포하였다. 본 연구는 미래기후조건에서의 유량변화 예측이 불확실하다는 것과, 이러한 불확실성의 가장 큰 원인이 전체 연구대상지역에 고려된 네 개의 GCMs 으로부터의 기후 예측상에서의 차이에서 기인한다는 것을 증명한다.

본 연구에서 도출된 결과는 향후 연구대상지역에서 기후변화 영향 하에서의 수자원관리를 위한 분석, 평가, 활용을 위해 유의미하게 참고될 수 있을 것으로 판단된다.

주요어: 기후변화, 수문학적 과정, 유량, SWAT, CMIP5, GCM, LARS-WG

학번: 2018-25580